8-1-2016

Tip110 is required for embryonic stem cell survival and embryonic development

Amanda J. Whitmill
University of North Texas Health Science Center at Fort Worth, amandajade.whitmill@gmail.com

TIP110 IS REQUIRED FOR EMBRYONIC STEM CELL SURVIVAL AND EMBRYONIC DEVELOPMENT

DISSERTATION

Presented to the Graduate Council of the
Graduate School of Biomedical Sciences
University of North Texas
Health Science Center at Fort Worth
in Partial Fulfillment of the Requirements

For the Degree of

DOCTOR OF PHILOSOPHY

By

Amanda J. Whitmill, B.S.
Fort Worth, Texas

June 2016

ACKNOWLEDGEMENTS

I would especially like to thank my family and friends for their praise and support during my time as a PhD student. I would also like to thank my major professor Dr. Johnny He for his encouragement, guidance, and unwavering commitment to produce exceptional research. I owe special thanks to my university member Dr. Andras Lacko and to my committee members Dr. Geoffrey Guttmann, Dr. Khalid Timani, and Dr. Yu-chieh Wang as each has directly assisted me with my research and my progress towards completion of my PhD. In particular, I owe thanks to Dr. Guttmann for providing his expertise and advice in embryology and developmental biology; to Dr. Timani for his constant support, encouragement, and advice; and to Dr. Wang for generously assisting me in my stem cell, embryoid body, and organoid culturing experiments in addition to graciously sharing his reagents and instrument with me. I would also like to thank Dr. Rance Berg for not only serving as my graduate advisor but for his assistance with our immune cell phenotyping experiments. In addition, I owe many thanks to Dr. Wang's student Victor Lin and Dr. Berg's student Alexandra Witter for their gracious guidance and support in the aforementioned experiments. Finally, I would like to thank my current and past lab members for their advice and assistance over the last five years with special thanks to Dr. Timani for teaching me a multitude of laboratory techniques and for the many times he assisted me in performing or troubleshooting experiments and in improving my abilities overall as a scientist.

Whitmill, Amanda J., Tip110 is Required for Embryonic Stem Cell Survival and Embryonic Development. Doctor of Philosophy (Biomedical Sciences), June, 2016, 171 pp., 3 tables, 36 illustrations, bibliography, 119 titles.

HIV-1 Tat-interacting protein of 110 kDa, Tip110, has roles in tumor antigen presentation, pre-mRNA splicing, transcription of viral and host genes, and protein degradation. Tip110 is also known to be up-regulated in a variety of cancers and to regulate and/or interact with a variety of transcription factors, oncogenes, and pluripotency factors. As such, Tip110 has been shown to effect pluripotency, proliferation, apoptosis, and the cell cycle when knocked down *in vitro*. However, the function of Tip110 in embryonic development remains largely uncharacterized.

One early study has shown that loss of a Tip110 ortholog leads to embryonic lethality in zebrafish. Our studies have shown that transgenic mouse embryos lacking expression of a functional Tip110 protein die several days post-implantation *in vivo*. In the present study, we determined how Tip110 knockout affects mouse embryonic development and investigated the underlying molecular mechanisms. We found that Tip110 loss did not impair embryo growth from the zygote to the blastocyst stage nor did it impair the blastocysts ability to implant into the uterine lining *in vivo*. Extended culture of blastocysts *in vitro* revealed that Tip110 loss impaired both blastocyst outgrowth formation and derivation of mouse embryonic stem cells from blastocysts. *In vivo* embryos could survive until the post-implantation stage where they eventually perished. The premature death of these embryos was characterized by a clear retardation in embryonic development resulting in underdeveloped or more commonly,

completely resorbed mouse embryos around 8.5 or 9.5 days post coitum. Microarray analysis of Tip110$^{-/-}$ cells derived from mouse blastocysts revealed that Tip110 loss favored differentiation but not self-renewal, pluripotency, or cell cycling through a complex regulatory network of stem cell factors. Tip110$^{-/-}$ cells also had perturbations in many other signaling and cellular processes including mRNA processing and proteasome degradation. Taken together, these findings document for the first time the lethal effects of complete loss of Tip110 on mammalian embryonic development and suggest that Tip110 is an important regulator of not only embryonic development but also stem cell factors.

TABLE OF CONTENTS

Page

LIST OF TABLES

LIST OF ILLUSTRATIONS

LIST OF ABBREVIATIONS

4f-rnp	4f RNA binding protein
5-FU	5’-fluorouracil
Akt1	V-Akt murine thymoma viral oncogene homolog 1
Apbb1/Fe65	Amyloid beta precursor protein binding family member 1
APC	Antigen presentation cell
AR	Androgen receptor
ARE	Androgen response element
BFU-E	Burst forming unit-erythroid
Brd4	Bromodomain containing 4
BSA	Bovine serum albumin
c-Myc	v-Myc avian myelocytomatosis viral oncogene homolog
CB	Cajal body
Cdk9	Cyclin-dependent kinase 9
Cdx2	Caudal type homeobox 2
CFU-GEMM	Colony-forming unit-granulocyte, erythrocyte, monocyte, megakaryocyte
CFU-GM	Colony-forming unit-granulocyte, monocyte
CIP	Calf intestinal phosphatase
CNS	Central nervous system
CODM	Cerebral organoid differentiation media
Cre	Recombinase
CT10	COOH-terminal 10 domain

CTL	Cytotoxic T lymphocyte
DAB	3,3’-diaminobenzidine
DAPI	4',6-diamino-2-phenylindole
Dkk1	Dickkopf-related protein 1 precursor
DMSO	Dimethyl sulfoxide
dpc	Days post coitum
dpf	Days post fertilization
DUB	Deubiquitinating enzyme
E-box	Enhancer box
EB	Embryoid body
EC	Expression console
EDTA	Ethylenediaminetetraacetic acid
Egr1	Early growth response protein 1
EGTA	Ethyleneglycoltetraacetic acid
egy	Earl grey
Endo H	Endoglycosidase H
Erk	Extracellular signal-related kinase
ESCM	Embryonic stem cell media
Esrrb	Estrogen-related receptor beta
FBS	Fetal bovine serum
Fgf4	Fibroblast growth factor 4
FoxD3	Forkhead box D3
Gapdh	Glyceraldehyde-3-phosphate dehydrogenase

Gata2/4/6	Gata binding protein 2/4/6
GCNF	Germ cell nuclear factor
GFAP	Glial fibrillary acidic protein
GFP	Green fluorescent protein
GP120	HIV-1 envelope glycoprotein 120
Gsk3	Glycogen synthase kinase 3
HAT	Half-a-tetracopeptide repeat
hCG	Human chorionic gonadotropin
hESC	Human embryonic stem cell
Hexim-1	Hexamethylene bis-acetemide inducible 1
HIF-1α	Hypoxia inducible factor 1 alpha subunit
HIV-1	Human immunodeficiency virus type 1
HLA	Human leukocyte antigen
HPC	Hematopoietic progenitor cell
HRP	Horseradish peroxidase
ICM	Inner cell mass
IFN-y	Interferon gamma
IgG	Immunoglobulin G
IP	Immunoprecipitation or intraperitoneal
IU	International unit
JAMM	Jab1/Mov34/Mpr1 Pad1 N-Terminal+ (MPN+)
KD	Knockdown
kDa	Kilodalton

Klf2/4/5	Kruppel-like factor 2/4/5
KOSR	Knockout serum replacement
KSOM+AA	Potassium simplex optimized media + amino acids
Larp7	La ribonucleoprotein domain family member 7
Lif	Leukemia inhibitory factor
Lifr	Leukemia inhibitory factor receptor
lncRNA	Long noncoding RNA
loxP	locus of X(cross)-over in P1
LTR	Long terminal repeat
MEF	Mouse embryonic fibroblasts
MEK	Mitogen-activated protein kinase kinase
mePCE	Methylphosphate capping enzyme
mESC	Mouse embryonic stem cell
MHC I	Major histocompatibility complex I
MIR-124	MicroRNA-124
mTOR	Mammalian target of rapamycin
n-Myc	v-Myc avian myelocytomatosis viral oncogene neuroblastoma derived homolog
Neo	Neomycin
NF-kB	Nuclear factor kappa B subunit
NLS	Nuclear localization sequence or signal
Nop25/Nol12	Nucleolar protein 12
NR	Nuclear receptor
NT	NH2(amino) terminus

NTC	Nineteen complex
Oct4	Octamer-binding protein 4/POU class homeobox 1
p300	E1A binding protein p300
p53	Tumor protein p53
Pax3	Paired box 3
PBMC	Peripheral blood mononuclear cell
PBS	Phosphate-buffered saline
PBSMT	Phosphate-buffered saline + Milk + Triton X-100
PBT	Phosphate-buffered saline + BSA + Triton X-100
PCNA	Proliferating cell nuclear antigen
PDAK	Peptide-pulsed dendritic cell-activated killer
pI	Isoelectric point
PMSG	Pregnant mare's serum gonadotropin
PPM1G	Protein phosphatase, Mg_{2+}/Mn_{2+} dependent 1G
Prl	Prolactin
Prp3/8/19	Pre-mRNA processing factor 3/8/19
pTEF-b	Positive transcription elongation factor-b
PTM	Post-translational modification
Raf1	Raf-1 proto-oncogene, serine/threonine kinase
RFP	Red fluorescent protein
RGD	Arginylglycylaspartic acid
Rif1	Replication timing regulatory factor 1
RNAPII	RNA Polymerase II

RNF157	Ring finger protein 157
RNP	Ribonucleoprotein
RNPS1	RNA-binding protein with a serine-rich domain 1
rRas	Related RAS viral oncogene homolog
RRM	RNA recognition motif
Sall4	Spalt-like transcription factor 4
Sap155	Splicing factor 3b subunit 1
SART3	Squamous cell carcinoma antigen recognized by T cells 3
scaRNA	Small Cajal body-specific RNA
SDS-PAGE	Sodium dodecyl sulfate-polyacrylamide gel electrophoresis
siRNA	Small interfering RNA
snRNA	Small nuclear RNA
snRNP	Small nuclear ribonucleoprotein
snoRNA	Small nucleolar RNA
Sox2	SRY-Box 2
STAT3	Signal transducer and activator of transcription 3
TAC	Transcriptome analysis console
TAR	Transactivating response element
Tat	HIV-1 transactivator of transcription
TBST	Tris-buffered saline + Tween 20
Tbx3	T-box 3
Tcf3	Transcription factor 3
Tcl1	T-cell leukemia/lymphoma 1A

TCR	T-cell receptor
TE	Trophoectoderm
TG	Transgenic
TGF-B	Transforming growth factor beta 1
Tip110	HIV-1 Tat-interacting protein of 110 kDa
TK	Tyrosine kinase
TPR	Tetracopeptide repeat
Tuj1/TUBB3	Tubulin beta 3 class III
Ub	Ubiquitin
UPS	Ubiquitin-proteasome system
Usp4/11/15	Ubiquitin-specific peptidase 4/11/15
UTR	Untranslated region
WM-IHC	Whole-mount immunohistochemistry
WT	Wild type
YB-1	Y-box binding protein 1
Zfp42	ZFP42 zinc finger protein
Zic3	Zic family member 3

CHAPTER I

INTRODUCTION

HIV-1 Tat-interacting protein of 110 kDa (Tip110), also referred to as squamous cell carcinoma antigen recognized by T cells 3 (Sart3), p110 or $p110^{nrb}$, was first discovered as KIAA0156 without any specific functions (*1*). Subsequent studies indicate that the ubiquitously expressed nuclear RNA binding protein is necessary for a variety of biological processes including pre-mRNA splicing (*2-15*), regulation of viral and host gene activation and transcription (*16-20*), regulation of protein degradation (*10, 19, 21*), and regulation of cell survival, proliferation and differentiation (*7, 22, 23*). Tip110 has also been extensively studied as a potential antigen for cancer immunotherapy (*24-32*) and has been shown to have roles in skin diseases including disseminated superficial actinic porokeratosis (*33-35*) and atopic dermatitis (*36, 37*).

Tip110 is also imperative for survival throughout embryonic development in *Drosophila melanogaster* (*38*) and in *Danio rerio* (*13*). In addition, Tip110 has been shown to be important in the maintenance and survival of stem cells in human embryonic and hematopoietic stem cell populations *in vitro* (*7, 22, 23*) and in the stem cell populations of regenerating *Schmidtea mediterranea* (*39*). Unfortunately, a complete understanding of what biological role Tip110 plays during mammalian development and why its loss induces an embryonic lethal phenotype has yet to be elucidated. This project aims to examine the specific biological role of Tip110 in both pre- and post-implantation embryonic development of the mouse as well as in stem cell development using a transgenic mouse model. To achieve this, pre- and post-implantation developmental milestones were studied in wild-type, $Tip110^{+/-}$, and $Tip110^{-/-}$ mice to pinpoint

the developmental defects caused by Tip110 deletion. In addition, we took advantage of Tip110$^{-/-}$ transgenic mice and performed whole transcriptome analysis using cells derived from mouse blastocysts to elucidate the molecular mechanisms whereby Tip110 controls embryo and stem cell development. We expect that this investigation will not only shed light on the role of Tip110 in the formation and survival of stem cells but in the development of the mouse and other organisms to better our overall understanding of its complete biological functions.

A literature review describing the characteristics and currently known biological roles of Tip110 is detailed below to provide a better understanding of the properties and functions of the protein and to provide a context for how its loss might perturb embryogenesis, development, and stem cell survival in our mouse model.

Physical Properties and Primary Structure of Tip110

Protein Characteristics and Conserved Domains

Tip110 is a 963-amino acid, nuclear RNA-binding protein. This protein has a predicted molecular weight of 110 kDa and a pI of 5.28. The amino terminal portion of Tip110 is more acidic than the carboxyl terminus such that amino acids 1-321 have a pI of 4.30, amino acids 322-642 have a pI of 6.04, and amino acids 643-963 have a pI of 9.77 in human Tip110 (*40*). This particular characteristic distinguishes Tip110 from other ribonucleoprotein (RNP) motif-containing proteins which are not typically acidic and suggests that Tip110 may be a member of a distinct subfamily of RNP proteins (*40*).

Several conserved domains and putative motifs have been identified within the human Tip110 primary amino acid sequence (**Fig. 1A**). The first motif can be found within the amino terminus of the protein and is the nuclear receptor box (NR box), characterized by the sequence LXXLL, where X is any amino acid. The NR box of Tip110 (LIRLL) spans amino acids 118-122 and is an important contributor to the co-regulation of nuclear steroid hormone receptors (*16, 41-43*). Specifically for Tip110, the NR box confers the ability to negatively regulate the androgen receptor (*16*). Next there is a conserved domain, COG5107, also known as the RNA14 motif (*44*). This particular domain is important for pre-mRNA 3'-end processing and modification such as cleavage and polyadenylation (Liu et al., unpublished data). There are 12 tetracopeptide repeats (TPR) also known as half-a-TPR (HAT) within and following the RNA14 motif that are necessary for many of the protein-protein interactions involving Tip110 and for *in vitro* splicing activity (*2, 8, 12, 20, 45, 46*). When this particular domain is deleted using mutagenesis, specific functions of Tip110 are abolished or diminished. A tyrosine phosphorylation kinase site exists at amino acids 309-316. This site is purported to be phosphorylated on the tyrosine at position 316 and as such may play a role in the metabolism of nuclear RNA due in part to the role of Tip110 as an RNA binding protein (*4, 32*). Unfortunately the phosphorylation state of Tip110 has not been concisely confirmed to be important for any of its cellular functions, with some disputing the functional significance of the tyrosine phosphorylation site altogether (*47*). Tip110 is able to function as a nuclear protein through two nuclear localization sequences (NLS), one spanning amino acids 612-619 and the other spanning amino acids 642-646 (*4, 32, 40*). Two RNA recognition motifs (RRM1 and RRM2) can be found near the carboxyl terminus of the protein with one spanning amino acids 705-778 and the other spanning amino acids 799-879 (*4, 32, 40*). The RRM itself consists of two highly conserved stretches of amino acids separated by ~30

amino acids. The first stretch of amino acids are a hydrophobic cement with 6 residues (RNP2) and the second stretch of amino acids are an octapeptide motif (RNP1) (*40*). The RRM are important for Tip110 to recognize and bind RNA (e.g. U6 snRNA) and for *in vitro* splicing activity. Additional motifs identified within the Tip110 protein sequence include the RGD cell attachment sequence at amino acids 742-744, which contributes to cellular adhesion and possibly caspase-3-mediated apoptosis (*32*), and the CT10 (C10 or LSm interaction motif) domain spanning the amino acids at the C-terminal end of the protein. The CT10 domain is necessary for Tip110 interaction with LSm proteins (*11, 12, 48*). These conserved domains and motifs all have a high degree of homology between species such that most are fairly similar between human and mouse Tip110 proteins (**Fig 1B & C**).

Expression and Cellular Localization

Tip110 is expressed ubiquitously at the mRNA level and can be detected in both normal and malignant cells and tissues. Interestingly, expression is highest in cells and tissues with cancerous phenotypes. There is notable Tip110 mRNA expression in a wide variety of cell lines (normal and malignant) and clear expression in the heart, brain, placenta, lung, liver, skeletal muscle, kidney, pancreas, spleen, thymus, testis, ovary, prostate, small intestine, colon, and in peripheral blood leukocytes (1, 32, 40). Regardless of its ubiquitous expression at the mRNA level, the Tip110 protein can only be found in the nucleus of malignant tumor cell lines, cancerous tissues, and the testis (4, 32, 50). Tip110 can be found in the cytoplasm of proliferating cells (both normal and malignant), the testis, and in the fetal liver (4). Within the nucleus the protein is dispersed rather evenly throughout the nucleoplasm with distinct exclusion from nucleoli and prominent expression in Cajal bodies (*9, 11, 12*). The expression in Cajal

A

B

Motif	# of Residues in Common	% Similarity
RNA14	364/397	91.7%
NR BOX	5/5	100.0%
TK PHOS SITE	8/8	100.0%
NOP25-LIKE SITE	69/98	70.4%
NLS 1	5/6	83.3%
NLS 2	5/5	100.0%
RRM1	64/74	86.5%
RGD	3/3	100.0%
RRM2	78/81	96.3%
LSM MOTIF	17/21	81.0%

C

Motif	# of Residues in Common	% Similarity
HAT 1	29/31	93.5%
HAT 2	27/31	87.1%
HAT 3	31/33	93.9%
HAT 4	34/35	97.1%
HAT 5	28/29	96.6%
Lα	22/26	84.6%
HAT 6	30/30	100.0%
HAT 7	29/31	93.5%
HAT 8	26/29	89.7%
HAT 9	45/50	90.0%
HAT 10	24/27	88.9%
HAT 11	30/30	100.0%
HAT 12	30/33	90.9%
HAT 12 EXT	26/26	100.0%

Figure 1. Conserved domains and motifs throughout the Tip110 protein. (**A**) The amino acid sequences of human Tip110 (top line) and mouse Tip110 (bottom line) were aligned using an NCBI BLAST alignment. A yellow highlight refers to amino acids that differ between mouse and human Tip110 while a grey highlight within the alignment refers to the absence of an amino acid at that position. Overall homology is detailed in the bottom right corner of **A**. A key for the conserved domains and motifs shown in **A** is provided in the first column of the tables in **B** & **C** along with the number of residues in common for a given domain or motif and the respective % similarity between human Tip110 and mouse Tip110. (**B**) shows all the underlined domains and motifs while (**C**) shows the 12 HAT repeats and the helix linker (Lα). Adapted from Whitmill et al., *Life Sci*., 2016 (*49*).

bodies is associated with its role as a recycling factor in pre-mRNA splicing and has contributed to bettering our understanding of the assembly of spliceosome components in these cellular compartments.

There is likely a specific demand for Tip110 in the nucleus of cells with a high metabolic demand (i.e. cancerous cells and tissues). This localization may be required for Tip110 to readily bind nuclear RNA, promote transcription of various oncogenes, interact with other nuclear proteins, or contribute to splicing processes. A cytosolic localization may be necessary in proliferating cells with active transcription and cellular processing. This would explain the expression of Tip110 in the testis and fetal liver as the processes that occur in the testis and fetal liver support this notion. In the testis, there is rapid production of spermatogonia by Sertoli cells and in the fetal liver there are various hematopoietic processes occurring prior to the switch to bone marrow mediated production of blood cells; both of these processes may depend on Tip110, either directly or indirectly, to occur.

Protein Stability and Post-Translational Modification

Previous work has indicated that both human (hTip110) and mouse Tip110 (mTip110) have a high degree of sequence homology. That is, mTip110 has ~80% homology to hTip110 at the nucleotide level and ~86% homology at the protein level (**Fig. 1**). mTip110 has an open reading frame (ORF) from nucleotides 15-2900 resulting in a 964 amino acid polypeptide with nearly all of the conserved domains and motifs previously described for hTip110. Despite this, hTip110 and mTip110 are not expressed and processed in identical fashions.

hTip110 and mTip110 have a theoretical molecular weight of 109,907 and 109,779 Da respectively, but hTip110 appears ~30 kDa larger than mouse after denatured polyacrylamide gel electrophoresis (**Fig. 2**). Also, hTip110 and mTip110 are expressed in a similar fashion at the protein level in human cell lines but not in mouse cell lines and tissues, despite being expressed in relatively comparable fashions at the RNA level. As such, hTip110 appears to be degraded or is otherwise less stable in mouse cell lines and tissues. A post-translational modification (PTM) is most likely responsible for the aforementioned size and expression differences observed between hTip110 and mTip110, although other possibilities cannot be excluded. Analysis for potential PTM on hTip110 has revealed that the protein possesses a tyrosine phosphorylation kinase site in addition to other potential sites for PTM including N-glycosylation, protein kinase C phosphorylation, casein kinase II phosphorylation, and N-myristoylation sites. The specific role or necessity for these PTM in the biological function of Tip110 has yet to be elucidated. Experiments designed to determine which PTM, if any, is responsible for the aforementioned differences between hTip110 and mTip110 can be found detailed further in the Perspectives and Future Directions section.

Biological Relevance of Tip110

RNA/Protein Interactions and Pre-mRNA Splicing

Tip110 can bind to >70 proteins, RNA, and other cellular factors. Many of which can be found using simple database analysis such as IntAct and NextProt. As mentioned, these interactions can occur through its N-terminal HAT domains which are important for protein-protein interactions and its C-terminal RRM which are important for its ability to bind RNA (*2, 4, 40*). Early studies

have revealed that Tip110 specifically plays a role in the regulation of pre-mRNA splicing because of it RNA binding property. Its most prominent role in pre-mRNA splicing is to serve as a recycling factor during the recycling phase of spliceosome assembly (*2, 3, 8*). Tip110 also possesses some other key characteristics that support its role in alternative splicing and that suggest it may have additional roles in RNA metabolism.

One of the first implications for a role for Tip110 in alternative splicing came when the protein was shown to bind to an RNA-binding protein with a serine-rich domain (RNPS1) (*4, 50*). RNPS1 is associated with activation of constitutive and alternative pre-mRNA splicing. The N-terminal region of RNPS1 interacts with Tip110 around amino acids 378-387 (*4*). When the two proteins are co-expressed the localization of Tip110 switches from a diffuse nucleoplasmic localization to a localization within nuclear speckles where RNPS1 is also found suggesting that the two proteins bind directly with one another and co-localize to the nuclear speckle regions within the nucleus to contribute to splicing associated processes there. Co-expression of both proteins promotes proximal 3' alternative splicing of the mRNA of a calcitonin-dehydrate reductase chimeric mini gene, further suggesting that the two proteins come together to form a complex with other proteins to regulate mRNA splicing *in vivo*. It has not been clearly shown whether the two interact together as a complex during the recycling phase of alternative splicing, although this and other data supports this notion. It may also be possible that the two interact and contribute to the role of Tip110 as a regulator of splicing.

Tip110, like its yeast homolog — Prp24, can recognize and bind U6 small nuclear RNA (snRNA) and the U4/U6 small nuclear RNP (snRNP) (*2, 8, 40, 48, 51*). The RRM (RRM1-

RRM4) of Prp24 bind U6 and U4 snRNP; in this regard Tip110 performs the identical function in humans except it possesses only two RRM (RRM1 and RRM2) (*2, 4, 40, 51, 52*). Tip110 interacts specifically with the hexanucleotide, ACAGAG, in the stem I region of 2', 3'-cyclic phosphate U6 snRNA and can bind to U6 snRNA via a direct interaction between nucleotides G38 and U57 of U6 snRNA (*2, 5, 51*). In mammalian systems the association of Tip110 with the U6 snRNP is only transient and the interaction takes place with only 10% of the free U6 snRNP (*5*). Tip110 also plays a role in regeneration of U4/U6 snRNP from free U4 and U6 snRNP as Tip110 can bring the U6 snRNP (either *de novo* synthesized or recycled from the spliceosome) into Cajal bodies (CB) from the nucleoplasm and promote the interaction of the U6 snRNP with the U4 snRNP (either *de novo* synthesized or recycled from the spliceosome) (**Fig. 3**) (*9, 11, 53*). Subsequently Tip110 will release and the U4-U6/U5 tri-snRNP will form and exit the CB and make its way to the spliceosome. As such, Tip110 is not static in the nucleus but rather, it shuttles from one nuclear compartment to another to contribute to spliceosome assembly and recycling. As previously noted, Tip110 only functions as a recycling factor during the recycling phase of spliceosome reassembly and has not been found in assembled and processed spliceosomes (*2*). Tip110 is particularly necessary as a recycling factor in splicing when pre-mRNA turnover is high and removal of Tip110 from *in vitro* systems results in dissociation of the U4/U6 snRNP (*8*).

Tip110 interactions with snRNP and other splicing related components all occur within the nucleus. As previously indicated, spliceosome recycling processes specifically occur within CB, where Tip110 is prominently expressed (*11, 12*). Co-staining for Tip110 and snRNP revealed that they co-localize strongly in the CB particularly when there is active transcription or splicing

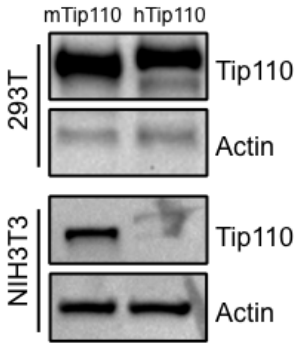
mTip110
hTip110
293T
Tip110
Actin
NIH3T3
Tip110
Actin

Figure 2. Size and expression differences between the mouse and human Tip110 proteins. Western blot analyses of cell lysates from 293T (Top) and NIH3T3 (Bottom) cells transfected with either the mouse Tip110 or human Tip110 plasmid are shown. β-Actin was included as a loading control for Western blotting. The data are representative of three independent experiments. Adapted from Whitmill et al., *Life Sci*., 2016 (*49*).

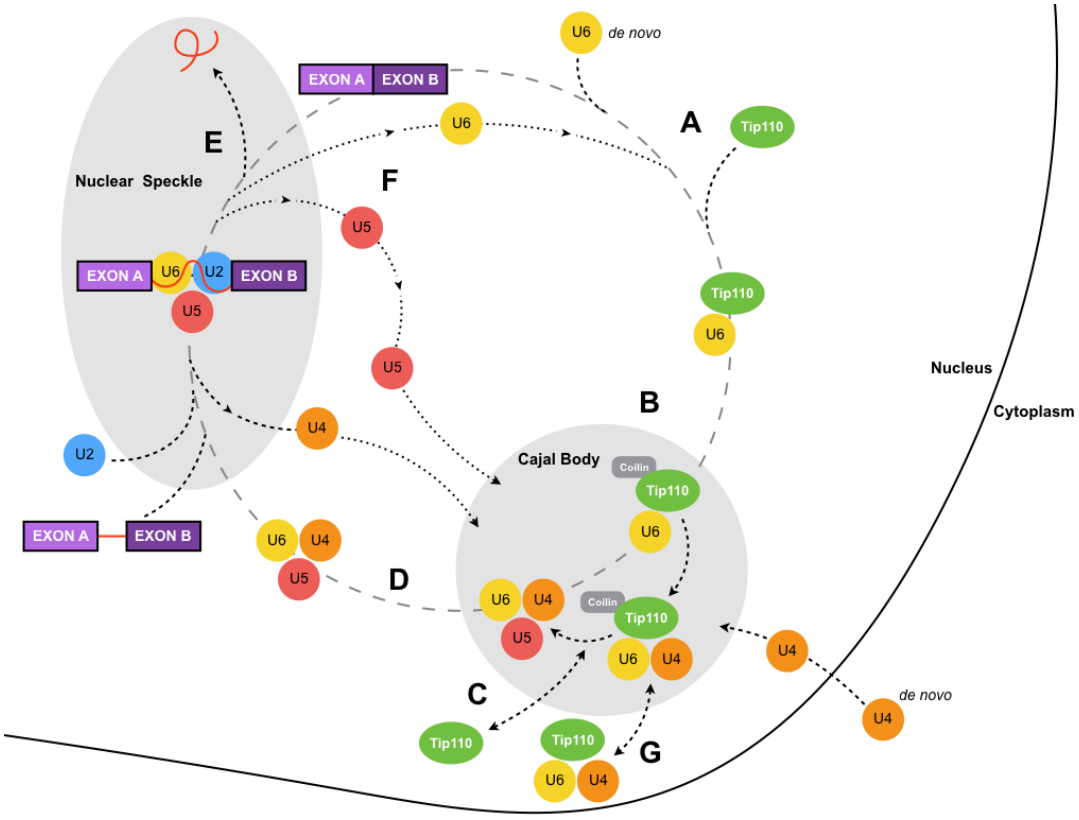
U6
de novo
EXON A
EXON B
U6
A
Tip110
E
Nuclear Speckle
F
U5
EXON A
U6
U2
EXON B
U5
Tip110
U6
U5
Nucleus
Cytoplasm
B
U4
U2
Cajal Body
Coilin
Tip110
EXON A
EXON B
U6
U4
U6
U4
U5
D
Coilin
Tip110
U5
U6
U4
U4
de novo
C
Tip110
Tip110
G
U6
U4
U4

Figure 3. Tip110 in pre-mRNA splicing. (**A**) Tip110 recognizes and binds U6 snRNA (either recycled from the spliceosome or *de novo* synthesized) and recruits it to Cajal bodies (CB). (**B**) In the CB, Tip110 binds to coilin and supports the interaction of the U6 snRNP with the U4 snRNP (either recycled from the spliceosome or *de novo* synthesized). Tip110 does release from coilin or the di-snRNP until the di-snRNP becomes a tri-snRNP (**C**) Tip110 releases after the U6 and U4 snRNP interact and can exit the CB and participate in subsequent rounds of U6 snRNA recruitment to CB or serve as a recycling factor. (**D**) The U5 snRNP binds the U4-U6 di-snRNP and the U4-U6/U5 tri-snRNP is formed. The tri-snRNP exits the CB and enters the spliceosome where the pre-catalytic (U1, U2, and U4-U6 snRNP) and catalytic (U2, U5, and U6 snRNP) spliceosomes form and promote splicing of pre-mRNA (**E**). (**F**) As the various catalytic steps of the spliceosome pass, snRNP exit the spliceosome and are recycled for reuse. (**G**) Tip110 assists in returning the U4-U6 di-snRNP back to the CB for subsequent rounds of splicing. Adapted from Whitmill et al., *Life Sci*., 2016 (*49*).

occurring in the cell, although both are evenly distributed throughout the nucleoplasm (*12*). The HAT domains of Tip110 are known to be a particularly important determinant for its CB localization such that deletion of HAT domains on the N-terminus of Tip110 results in prominent expression of Tip110 in nucleoplasm and nucleoli with only low levels detected in CB (*12*). Recruitment of Tip110 and snRNP to CB is dependent on expression of coilin, a marker for CB (*9, 11, 12, 14*). Tip110 can interact with coilin in CB and has been shown to act as a sort of anchor whereby it holds on to incomplete di-snRNP and coilin in the CB until the snRNP form into tri-snRNP (**Fig. 3**) (*9*). Tip110 can also interact with LSm proteins through its CT10 domain or LSm motif. This interaction stabilizes the interaction between Tip110 and the U6 snRNP and promotes formation of the U4/U6 snRNP complex (*11, 12*). Because Tip110 interacts with U6 snRNA, it is responsible for and required for U6 snRNP targeting to CB through the aforementioned CT10 or LSm domain. Tip110 cannot effectively perform its functions as a recycling factor and regulator of splicing without CB. This notion is further confirmed by data that shows that CB containing Tip110 are induced to form when snRNP accumulate in the cell (*14*).

Splicing or rather the assembly of the spliceosome, is regulated by protein ubiquitination. That is, the stability of the U4/U6.U5 tri-snRNP is regulated through ubiquitination of the U4 snRNP (**Fig. 4**) (*10*). Prp19, which is part of the Nineteen Complex — NTC, has been shown to function as an E3 ligase (*10*). Specifically, Prp19 can ubiquitinate Prp3 (a component of the U4 snRNP) with K63 chains. The K63 chains of the ubiquitinated Prp3 are then recognized by the JAMM domain of Prp8 (a component of the U5 snRNP) (*10*). As such, Prp8 preferentially interacts with the K63 chain of Prp3 and stabilizes the U4/U6.U5 tri-snRNP allowing the complex to enter the

spliceosome for productive splicing. When the tri-snRNP is recruited to the spliceosome, Prp3 is released after deubiquitination by Usp4. Tip110 interacts with Usp4, a deubiquitinating enzyme, and the Usp4:Tip110 complex ($Usp4^{Tip110}$) deubiquitinates Prp3 weakening the interaction between Prp3 and Prp8 and promoting U4 snRNP dissociation from the spliceosome (*10*). Without ubiquitination a stable tri-snRNP cannot form and enter the spliceosome as such this step serves a regulatory purpose in the cell. After dissociation the components are recycled (in processes that also require Tip110) for further rounds of splicing. These findings are interesting because prior to this Tip110 was only shown to function as a recycling factor that promoted the assembly of the U4/U6 snRNP. This data shows that Tip110, or more specifically, $Usp4^{Tip110}$ is also necessary for the disassembly of the U4/U6.U5 tri-snRNP and that Tip110 further contributes to regulation of splicing as a result.

In addition to these roles Tip110 can specifically regulate the alternative splicing of OCT4 mRNA in human embryonic stem cells (hESC). Specifically, the splice variants - Oct4a and Oct4b - of OCT4 are affected by modulating Tip110 levels (*7*). Oct4a is expressed in self-renewing pluripotent ESC and helps maintain these pluripotent cells in their undifferentiated state while Oct4b is expressed in a variety of non-pluripotent cells and is not involved in maintaining either the self-renewal or the pluripotency of ESC. Increasing Tip110 and OCT4, results in more efficient splicing of an OCT4 mini-gene in the Oct4a form (*7*). When Tip110 is down-regulated the mini-gene cannot splice in the Oct4a form efficiently while the Oct4b levels remained unchanged in either case (*7*). Tip110 does not affect Oct4a splicing through activation of the OCT4 promoter, which suggests that its effects are specifically through alternative splicing. Because Tip110 preferentially induces splicing of OCT4 in the Oct4a form it is likely

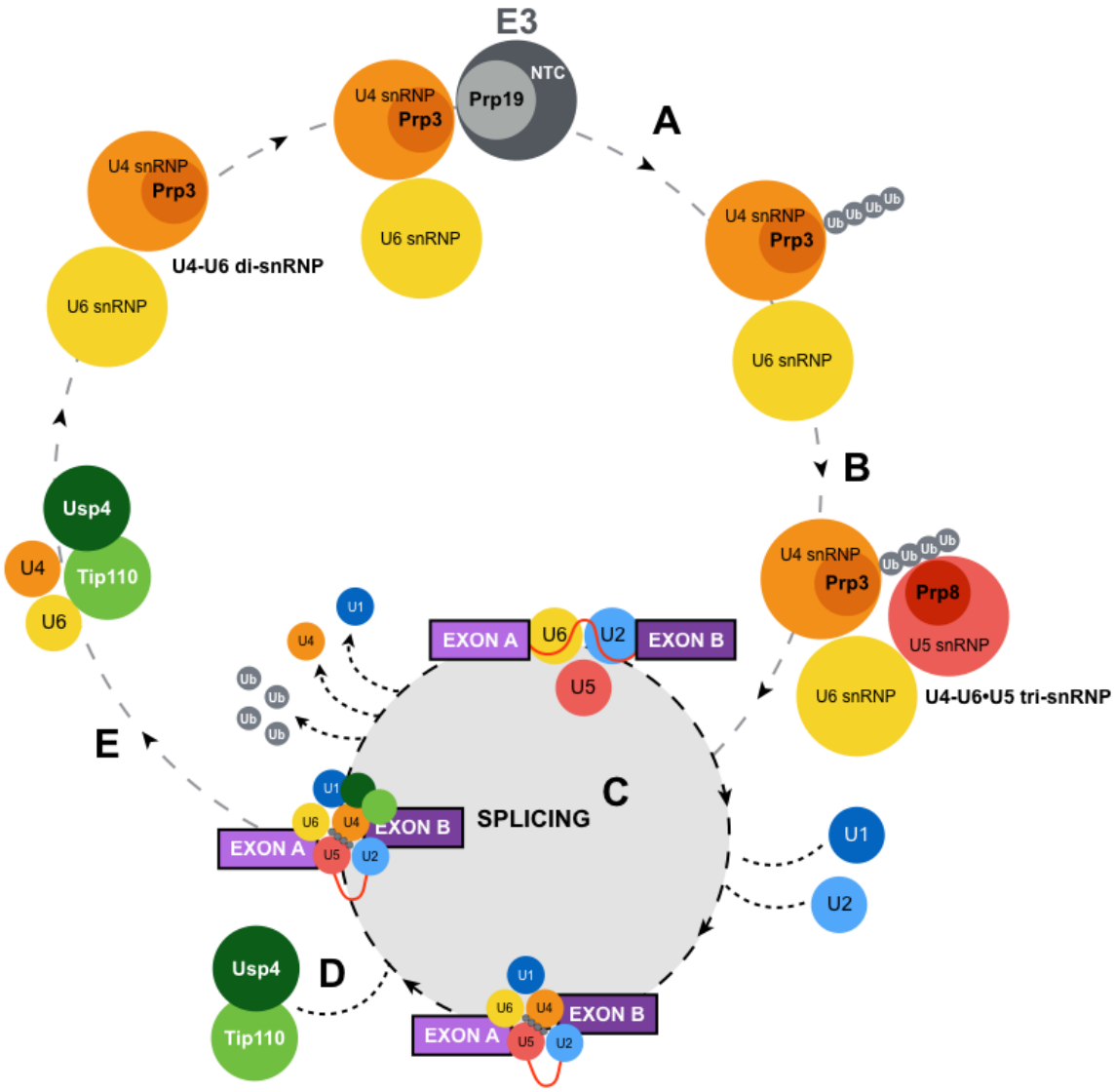
E3
NTC
Prp19
U4 snRNP
Prp3
A
U6 snRNP
U4-U6 di-snRNP
Ub
B
Prp8
U5 snRNP
U6 snRNP
U4-U6•U5 tri-snRNP
Usp4
Tip110
U4
U6
E
U1
U2
U5
EXON A
EXON B
SPLICING
C
D

Figure 4. Tip110 in UPS-mediated deubiquitination of the U4 snRNP. Ubiquitination of the Prp3 component of the U4 snRNP is necessary for successful participation of the U4-U6/U5 tri-snRNP in the spliceosome. (**A**) The Prp19 E3 ligase ubiquitinates Prp3 with K63 ubiquitin (Ub) linkages. (**B**) Subsequently, the JAMM domain of Prp8 recognizes and binds the K63 Ub chains of Prp3 forming the U4-U6/U5 tri-snRNP. (**C**) The stabilized tri-snRNP is recruited to the spliceosome where the steps of the splicing proceed as outlined in Fig. 4. (**D**) The tri-snRNP can be destabilized by interaction with the Usp4:Tip110 complex which deubiquitinates Prp3. Deubiquitination of the U4 snRNP causes it to release from the spliceosome. (**E**) Subsequently Tip110 interacts with released or free U6 snRNA (which can bind the U4 snRNP) and recycles the U4-U6 di-snRNP back into the cycle for additional rounds of splicing. Adapted from Whitmill et al., *Life Sci*., 2016 (*49*).

that Tip110 expression is important for maintenance of stem cells in an undifferentiated state. This information coupled to additional data in the (Stem) Cell Growth, Survival and Differentiation section suggests an important role for Tip110 in maintaining and regulating the differentiation of stem cell populations. All of these findings highlight the critical role of Tip110 in RNA binding and splicing processes and may suggest that when lost during development these processes will likely be perturbed to some degree affecting various splicing and other homeostatic processes occurring in developing cells and tissues.

Gene Expression and Transcription Regulation

Tip110 has been shown to play some critical roles in the transcription activation and repression of a variety of genes including the HIV-1 LTR and the androgen receptor. HIV-1 Transactivator of Transcription (Tat) is a regulatory protein that is essential for HIV-1 gene expression and viral replication (*17*). Tat can transactivate HIV-1 transcription from the viral LTR promoter (HIV-1 LTR) through interaction with transactivating response element (TAR), which is found 3' of the LTR start site. Similarly, Tip110 can regulate HIV-1 gene expression through direct activation of the HIV-1 LTR promoter and through interaction with HIV-1 Tat where it increases Tat-mediated transactivation activity (*17*). Tip110 binds to Tat (independent of TAR) via direct interaction between the HAT-rich domain on the N-terminus of Tip110 and the core domain (aa 38-48) of Tat (*17, 54*). Tip110 does not bind to TAR directly or otherwise (*17*). Tat and Tip110 can independently transactivate the HIV-1 LTR promoter in HIV-1 gene expression, although Tat does so more efficiently. The proteins work synergistically in enhancing Tat transactivation activity in a TAR-dependent fashion when they bind directly to one another. In this way Tip110 supports Tat-mediated enhancement of HIV-1 gene transcription and replication. In fact 293T

cells co-expressing recombinant HIV-1 proviral DNA (pNL4-3) and recombinant Tip110 display a 3.5-fold increase in HIV-1 virus production; where the interaction between Tip110 and Tat is required for the increase and down-regulation of Tip110 induces inhibition of HIV-1 viral gene expression (*17*).

Tip110 can also enhance HIV-1 LTR transcription through direct interaction with unphosphorylated RNA polymerase II (RNAPII) (**Fig. 5**). Specifically, the combined interaction between Tip110, Tat, and RNAPII leads to the recruitment of more positive transcription factor b (P-TEFb) – CDK9 and cyclin T1 – to the transcriptional complex (*20*). This effectively enhances phosphorylation of serine 2 and serine 5 of RNAPII. Together these interactions lead to a higher efficiency of transcription elongation of the HIV-1 LTR. Interestingly, endogenous Tip110 can be found at the HIV-1 LTR promoter *in vivo* independent of Tat indicating that Tip110 may first complex with RNAPII on the HIV-1 LTR followed by recruitment of the Tat-PTEF-b complex (*20*). The entire complex initiates phosphorylation of serine 2 of RNAPII leading to HIV-1 LTR transcription elongation and synthesis of full length mRNA.

Tip110 is not only important in increasing viral gene expression but is also important for activation of expression of other genes. This is because Tip110 can interact with the transcriptionally inactive P-TEFb complex which consists of 7SK RNA, Hexim1, MePCE, Larp7, and P-TEFb components cyclin T1 and CDK9 (**Fig. 5**) (*54-56*). The disruption of the complex and the initiation of formation of the active P-TEFb complex occurs upon introduction of the Tat protein, as Tat can recruit protein phosphatase 1 G (PPM1G) to the complex (*54*). PPM1G dephosphorylates the T-loop of CDK9 and destabilizes the complex causing it to

dissociate. Because of this Tip110 cannot be found complexed with the transcriptionally inactive P-TEFb complex and Tat simultaneously. The dissociation of the complex activates the switch from initiation to elongation. P-TEFb is subsequently autophosphorylated and recruited to phosphorylate RNA polymerase II and further promote transcription elongation. This phenomenon has been shown for HIV-1 gene expression/viral replication and for NF-**κ**b mediated transcription of inflammatory response genes/anti-apoptotic genes but likely occurs in many other systems. As such, it is very likely that Tip110 can potentiate transactivation of other viral and host promoters and thus drive synthesis of a variety of other mRNA transcripts *in vivo*

In addition to its role in regulating viral gene expression Tip110 can also regulate host genes. Specifically, Tip110 possesses a NR box (LIRLL) on its N-terminus that gives the protein the ability to regulate nuclear steroid hormone receptors (*16*). Thus far Tip110 has been shown to be a negative regulator of the androgen receptor (AR). The AR is a transcription factor that binds DNA to control expression of androgen-responsive genes (**Fig. 6**) (*57, 58*). Tip110 is able to bind the AR through its NR box, and although there is no complex formation between Tip110 and the AR, Tip110 can serve as a co-repressor of AR-mediated gene expression in a dose-dependent manner (*16*). The inverse is also true. That is, when Tip110 expression is down modulated using antisense RNA there is an increase in AR-mediated gene expression. Tip110 is able to exert its functions as a negative regulator of AR transactivation by binding to the AR with its NR box and effectively blocking the complex formation between the AR and the androgen response elements (ARE) (*16*). This study defines yet another role for Tip110 in modulation of gene expression and could have potential implications for roles for Tip110 and the AR in male infertility, androgen insensitivity, diabetes, metabolic syndrome, Alzheimer's disease and even tumorigenesis (i.e. in

.

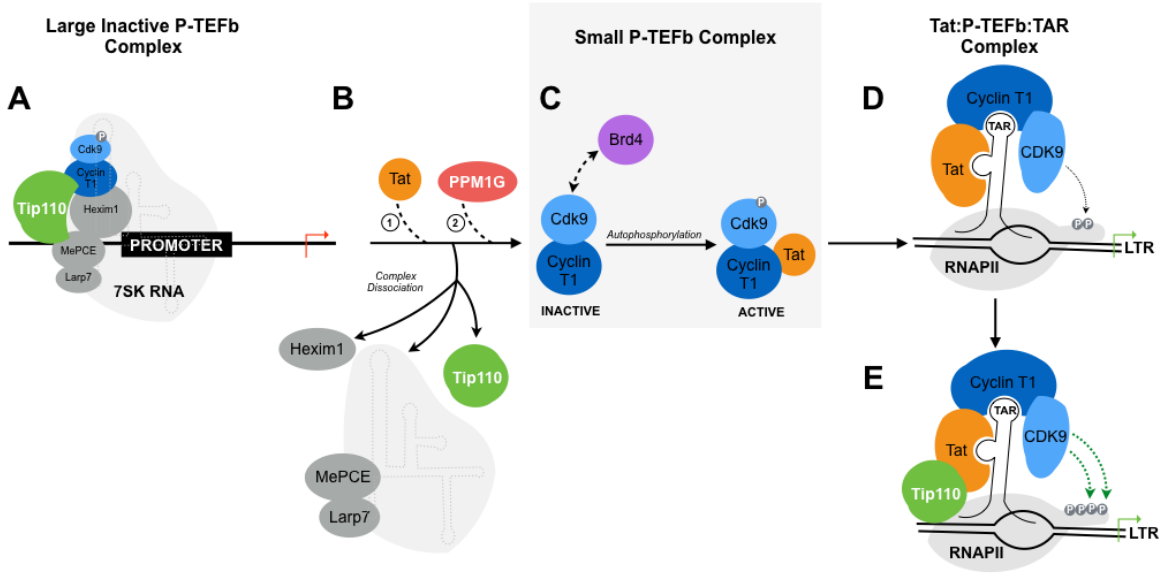
Large Inactive P-TEFb Complex
A
Cdk9
Cyclin T1
Tip110
Hexim1
MePCE
Larp7
PROMOTER
7SK RNA
B
Tat
PPM1G
1
2
Complex Dissociation
Hexim1
Tip110
MePCE
Larp7
Small P-TEFb Complex
C
Brd4
Cdk9
Cyclin T1
INACTIVE
Autophosphorylation
Cdk9
Cyclin T1
Tat
ACTIVE
Tat:P-TEFb:TAR Complex
D
Cyclin T1
TAR
Tat
CDK9
RNAPII
LTR
E
Cyclin T1
TAR
Tat
CDK9
Tip110
RNAPII
LTR

Figure 5. Tip110 in regulation of viral gene transcription. (**A**) Tip110 can be found bound to the transcriptionally inactive P-TEFb complex. (**B**) The Tat protein can also interact with the complex but it recruits PPM1G which dephosphorylates CDK9 and quickly destabilizes the complex. (**C**) P-TEFb which is stabilized by Brd4 can then be autophosphorylated (for further stabilization) and can interact with and be recruited by Tat to RNA Polymerase II (RNAPII) for elongation. (**D**) The Tat:P-TEFb:TAR complex is active and as such CDK9 can phosphorylate RNAPII to promote elongation. (**E**) When Tip110 is introduced to the Tat:P-TEFb:TAR complex and RNAPII it promotes further phosphorylation of RNAPII and enhances transcription elongation of the LTR promoter. Adapted from Whitmill et al., Life Sci., 2016 (*49*).

prostate and breast cancer) and may also suggest a role for Tip110 as a co-repressor of other genes (*16, 57, 58*).

In addition to its direct regulation of HIV-1 and AR-associated gene expression Tip110 can regulate gene expression and transcription by serving as a histone chaperone that assists in histone deubiquitination. Through its N-terminal domain the deubiquitinating enzyme USP15 has been shown to directly interact with Tip110 (*19, 21, 59*). The interaction between the two proteins alters the localization of USP15, causing it to change from a primarily cytoplasmic localization to a distinct co-localization with Tip110 in the nucleoplasm when the two are co-expressed suggesting that they work together in this cellular compartment (*19, 21*). Both Tip110 and USP15 can interact with histones H2A and H2B where Tip110 binds to histones and acts as a histone chaperone that functions in substrate recruitment while USP15 binds to histones and deubiquitinates them (*21*). Histones can be ubiquitinated for variable reasons. H2A ubiquitination is associated with gene silencing while H2B ubiquitination is associated with active gene transcription (*21, 60*). When H2B is ubiquitinated it is released from nucleosomes as they are disassembled during transcription (*21*). After eviction from active transcription sites ubiquitinated H2B (ubH2B) can be recycled back into nucleosomes after deubiquitination by a DUB such as USP15. The interaction with the DUB is mediated by histone chaperones like Tip110. Tip110 can bind both ubH2B and USP15 to contribute to the enhancement of ubH2B deubiquitination by USP15 (*21*). Tip110 can also, to a lesser extent, promote nucleosome formation through conversion of relaxed circular DNA to supercoiled DNA (*21*). If we couple these findings to the role of Tip110 in pre-mRNA splicing it seems that this data supports the notion of transcription being tightly coupled to pre-mRNA processing. That is, ubH2B

ubiquitination and deubiquitination could affect (either directly or indirectly) chromatin disassembly and reassembly in both transcription and mRNA processing of certain target genes.

The aforementioned data clearly highlights roles for Tip110 in various aspects of regulation of gene expression. It is also important to note though, that Tip110 has the ability to regulate or be regulated by many oncogenes, oncoproteins, and transcription factors (i.e. p53, HIF-1α, YB-1, USP15, USP4, c-MYC) (*7, 18, 19, 21, 23, 59*). This suggests a role for the protein not only as a regulator of general transcription functions but also suggests that Tip110 is important in cancer and can contribute to promoting or suppressing cancerous or cancer-like phenotypes.

Lastly, although Tip110 has various interactions and functions that implicate it in cancer its expression is almost exclusively studied under normal oxygen conditions. To better understand its role as an oncogenic protein in tumors, the regulation of Tip110 under hypoxic conditions has been investigated. Hypoxia inducible factor 1α (HIF-1α) and p53 are both transcription factors that can be regulated by the oxygen state of the microenvironment. Under normoxia HIF-1α and p53 levels remain low because of UPS-mediated degradation processes (*61*). However, under hypoxia HIF-1α and p53 are stabilized and can serve to activate either pro-survival or pro-apoptotic genes (*61*). Interestingly, Tip110 can be regulated by both HIF-1α and p53. That is, in the hypoxic state, there is UPS-mediated degradation of Tip110 that is induced by p53 destabilization of Tip110 (*61*). The destabilization of Tip110 by p53 is possible, in part, because of the ability of Tip110 to first stabilize p53 under hypoxia (*61*). Tip110 can also regulate HIF-1α and p300 - a coactivator of HIF-1α and p53 (*61*). These data indicate that the oxygen state of

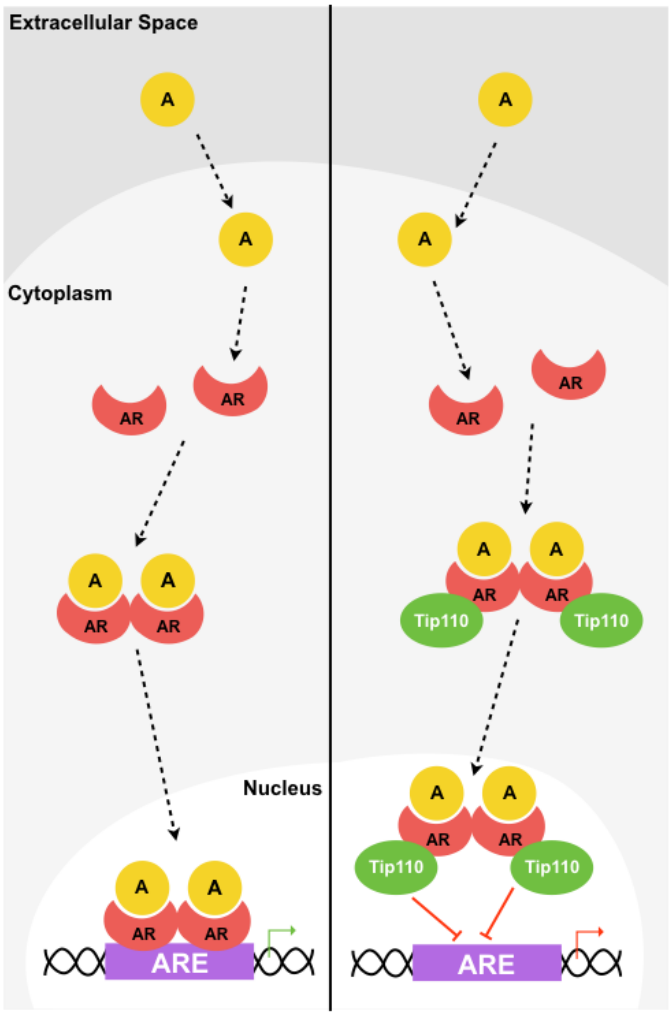
Extracellular Space
Cytoplasm
Nucleus
A
AR
Tip110
ARE

Figure 6. Tip110 as a negative regulator of androgen receptor-mediated transcriptional activation. Left - Under basal conditions androgens (A) bind the androgen receptor (AR) which dimerizes and translocates to the nucleus. In the nucleus the androgen receptor binds to the androgen response element (ARE) and promotes the transcriptional activation of a variety of genes. Right - Overexpression of Tip110 promotes Tip110 binding to the AR. Although the AR can still translocate to the nucleus it cannot bind ARE and promote transcriptional activation as Tip110 prevents the interaction of the AR with the ARE. Adapted from Whitmill et al., *Life Sci*., 2016 (*49*).

the tumor and changes in the expression of proteins and transcription factors like Tip110, p53, HIF-1α and p300 are critical to the fate of the tumor and may even be predictors for the severity of cancer and metastasis. This is because cell-type and oxygen status of a tumor can determine if there will be a switch to a cell survival or cell death state. Understanding this dynamic balance is crucial for enhancing our understanding of Tip110 in cancer and other diseases states.

All together these data show the critical role Tip110 plays in gene regulation and protein turnover processes. These data also provide further insights into the biological processes where Tip110 expression is critical for proper maintenance of cell homeostasis and provides clues into where the loss of Tip110 might perturb these processes during development.

(Stem) Cell Growth, Survival and Differentiation

Tip110 mRNA and protein expression can be detected in hematopoietic stem and progenitor cells isolated from human cord blood in the first days of culture and are diminished overtime (*23*). That is, there is high detection of Tip110 mRNA and protein in various $CD34^+$ populations but as the cells begin to cycle and develop into mature hematopoietic cells (i.e. $CD14^+$, $CD16^+$ or $CD36^+$ cells) Tip110 levels decline. This down-regulation of Tip110 during hematopoietic stem cell differentiation is initiated through an interaction of microRNA-124 (mir-124) with the 3'-untranslated region (3'UTR) of Tip110 (*6*). In contrast to Tip110, mir-124, which normally has low-level expression, is up-regulated during the differentiation of $CD34^+$ cells (*6*). The expression changes in Tip110 as stem cells develop and differentiate establishes Tip110 as a marker for undifferentiated cells of hematopoietic lineage and implicates it in the development of hematopoietic cells.

Analysis of the hematopoietic cell and tissue lineages in Tip110 transgenic mice ($Tip110^{TG}$) overexpressing hTip110 showed that $Tip110^{TG}$ mice have significant increases in CFU-GM, BFU-E, and CFU-GEMM per femur and spleen (*23*). These mice also have a significant increase in the percentage of marrow and spleen HPC in the S phase of the cell cycle and a non-significant decrease in nucleated femoral cellularity and a non-significant increase in nucleated spleen cellularity with circulating blood levels remaining within the normal range. Analysis of the hematopoietic cell and tissue lineages in Tip110 haploinsufficient mice under the hematopoietic lineage specific promoter Tie2-Cre ($Tip110^{+/-}$) showed that $Tip110^{+/-}$ mice have significant decreases in CFU-GM, BFU-E, and CFU-GEMM per femur and spleen. These mice also have slowly or non-cycling bone marrow and spleen HPC, an insignificant increase in nucleated cellularity in femoral marrow, and an insignificant decrease in nucleated spleen cellularity with circulating blood levels remaining within the normal range (*23*).

From these data it is clear that modulation of Tip110 expression results in an inverse response in $Tip110^{+/-}$ mice compared to $Tip110^{TG}$ mice, with $Tip110^{+/-}$ mice exhibiting an overall decrease in HPC numbers and cycling and TG mice showing an increase in both. These data together suggest that Tip110 expression can regulate the proliferation and number of HPC possibly through effects on HPC cycling. Moreover, when cell cycle specific drug 5-FU was administered to WT, $Tip110^{TG}$, and $Tip110^{+/-}$ mice, overall $Tip110^{+/-}$ mice seemed to be protected from the 5-FU administration most likely because at the time of administration $Tip110^{+/-}$ HPC were slowly or non-cycling making them less vulnerable to the effects of 5-FU (*23*). On the other hand $Tip110^{TG}$

mice seemed to be more vulnerable to the 5-FU administration most likely because at the time of administration their HPC were in a state of increased cycling (*23*).

These data indicate clearly that Tip110 overexpression resulted in an increase in $CD34^+$ cell numbers compared to controls, a decrease in apoptosis, an increase in cell cycling, and an increase cell survival and proliferation, while Tip110 knockdown had the opposite effect (*23*). Transcription factors c-MYC and GATA2 can be implicated in the mechanism of action of Tip110 in modulation of HPC processes, as increases in Tip110 are associated with coordinated increases in c-MYC and GATA2, while Tip110 decreases result in the opposite trend (*23*). Tip110 and c-MYC can reciprocally regulate each other's gene expression while GATA2 can regulate Tip110 gene expression (*23*). This is important because c-MYC is a known regulator of hematopoiesis while GATA2 is crucial for the maintenance and expansion of HSC. Other information about the role of c-MYC in stem cells coupled to this allows us to postulate that the regulation of Tip110 by c-MYC might be mediated through transcriptional pause release mechanisms as c-Myc was shown to affect Pol II pause release and thus affect gene expression particularly in stem cells (*62*). If this is true, then in cells with active transcription, particularly embryonic stem cells or in our case hematopoietic stem cells, high levels of c-MYC can lead to recruitment of P-TEFb to Pol II (*62*) at the Tip110 promoter causing pause release and a subsequent increase in Tip110 gene expression. The increase in Tip110 expression can then stimulate more c-MYC expression resulting in a feedback loop promoting both Tip110 and c-MYC expression in these cells. More interestingly as well, is that it is already known that Tip110 itself can affect transcriptional elongation of RNA Pol II by contributing to the phosphorylation

and activation of RNA Pol II so it may also be the case that this regulation is also a part of this particular feedback loop.

To further understand the biological role of Tip110 in stem cells, Tip110 expression was studied in human embryonic stem cells. These studies revealed that Tip110 is expressed in hESC, where its promoter is activated by the transcription factor/oncoprotein c-MYC (*7, 22*). c-MYC binds to a putative E-box region (CACGTG) within the Tip110 promoter (-687 - +1 bp) in order to initiate its activation (*7*). After ESC differentiation, c-MYC levels and Tip110 levels are decreased significantly. That is, c-MYC and Tip110 are not expressed in quiescent $CD34^+$ cells but are expressed in cytokine-stimulated undifferentiated $CD34^+$ cells where expression of both decreases as the cells differentiate as mentioned above (*22*). This is similar to the aforementioned trend in HSC and HPC.

c-MYC expression can affect Tip110 expression through its interaction with the Tip110 promoter. When c-MYC is over-expressed, Tip110 expression increases and when C-MYC is knocked down Tip110 expression (mRNA and protein) is reduced (*7*). c-MYC not only effects Tip110 but also impacts pluripotency factors OCT4, SOX2, and NANOG in an identical fashion (*7, 22*). Increasing Tip110 levels can also result in a slight increase in the levels of OCT4, SOX2, and NANOG. As hESC differentiate Tip110, OCT4, SOX2, and NANOG have all been shown to decrease with greater than 70% loss of expression in all cases (*22*). Overexpression of Tip110 contributes to maintenance of hESC in the undifferentiated state while Tip110 knockdown contributes to induction of differentiation of hESC (*22*). These effects appear to be due in part to the ability of Tip110 to regulate NANOG, OCT4, and SOX2 (*22*). These results

suggest that Tip110 may be an effective marker for early undifferentiated cells and that is has some role in the regulation and maintenance of pluripotency of stem cells. This implies that Tip110 is important in development although it is possible that in the absence of Tip110 there are other factors that can substitute it as a pluripotency regulator.

Lastly, E3 ligase RNF157 is shown to promote the health, integrity, and survival of neurons (*63*). Interestingly this protein and Tip110 both interact with amyloid beta precursor protein-binding, family B, member 1 (APBB1 or Fe65) where each interacting pair has been shown to function differently (*63*). RNF157 and Fe65 are expressed primarily in neuronal tissues (i.e. hippocampus, cerebellum, and cortex) and neurons with little to no expression in non-neuronal tissues (*63*). Fe65 is a substrate of the E3 ligase RNF157 and receives a K63 ubiquitin chain which targets it for proteasomal degradation in neurons (**Fig. 7**) (*63*). When Fe65 is overexpressed it promotes neuronal apoptosis particularly when it is localized in the nucleus (*63*).

Tip110 has been shown to be localized in the nucleus of neurons and it is also expressed in the hippocampus and cortex (*63*). Overexpression of Tip110 in neurons induced cell death. More specifically, it was shown that the Tip110 and Fe65 interaction is necessary to induce neuronal apoptosis. Although it was already established that Tip110 possesses an RGD cell attachment motif that not only contributes to cellular adhesion but potentially to caspase-3-mediated apoptosis this is the first time that a specific role for Tip110 has been elucidated in neurons and the first time is has been described specifically as a pro-apoptotic and anti-survival protein (*32, 63*). These studies detail concisely the role for Tip110 in maintenance of stemness, pluripotency and survival of stem cells and provide additional insight into the mechanisms through which

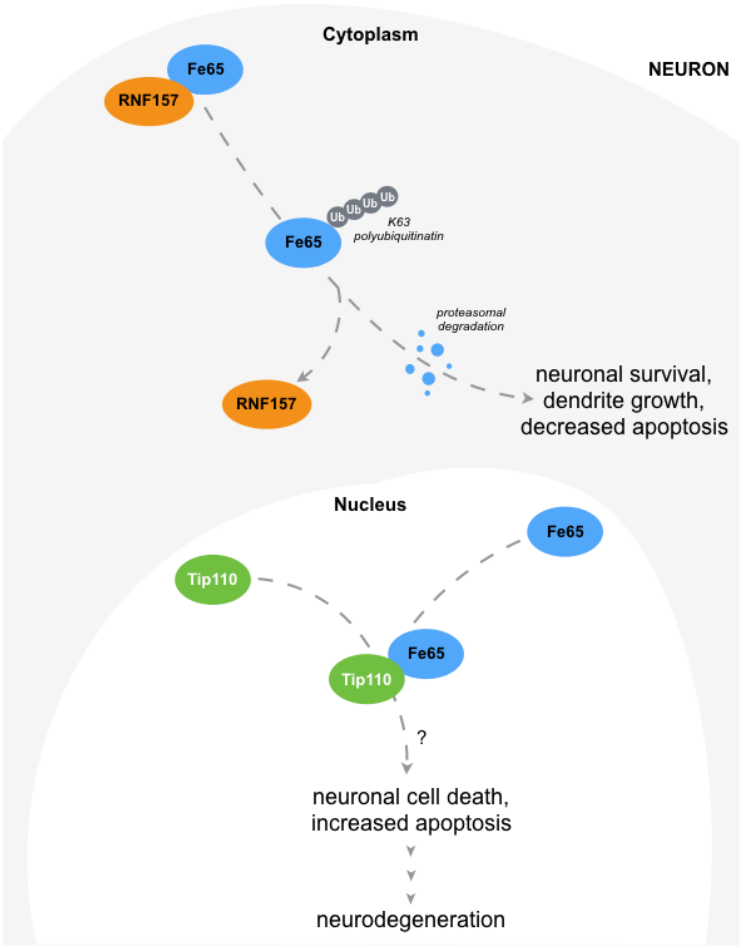
Cytoplasm
NEURON
Fe65
RNF157
Ub
Ub
Ub
Ub
K63
polyubiquitinatin
Fe65
proteasomal
degradation
RNF157
neuronal survival,
dendrite growth,
decreased apoptosis
Nucleus
Fe65
Tip110
Fe65
Tip110
?
neuronal cell death,
increased apoptosis
neurodegeneration

Figure 7. Tip110 in neuronal apoptosis. In neuronal tissues, E3 ligase RNF157 ubiquitinates Fe65 with K63 ubiquitin (Ub) linkages. This targets Fe65 for proteasomal degradation and promotes neuronal survival and growth. When Fe65 is not targeted to the proteasome, it can translocate to the nucleus where it can interact with Tip110. Co-expression of the two proteins in neurons promotes neuronal cell death. Adapted from Whitmill et al., *Life Sci*., 2016.

Tip110 might promotes cell growth and survival. Because the if the critical role Tip110 plays in these process it is not too farfetched to conjecture that it might also play these roles in the early pre-implantation portion of development of the mouse embryo thus leading to a disruption in the health and growth of the the early embryo that might contribute to its eventual demise.

Cancer Immunotherapy

Several peptides of the mouse and human Tip110 protein have been identified as tumor epitopes that can induce human leukocyte antigen (HLA)-Class I-A restricted and tumor-specific cytotoxic T lymphocytes (CTL) in the peripheral blood mononuclear cells (PBMC) of cancer patients but not healthy donors (*32*). This is because these peptides are expressed only in malignant and cancerous tissues and not in normal tissues. A great deal of research has been conducted to better understand the potential for these peptides to be used in specific immunotherapy for cancer patients of different HLA types such that one day custom vaccine therapy might be a plausible cancer treatment. The details of all the studies concerning Tip110 peptides in cancer immunotherapy can be found in the literature (*25-32, 36, 49, 64-80*) but will be briefly described below.

Peptides 109-118 and 315-323 of hTip110 and 316-324 of mTip110 (**Fig. 8**) can be recognized by a variety of stimulated HLA restricted CTL for subsequent induction of IFN-γ producing HLA-restricted and tumor-specific CTL derived from the PBMC of cancer patients (*26, 32*).

Tip110 peptides have been proven to induce HLA-restricted CTL recognition of bladder, breast, brain, cervical, colorectal, epithelial, gastric, musculoskeletal (i.e. osteosarcoma or malignant

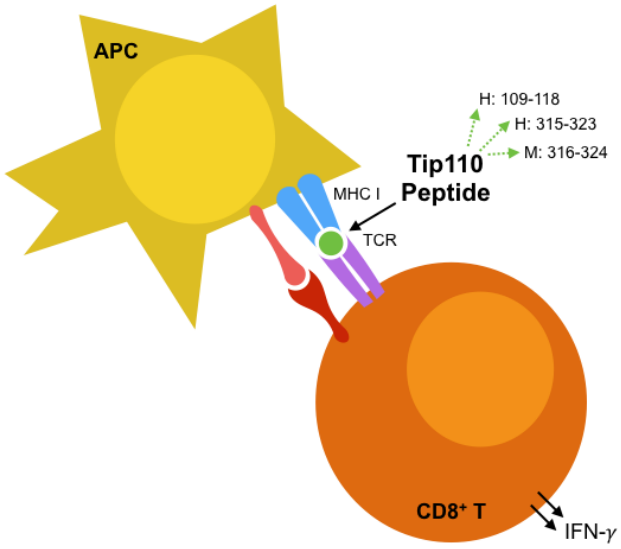
APC
H: 109-118
H: 315-323
M: 316-324
Tip110
Peptide
MHC I
TCR
CD8+ T
IFN-γ

Figure 8. Tip110 peptides presented on APC to $CD8^+$ T cells. Several different Tip110 peptides can be presented to antigen presentation cells for activation of $CD8^+$ T cells and subsequent interferon-ɣ release.

fibrous histiocytosis), oral, ovarian, pancreatic, prostate, and renal cancer types (*1, 28, 36, 65, 67, 69, 70, 72-80*). This would suggest that Tip110 peptides could potentially be used immunotherapeutically to treat a wide variety of cancers. Because A2 and A24 subtypes, and A3 supertypes can all be stimulated with Tip110 peptides it also broadens the diversity of patients that can potentially be treated with Tip110 tumor-epitope based therapies (*29*). The likelihood of expressing A2, A24, or A3 HLA types varies based on an individual's ethnic background but exploiting this property, would allow for a more personalized Tip110 peptide based immunotherapy for patients and would allow for physicians to know which ethnic groups are more or less likely to respond positively to a given treatment.

It is likely that hTip110 and mTip110 peptides are generated as byproducts of the protein entering the 26S proteasome. After degradation the peptides are processed and loaded on the HLA class I groove for presentation. Reasons for why Tip110, which is a self-antigen, gets presented to T cells is not apparent. It may be simply because the protein is highly expressed in cancer and as such, an immune response is mounted against cells and tissues with abundant Tip110 in an attempt to eliminate cancerous cells from propagating further.

There are also several studies that investigate the efficacy of Tip110 peptides as potential vaccine candidates especially when coupled with other immunotherapies such as peptide-pulsed dendritic cell-activated killer (PDAK) cells, OK-432 with oil- based adjuvants, and polyplex micelles coupled to better determine the best method to induce a clinical response in patients (*25, 27, 30, 31*). These studies prove that Tip110 peptides - when paired with the appropriate therapy - seem to have great potential to be used for immunotherapy based treatment of cancer. Such that,

coupling of the aforementioned therapies with preexisting treatments might induce a greater clinical response, promote tumor regression, or prevent cancer recurrence.

Role of Tip110 in Development

As previously mentioned, there are a few studies that suggest that Tip110 might have some roles in various aspects of development and embryogenesis. Tip110 is imperative for survival through embryonic development in *Drosophila melanogaster* – fruit fly (38) and in *Danio rerio* – zebrafish (13). Tip110 has also been shown to be important in the maintenance and survival of stem cells in human embryonic and hematopoietic stem cell populations (7, 22, 23) and in the stem cell populations of regenerating *Schmidtea mediterranea* (39).

In the fruit fly a homozygous loss of function mutation in *4f-rnp (*the *drosophila* homolog to Tip110) results in a lethal phenotype (*38, 81*). The *4f-rnp* gene codes for a 943 amino acid product that has only 16% similarity to Tip110. It does however have 3 HAT motifs, 1 RRM, and the CT domain. These particular conserved motifs are likely what contribute to a specific role for *4f-rnp* or Tip110 in development (*2, 26*). The *4f-rnp* is ubiquitously expressed in the cells of the fly throughout embryogenesis but is expressed highly in the central nervous system (CNS) (*81*). *Drosophila* larvae lacking *4f-rnp* do not hatch, as they die during the larval period, and have developmental abnormalities in the CNS where *4f-rnp* happens to be abundantly expressed. These and other data suggest a role for Tip110 in the CNS during embryogenesis (*38*).

Because of the highly conserved nature of the various domains of Tip110 it would be expected that the role of Tip110 as a recycling factor in spliceosome assembly would be conserved as well amongst different species. This was confirmed in studies that identified a zebrafish mutant with a genomic aberration causing an insertion in intron 15 of the zebrafish Tip110 ortholog (*13*). These mutant zebrafish, coined *earl grey (egy)* mutants, exhibit a reduction in the U4/U6 snRNP interaction, partial degradation of U4 snRNA, and a reduction in U6 snRNA levels (*13*). Using microarray analysis, it was found that a combined 76 genes with human homologs were up-regulated in 3- and 5-days post fertilization (dpf) zebrafish, with 50 genes being in common between both 3- and 5-dpf zebrafish. Fifty percent of the up-regulated genes were snRNP-related or splicing-related factors (*13*). The authors conclude that there is a network of co-regulated factors involved in the spliceosome cycle and in snRNP biogenesis such that in the absence of Tip110 there is induction of a compensatory mechanism that results in an increase in Tip110 related splicing factors to ameliorate the block in the spliceosome recycling phase and to allow more synthesis of tri-snRNP, stimulate snRNA transcription, and stabilize U6 snRNA/P assembly. Microarray analysis also revealed what genes were down-regulated in *egy* mutants. Many of these down-regulated genes had an organ-specific pattern of expression so that the aforementioned compensatory mechanism was not sufficient to reverse the observed organ-specific phenotypes thus causing a lethal phenotype in the affected zebrafish (*13*). Interestingly, when Tip110 is lost in zebrafish there are mechanisms in place to compensate for its inability to function in splicing but not for its other roles in cells and tissues. This would suggest that the zebrafish that perish as a result of Tip110 loss, do not die because of defective pre-mRNA splicing but likely because of loss of Tip110 as a contributor to regulation of gene expression and cell growth, survival, and differentiation.

Most recently, Tip110 has also been shown to be necessary for stem cell maintenance in planarians during tissue regeneration processes, which further supports the aforementioned notions (*39*). In this study microarray analysis revealed several genes, including Tip110, that were expressed in the regenerating and non-regenerating head and CNS tissues of planarians. Tip110, or *Smed-sart3* in planarians, was particularly found to be necessary for stem cell or neoblast maintenance during the regeneration process. In this study it was also shown that knockdown of *Smed-sart3* produced a phenotype with loss of stem cells. This type of loss was thought to affect blastemal formation, head regression, lesions, ventral curling, and lysis and contributed to a reduction in the number of mitotic cells present (*39*). This study shows yet another role for Tip110 in stem cell maintenance and survival and further implicates it in neurogenesis and development.

Our initial attempts to study Tip110 in mouse development revealed first that a constitutive transgenic mouse knockout of Tip110 could not be produced and second that intercrossing $Tip110^{+/-}$ mice with one another would produce an embryonic lethal phenotype. There are no other studies in the literature that investigate Tip110 loss in mice or in any other mammalian system. This information coupled to the aforementioned studies that clearly highlight roles for Tip110 in the development of several other species serve as the basis to further explore the role of Tip110 in development in order to better understand its biological roles in general and in mammalian embryogenesis.

Overview of Mouse Development

Pre-implantation Development

Embryonic development initiates with the fertilization of an egg or oocyte. More specifically, with the fertilization the pre-implantation portion of embryonic development commences. Pre-implantation development begins at fertilization and ends when the blastocyst begins to implant into the lining of the uterus. The processes that occur during pre-implantation development include: cleavage, compaction, and cavitation [**Fig. 9,** (*82, 83*)]. In these processes the embryo completes many successive rounds of division and eventually coalesces and forms a blastocyst consisting of two distinct cell types – the inner cell mass which consists of mouse embryonic stem cells and the trophoectoderm layer which consists of trophoblast stem cells. The cells of the inner cell mass will make up the body of the embryo, while the trophoectoderm cells will primarily make up the extraembryonic tissues of the embryo including the placenta.

Post-implantation Development

Implantation itself commences when the highly invasive trophoectoderm cells invade into the lining of the uterus and establish a place for the developing embryo to safely grow (*84*). Post-implantation development begins just after the embryo implants into the lining of the uterus and ends at birth when perinatal development initiates (**Fig. 10**). The major processes that occur during post-implantation development include: gastrulation and organogenesis (*85, 86*). In these processes the embryo divides and develops into the three distinct germ layers (ectoderm, endoderm, and mesoderm) and different organs begin developing.

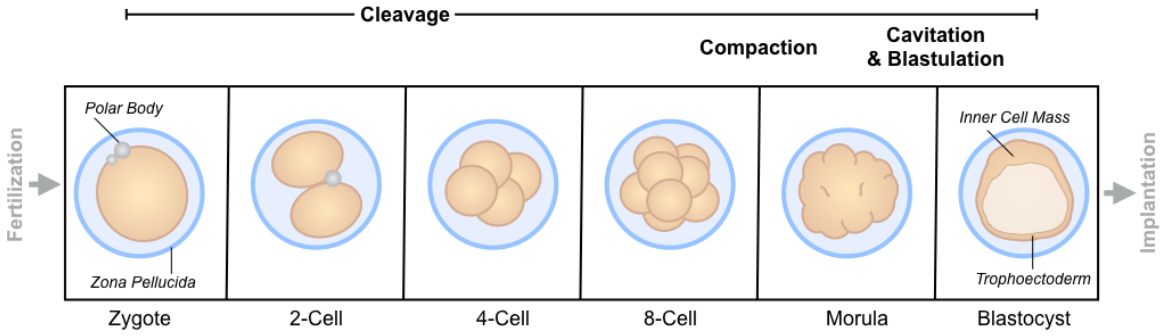
Cleavage
Compaction
Cavitation
& Blastulation
Fertilization
Polar Body
Zona Pellucida
Inner Cell Mass
Trophoectoderm
Implantation
Zygote
2-Cell
4-Cell
8-Cell
Morula
Blastocyst

Figure 9. Fertilization, cleavage and blastocyst formation. After fertilization, the one-cell zygote begins the cleavage process whereby multiple successive rounds of cell division take place to form the blastocyst. To initiate blastocyst formation, compaction processes initiate around the 8-16 cell stage to form a morula. The morula then undergoes cavitation and the blastocyst cavity is formed. The resulting blastocyst consists of two distinct cell types: the inner cell mass cell and trophoectoderm cells that form the body of the embryo and the extra embryonic tissues respectively.

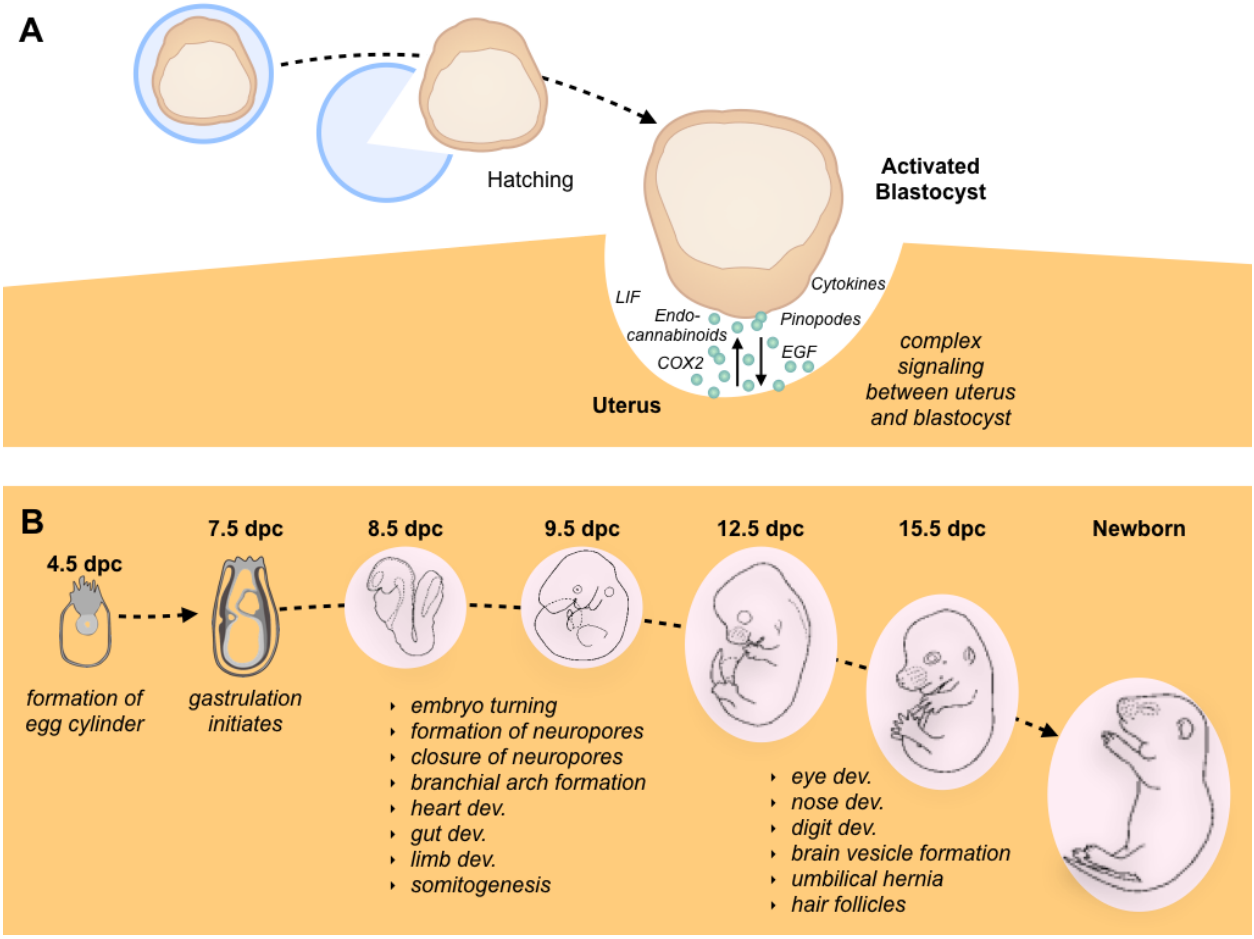
A
Hatching
Activated Blastocyst
LIF
Endo-cannabinoids
COX2
Cytokines
Pinopodes
EGF
Uterus
complex signaling between uterus and blastocyst
B
4.5 dpc
7.5 dpc
8.5 dpc
9.5 dpc
12.5 dpc
15.5 dpc
Newborn
formation of egg cylinder
gastrulation initiates
embryo turning
formation of neuropores
closure of neuropores
branchial arch formation
heart dev.
gut dev.
limb dev.
somitogenesis
eye dev.
nose dev.
digit dev.
brain vesicle formation
umbilical hernia
hair follicles

Figure 10. Implantation and embryogenesis. (**A**) Blastocysts hatch from their zona pellucida and position themselves to implant into the lining of the uterus. Complex signaling events occur to support reception of the blastocyst into the uterus. (**B**) After implantation embryonic development proceeds until birth. The embryo completes several critical developmental milestones, as shown, including gastrulation and organogenesis before birth.

mESC and hESC

Although mouse and human developmental processes are comparable on many levels, there are some fundamental differences between mouse and human ESC in terms of their requirements for maintenance of stemness. The data presented here are expectantly applicable to both mESC and hESC but the differences between the two must be noted. For example, hESC and mESC differ in their signaling requirements for maintenance of self-renewal and pluripotency. Most notably, hESC require FGF while mESC require LIF signaling. FGF and IGF signaling are associated with undifferentiated hESC, while LIF/Stat3 signaling is associated with undifferentiated mESC (*87, 88*). Other aspects of hESC and mESC self-renewal and cell fate determination processes such as Wnt, Tgf-β, Oct3/4, and Nanog mediated signaling are fairly similar but certainly not identical (*87*). In essence, both mESC and hESC rely on Oct4, Sox2, and Nanog but the specific role for each transcription factor and their respective targets have been shown to differ between species. In addition, alterations in the expression or regulation of these factors results in different cell fate outcomes between species (*87*).

Markers that identify the differentiation state of the stem cell have also been shown to differ between mESC and hESC grown in the same conditions (*88*). In addition, there are certain morphological characteristics that can be used to distinguish growth of mESC and hESC *in vitro* as well as species-specific differences in genes associated with cell cycle, apoptosis, and cytokines (*88*). Collectively, these findings show that mESC and hESC do possess clear differences in both their requirements for self-renewal and pluripotency in addition to differences in their morphology and gene expression profiles. So, although mESC and hESC are comparable

they are not identical and one must use caution when making comparisons or extrapolations between the two.

Embryonic Lethal Phenotypes

There are many genes that result in embryonic lethal phenotypes in humans and mammalian models (*89*). The time at which a gene induces a lethal phenotype says a lot about its function. Most often a peri-implantation death suggests that some defect might be occurring in basic molecular functions (i.e. metabolism, cell cycle, etc.), while death at the organogenesis stage or during fetal development on the other hand, often suggests a defect in vascular circulation, hematopoiesis, or chorioalloantoic placenta formation (*90, 91*).

Interestingly, there are not many genes that affect the ability to derive mESC populations from knockout cells. The genes that fall into this category are often categorized as essential or housekeeping genes. For example, genes like mTOR and Stat3 which are now well accepted genes contributing to signal transduction processes and ESC development have been shown to affect stem cell survival and embryonic development *in vivo* and *in vitro*. mTOR mutant mice cannot survive *in vivo* past 12.5 dpc (*92*). The embryos of $mTOR^{-/-}$ mice also have arrested and aberrant development at 5.5 dpc and a clear inability to establish mESC from $mTOR^{-/-}$ embryos *in vitro* (*92*). These data suggest a critical role for the protein in pre-implantation development and survival of the mouse. Stat3 deficient mice cannot survive beyond 6.5 or 7.5 dpc and have clear impairments in the *in vitro* survival and proliferation of blastocyst outgrowths (*93*). These data clearly show that genes that are critical for cell signaling and cell growth processes play

indispensable roles in development, embryogenesis and stem cell survival. Tip110, not unlike these proteins, should be grouped into the same category as proteins like mTOR and Stat3 as the findings reported here clearly describe an important role for Tip110 in these and other mammalian cellular and developmental processes.

Significance

Embryonic development is a complex and highly controlled process with a dynamic relationship existing between the proteins and signaling molecules that function in initiating, maintaining, and terminating the cellular events related to the proliferation, differentiation, and even death of the cells of the embryo. Proteins that when lost, result in an embryonic lethal phenotype are crucial to study to gain insights into the inner workings of the aforementioned processes. Because very little is known about the mechanisms through which Tip110 induces embryonic lethality in knockout mouse models, this particular subject is of most interest to us. This dissertation summarizes the results of our investigation into the role of Tip110 throughout pre-implantation and post-implantation embryonic development of the mouse. The ultimate goal of this project is to fully characterize the phenotype of our embryonic lethal Tip110 knockout mouse model and to eventually decipher what human disease states and/or congenital anomalies it may have direct ties to. The specific objective of this study is to determine the actual time point at which embryonic lethality occurs and the specific cellular processes in the pre- and post-implantation developing mouse embryo that are most adversely impacted by Tip110 knockout.

Hypothesis

We hypothesize that Tip110 is an important regulator of the cellular processes occurring throughout embryonic development and that it has essential roles during both pre- and post-implantation development of the mouse.

This hypothesis was evaluated in the following specific aims:

- *Specific Aim 1:* Determine the effect of Tip110 knockout on inner cell mass formation and trophoectoderm development of the blastocyst during pre-implantation development of the mouse embryo.
- *Specific Aim 2:* Identify the specific time point of lethality and the mechanism behind the defect that results in the lethality of Tip110 knockout embryos during post-implantation development using our previously established $Tip110^{+/-}$ mice.

CHAPTER II

MATERIALS AND METHODS

Mice, Breeding, and Animal Care

All animal experiments were conducted in compliance with protocols approved by the Institutional Animal Care and Use Committee of the University of North Texas Health Science Center, in accordance with guidelines of the National Institutes of Health. Mice and embryos used were either of the wild-type, Tip110 knockdown ($Tip110^{+/-}$), or Tip110 knockout ($Tip110^{-/-}$) genotype (**Fig. 11**). Each of these mice is of the C57BL/6 background and were derived from many rounds of cross-breeding. Wild-type and $Tip110^{+/-}$ adult mice were stably generated while $Tip110^{-/-}$ mice could only be derived at the embryonic stage from a successful mating between two $Tip110^{+/-}$ mice.

Disruption of the Tip110 Gene

To disrupt the Tip110 gene in mice, the genomic loci containing exons 9-12, 13-18, and 19 of Tip110 were obtained by high-fidelity genomic DNA PCR and cloned into the pEasyFlox vector (*93*) over several successive steps. The pEasyFlox vector contains a neomycin resistance sequence (neo) and 3 *loxP* sites to allow for conditional gene targeting under the tri-loxP strategy. The newly generated Tip110 transgenic vector was then used to generate transgenic mice by the Transgenic and Knockout Core at Indiana University School of Medicine. These

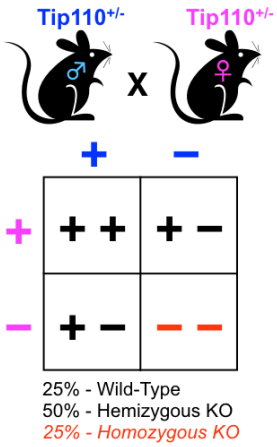
Tip110+/-
Tip110+/-
x
+
−
+
−
+ +
+ −
+ −
− −
25% - Wild-Type
50% - Hemizygous KO
25% - Homozygous KO

Figure 11. Breeding scheme and predicted Tip110$^{+/-}$ intercross offspring outcomes. To obtain Tip110$^{-/-}$ embryos, Tip110$^{+/-}$ mice are mated around 6-8 weeks of age for natural mating, while females can be as young as 3-4 weeks of age when superovulated. The resulting offspring produced from this intercross are 25% likely to be wild-type (Tip110$^{+/+}$), 50% likely to be hemizygous knockouts or knockdown mice (Tip110$^{+/-}$), and 25% likely to be homozygous knockouts (Tip110$^{-/-}$).

mice were back-crossed at least 8 generations to a C57Bl/6 strain background. The genotypes of these mice were confirmed with genomic DNA PCR as previously described (*23*).

Mating Mice

Superovulation

Superovulation was performed on sexually immature (3-4 weeks old) or sexually mature (6-8 weeks old) Tip110$^{+/-}$ female mice, as described [(*94*), **Fig. 12A,** Top]. Lyophilized gonadotropin, pregnant mare's serum (PMS-G; Sigma, G4527 or National Hormone and Peptide Program at UCLA) and human chorionic gonadotropin (hCG; Sigma, C8554) were first dissolved in sterile-filtered 0.9% NaCl solution (pH 7.0) and stored in aliquots at -20°C (short term) or -80°C (long term) until use. Superovulation was initiated by administering a 0.1 ml intraperitoneal (i.p.) injection of PMS-G at a working concentration of 50 IU/ml around 11:00 AM or 12:00 PM to each experimental female. Injected females were then housed together. Superovulation was completed by administering a 0.1 ml i.p. injection of hCG at a working concentration of 50 IU/ml, 46-48 hrs. after the initial PMS-G injection. Immediately after the hCG injections female mice were separated and housed in individual cages with one stud Tip110$^{+/-}$ male mouse. The next morning, males were removed from each cage and each female was checked for the presence of a vaginal copulatory plug. Although the presence of a plug suggests strongly that the female mouse is pregnant, embryos were often isolated from females with no visible plug after superovulation. Because of this each superovulated female was sacrificed for embryo isolation regardless of the presence of a plug as a precaution. The day after mating was considered 0.5 days post coitum (dpc) because we presume that the mice will mate around midnight. 2-cell

embryos were collected at 1.5 dpc while blastocysts were collected at 3.5 dpc as detailed in **Fig 12B** (Bottom).

Natural Mating

In situations where superovulation was either impractical or unnecessary, natural matings were performed (**Fig. 12A,** Bottom). For most natural matings, the Tip110$^{+/-}$ female mice used were between 6-weeks and 9-weeks old to increase the likelihood of a successful mating. To initiate mating, at ~5:00 PM, 1-4 female mice were housed together with a single stud Tip110$^{+/-}$ male mouse overnight. The next morning, females were removed and checked for copulatory plugs. Females were only sacrificed for embryo collection if a copulatory plug was present. The day after mating was considered 0.5 days post coitum. 2-cell embryos were collected at 1.5 dpc while blastocysts were collected at 3.5 dpc. Post-implantation embryos were collected between 5.5 dpc and 15.5 dpc as detailed in **Fig. 12B** (Bottom).

In Vitro **Techniques**

Embryo Isolation and Culture

2-cell embryos were isolated from the oviducts of plugged females at 1.5 dpc as described (*95*). Embryos were collected in M2 media (Sigma, M7167) and subsequently washed through three 200 µl drops of M2 media surrounded by ovoil (Vitrolife, 10029) before being transferred to potassium simplex optimized media with amino acids (KSOM+AA; Caisson Labs, IVL04) in a 96-well culture dish. Blastocysts were flushed from the uterine horns of plugged females at 3.5 dpc as described (*95*). Blastocysts were collected in M2 media and washed through three 200 µl

A

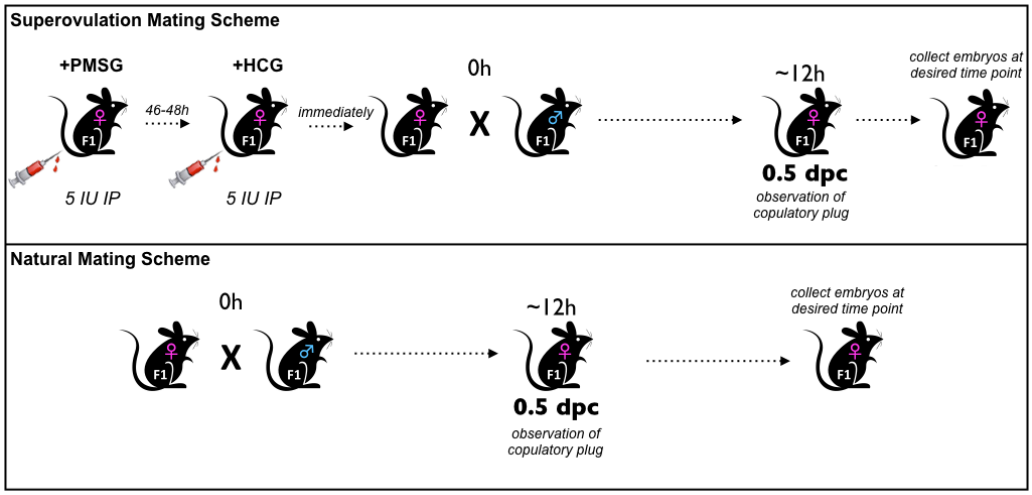
Superovulation Mating Scheme
+PMSG
+HCG
0h
~12h
collect embryos at desired time point
46-48h
immediately
5 IU IP
5 IU IP
0.5 dpc
observation of copulatory plug
Natural Mating Scheme
0h
~12h
collect embryos at desired time point
0.5 dpc
observation of copulatory plug

B

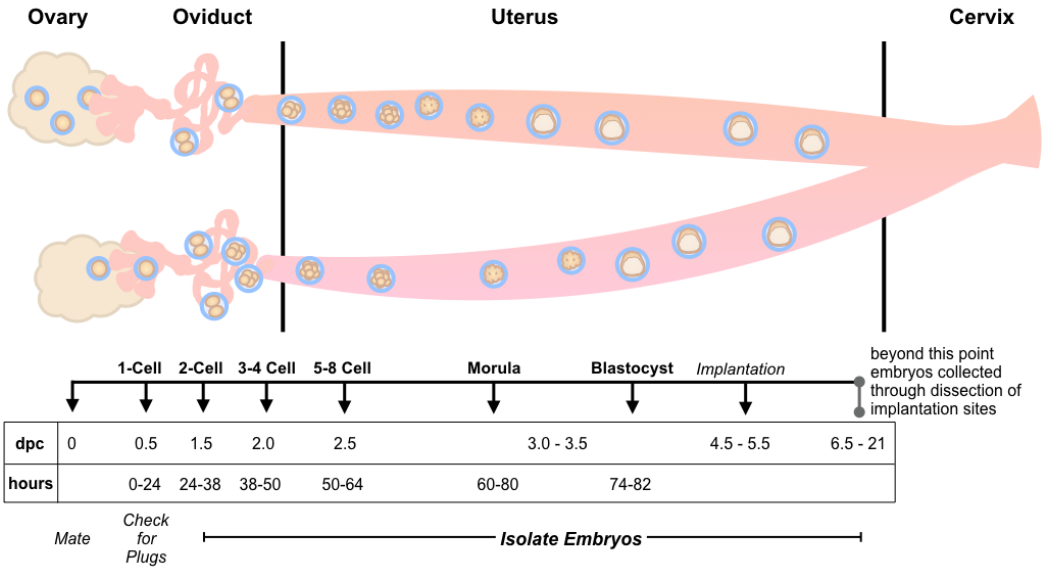
Ovary
Oviduct
Uterus
Cervix
1-Cell
2-Cell
3-4 Cell
5-8 Cell
Morula
Blastocyst
Implantation
beyond this point embryos collected through dissection of implantation sites
dpc
0
0.5
1.5
2.0
2.5
3.0 - 3.5
4.5 - 5.5
6.5 - 21
hours
0-24
24-38
38-50
50-64
60-80
74-82
Mate
Check for Plugs
Isolate Embryos

Figure 12. Timing of mating and embryo collections. To isolate embryos at different time points timed breeding must be performed with the assistance of hormones (**A**, Top) or without (**A**, Bottom). For hormone assisted or superovulation matings 3-8 week old female mice were first injected with PMSG (5 IU), then HCG (5 IU, ~46-48 hrs. later). Mice were immediately mated and checked for plugs the next day. For natural matings ~8 week old mice were mated in the evening, checked for plugs and embryos and collected from a given section of the uterus. (**B**) Embryos can be found in various parts of the uterus early after mating. Embryos that have not yet implanted can be flushed from these different locations using culture media (KSOM, M2, or KOSR-ESCM) or PBS. 1-cell embryos can be found in the ampulla, 2-cell embryos in the infundibulum of the oviducts or the (upper oviduct), 3-4 cell embryos in the mid-lower oviduct, 5-8 cell embryos in the lower oviduct or uterus, and morula or blastocysts in the uterus. Embryos beyond 3.5 dpc are difficult to dissect as they are too small and have likely initiated implantation processes, but could be found in the early forming implantation site. Embryos beyond 6.5 dpc can be found growing in well-defined implantation sites and must be manually dissected.

drops of M2 media surrounded by ovoil before being transferred to knock-out serum replacement embryonic stem cell media (KOSR-ESCM) (*96*) in a 0.1% gelatin-coated (Sigma, G9391) 96-well culture dish. It is important to note that all media used for embryo and stem cell culture was equilibrated to 37°C, 5% CO_2 for at least 18 hrs. before introducing embryos or cells to culture.

Blastocyst-Derived Outgrowth and Mouse Embryonic Stem Cell Culture

Outgrowths were derived from 3.5 dpc blastocysts (collected and cultured as previously described) that hatched from the zona pellucida and attached to the culture dish *in vitro*. These so-called "blastocyst-derived outgrowths" were also cultured in KOSR-ESCM prior to disaggregation or RNA isolation as described (*96*). Typically, these outgrowths were cultured no longer than 9-11 days as the more dense they became the less stemness they possessed. To derive mouse embryonic stem cell populations, blastocyst-derived outgrowths were enzymatically disaggregated in a trypsin solution (Sigma, T4049). After disaggregation the cells were cultured in fetal bovine serum embryonic stem cell media (FBS-ESCM) to promote formation of embryonic stem cell colonies.

Embryoid Body and Organoid Culture

Embryoid bodies (EB) were derived from disaggregated mESC colonies and cultured in mouse embryonic stem cell embryoid body (mESC EB) media which consists of the same ingredients as the KOSR-ESCM media except no LIF was included (*97*). Culture of EB in mESC EB media with 10% FBS was used to promote their differentiation over a 2-week period. To initiate generation of cerebral organoids, EB were first cultured in neural induction media then transferred to Matrigel droplets as described in the literature (*98*). The inhibitors used for culture

in these experiments were the MEK inhibitor PD0325901 (s1036; Selleckchem) and the GSK-3 inhibitor CHIR99021 (S2924; Selleckchem) in lieu of SB431542 and DKK1. Organoid culture was carried out on an orbital shaker rather than a spinning bioreactor for 40 days.

Genotyping

Embryos and Outgrowths

Pre-implantation embryos (2-cell embryos and blastocysts) were lysed at 55°C for 5 hrs. in 20 µl of embryo lysis buffer (10 mM Tris, pH 8.4, 50 mM KCl, 2 mM $MgCl_2$, 0.45% NP-40, 0.45% Tween-20, and 180 µg/ml proteinase K (Sigma, P-6566; added immediately before use) (*99*). Embryo lysis was followed by incubation at 95°C for 10 minutes for proteinase K inactivation. 1-5 µl of lysate was used for PCR. PCR analysis to detect the mutated Tip110 allele lacking exons 12-18 but containing the neomycin cassette "neo" was accomplished with the following primers: 12A 5'-CCT CAC TGT GCT GCA AGC TCT G-3' and NEO 5'-CGT GCA ATC CAT CTT GTT CAA TGG CCG ATC CCA T-3' which gives rise to an 850 bp product when neo is present and the absence of a product when neo is not present. Primers 12A 5'-CCT CAC TGT GCT GCA AGC TCT G-3' and 12B 5'-GAA TCA TGG CTA TAG GAG CCC CCC-3' were used to detect the wild-type Tip110 allele lacking neo and containing exons 12-18. Primers 12A and 12B gives rise to a 516 bp product. PCR analysis to detect the presence of exon 12 in the frameshift mutated Tip110 allele was accomplished with 12A and 12B primers which gives rise to a 516 bp product when exon 12 is present (wild-type) and a 350 bp product when exon 12 is absent ($Tip110^{+/-}$ or $Tip110^{-/-}$).

Blastocyst-derived outgrowths were genotyped following RNA isolation via the RNeasy Micro Kit (Qiagen, 74004) and subsequent cDNA generation via the Titan One Tube RT-PCR System (Roche, 11855476001). cDNA obtained from blastocyst-derived outgrowths was genotyped using the following primers to amplify a region between exons 9 and 14: 5'-CCTTCGAGAACGCTCTGAGTG-3' and 5'- CAT TCT CTG CTC ATT CAC ACG-3' followed by a nested PCR using primers 5'- CCA GGC CAC TGA CTA TGT GGA-3' and 5'-GCT AGA TCC CAA TCT TCT AAG G-3'. Primers 5'-CCT TCG AGA ACG CTC TGAGTG-3' and 5'- CAT TCT CTG CTC ATT CAC ACG-3' produce a 540 bp band when exon 12 is present and a 430 bp band when exon 12 is absent while 5'- CCA GGC CAC TGA CTA TGT GGA-3' and 5'-GCT AGA TCC CAA TCT TCT AAG G-3' produce a 459 bp band when exon 12 is present and a 349 bp band when exon 12 is absent.

Post-implantation Embryos and Pups

Post-implantation embryos were genotyped using the Genomic DNA Purification Kit (Promega, A1120) if an ample amount of embryonic yolk sac or embryonic tissue could be harvested. If only a small amount of either tissue was isolated embryos were genotyped using embryo lysis buffer and simple PCR as described above. Pups were genotyped using the Genomic DNA Purification Kit as well, where either a small piece of tail or ear tissue was used for this purpose. To lyse the tail or ear tissue the sample was incubated at 55°C for 3 hours or overnight in a solution of 500 μl nuclei lysis solution, 120 μl of 0.5M EDTA, and 17.5 μl of proteinase K in a 1.5 ml Eppendorf tube. When the sample was completely digested it was cooled to room temperature and 200 μl of protein precipitation solution was added. After a 20 second vortex and 5 minutes on ice the sample was centrifuged for 5 minutes at max speed. The supernatant

containing the DNA was transferred to a new tube containing 600 ul of room temperature isopropanol. Gentle inversion of the tube induces precipitation of the DNA which was spun down at max speed for 1 minute. The DNA pellet was washed with 600 μl of 70% ethanol and spun down again at max speed for 1 minute. The 70% ethanol was then removed either by inversion or aspiration. The pellet was then allowed to dry for 10-15 minutes before being resuspended in 100 μl dH_2O.

RNA Isolation and qRT-PCR RNA Quantification

RNA was isolated from blastocyst-derived outgrowths using the RNeasy Micro Kit (Qiagen, 74004). RNA was typically eluted twice in 14 μl before storage at -80°C. To quantify RNA from such a small sample size the VeriQuest SYBR Green One-Step qRT-PCR Assay (Affymetrix, 75705) was used to estimate the RNA concentration of each sample using provided total RNA from HeLa cells to generate a standard curve and 18S rRNA primers for each sample.

Western Blotting

Western analysis was performed by washing cells in cold PBS and lysing in lysis buffer (50 mM Tris HCl (pH 8.0), 280 mM NaCl, 0.5% NP-40, 0.2 mM EDTA (pH 8.0), 2 mM EGTA (pH 8.0), 10% glycerol) with protease inhibitor freshly added for 20 minutes on ice. The cell lysate was cleared of debris by spinning at 14,000 rpm for 10 minutes. After SDS-PAGE, transfer to a nitrocellulose membrane, and blocking in 5% milk in Tris-Buffered Saline with Tween-20 (TBST) for 30 minutes. Primary antibody was added for either 2 hours or overnight. The

antibodies used were β-Actin (1:3000; A1978, Sigma), Brachyury (1:500; AF2085; R&D Systems), GFAP (C-19, sc-6170; Santa Cruz Biotechnology, Inc.), Egr1 (588, sc-110; Santa Cruz Biotechnology, Inc.), Nanog (1:500; H-155, sc-33759; Santa Cruz Biotechnology, Inc.), Oct4 (1:500; C-10, sc-5279; Santa Cruz Biotechnology, Inc.), Pax3 (1:500; MAB2457; R&D Systems), PCNA (PC-10, sc-56; Santa Cruz Biotechnology, Inc.), Sox2 (1:500; H-65, sc-20088; Santa Cruz Biotechnology, Inc.), Sox17 (1:500; AF1924; R&D Systems), Tuj1 (1:1000; 801201; Biolegend, San Diego, CA), Vimentin (ab7783-500, abcam; Cambridge, MA), and Tip110 [1:200; (*23*)].

Immunofluorescence Staining

Blastocysts were flushed from uterine horns at 3.5 dpc in PBS and subsequently fixed in 4% paraformaldehyde, pH 6.9 in PBS for 30 min at room temperature. After fixation blastocysts were washed 3 times in PBS and permeabilized in a solution of 0.3% Triton-X-100 in PBS for 20 min at room temperature. They were then washed again 3 times in PBS and blocked in a solution of 3% BSA and 0.05% tween in PBS overnight at 4°C. The next day the embryos were washed in PBS and incubated overnight at 4°C in a humidified chamber in primary antibody against Tip110 in 3% BSA in PBS (1:5000) or Oct4 in 3% BSA in PBS (1:500). A no antibody control and pre-bleeding control were used as well. The next day, blastocysts were washed 3 times in PBS and incubated in secondary antibody in 3% BSA in PBS (1:1000) in a humidified chamber for 2 hr. They were then washed again 3 times in PBS and incubated in a DAPI (0.5 mg/ml, 1:250) solution for 10 min at room temperature. Embryos were then washed 3 times in PBS before being mounted on coverslips in a 1:1 mixture of PBS and Fluoromount G solution (0100-

01, Southern Biotech). They were photographed using a Zeiss LSM 510 confocal microscope after allowing the blastocysts to settle for 5-10 min. It is important to note that the blastocysts were mounted directly onto #1½ coverslips (72204-04; Electron Microscopy Sciences) with no additional cover, rather than slides to avoid crushing the blastocyst and disturbing its hollow ball-like morphology.

Whole-Mount Immunohistochemistry Staining

Whole mount-immunohistochemistry (WM-IHC) was performed following a protocol established by the Graef Lab at Stanford University (*100*). Embryos were dissected from their implantation sites at 8.5 and 9.5 dpc. Each embryo was fixed in 4% paraformaldehyde (pH 6.9) at 4°C overnight. The next day embryos were washed twice in PBS for 10 min at room temperature. To dehydrate the embryos, they were washed for 15 min each in 25% methanol in PBS, 50% methanol in dH_2O, 80% methanol in dH_2O, and 100% methanol. Next the embryos were bleached in 5% H_2O_2 for 4-5 hrs. at room temperature. After dehydration and bleaching the embryos were rinsed briefly in methanol twice before being rehydrated. To rehydrate the embryos, they were placed in 80% methanol in PBS, 50% methanol in PBS, 25% methanol in PBS, and PBS for 15 min each at room temperature. To block non-specific antibody binding, the embryos were incubated in 3% milk and 0.1% Triton X-100 in PBS twice (PBSMT) for one hour at room temperature. The primary antibody against Tip110 (rabbit-α-hTip110) was diluted 1:1000 in PBSMT and incubated with the embryos at 4°C for 48 hrs. (no antibody control and pre-bleeding control were used as well). After this incubation embryos were washed five times in PBSMT at 4°C for one hour each wash. The secondary antibody (anti-rabbit IgG HRP) was

diluted 1:500 in PBSMT and incubated with the embryos at 4°C overnight. After this incubation embryos were washed five times in PBSMT at 4°C for one hour each wash. Next the embryos were washed in 0.1% Triton X-100 and 0.2% BSA in PBS (PBT) for 20 min at room temperature. After this wash the embryos were incubated for 20 min at room temperature in a freshly prepared and well dissolved solution of .3 mg/ml 3,3'-diaminobenzidine (DAB; D8001, Sigma) and 5 mg/ml nickel (II) chloride (NiCl; 339350, Sigma) in PBT. After 20 min 1 μl of 30% H_2O_2 was added to the 1 ml solution of DAB-NiCl-PBT to make a solution of 0.03% H_2O_2 in DAB-NiCl-PBT. Color was allowed to develop for 5-7 min before washing with 0.1% Triton X-100 in PBS. Stained embryos were post-fixed in 2% paraformaldehyde in PBS overnight at 4°C. The next day embryos were photographed in PBS using a Nikon SMZ745T stereoscopic microscope with a DsFiJ camera attachment. Each step was carried out in 1.5 ml Eppendorf tubes on a shaker either at room temperature or at 4°C.

Microarray Analysis

Total RNA was isolated and pooled from up to three wild-type and Tip110$^{-/-}$ blastocyst-derived outgrowths. After quantification samples were processed at the UT Southwestern Microarray Core (Dallas, TX) using the GeneChip Whole Transcriptome Pico Kit (902622; Affymetrix) and the GeneChip Mouse Transcriptome Pico Assay 1.0 (902663; Affymetrix). The array output was analyzed using the Expression Console (EC) and Transcriptome Analysis Console (TAC) software from Affymetrix, the PANTHER classification system (*101*), and Wiki Pathways Beta (*102*). Array data were representative of technical triplicates obtained by pooling RNA from six

outgrowths into two separate groups of three for each genotype. 150 pg of RNA was used for microarray analysis.

Statistical Analysis

Values were mean ± S.E.M. from triplicate experiments. Comparisons were made using wild-type mice as the control in a two-tailed Student's t-test unless stated otherwise. A p-value of ≤ 0.05 was considered statistically significant (*). All data represent three or more independently repeated experiments.

CHAPTER III

TIP110 IN THE POST-IMPLANTATION DEVELOPMENT OF THE MOUSE

Rationale

Because preliminary experiments have revealed that Tip110 constitutive knockout mice cannot be derived (unpublished data) and that Tip110 loss results in a non-viable phenotype in transgenic mice, a closer look into when and how these mice come to their demise is necessary to understand how Tip110 induces embryonic lethality. To this end, embryos from $Tip110^{+/-}$ intercrosses were collected at various points during their post-implantation development to first determine when they die *in utero* and what specific phenotype they possess. In addition, the expression of Tip110 in the post-implantation embryo was analyzed to determine where it may be highly expressed during embryogenesis. Together these data will answer when, why, and how Tip110 loss results in an embryonic lethal phenotype in mice.

Results

Generation of Tip110-Deficient Mice

To generate Tip110-deficient mice, a targeting vector was designed and constructed using a tri-flox transgenic strategy based on the Tip110 genomic locus (**Fig. 13A**). In this design exons 12-18 of the Tip110 gene are to be deleted. These exons code for the nuclear localization signals, the RNA recognition motifs, and the LSm interaction motif of Tip110 (*23, 49*), which are

essential for a functional Tip110 protein. Tip110 tri-flox transgenic founder mice were generated and crossbred with EIIa-Cre transgenic mice, which have *cre* expression under the adenovirus EIIa promoter to express the Cre recombinase as early as the zygote stage (*103*). Such breeding would result in complete Cre recombinase-mediated excision of the loxP flanked gene segment (*103-105*) and desegregation of transgenic mice carrying a flox (exon 12-18) conditional knockout (CK) allele, a flox (neo) knockout allele, or a exon 12-18-deleted and neo-deleted knockout allele [flox (Δneo)] (**Fig. 13A**). Interestingly, subsequent mating and genotyping analysis of flox (exon 12-18) mice revealed that homozygous Tip110-CK mice could not be produced even after many rounds of mating and that only Tip110 transgenic mice with a single floxed allele could ever be produced. Further investigation revealed that an error was introduced during construction of the targeting vector so that exon 12 of the Tip110 gene was inadvertently deleted. This deletion resulted in a frameshift mutation in the Tip110 gene and introduced the stop codon, TGA, early on in exon 13 of Tip110 resulting in mice carrying a flox (exon 12-18) conditional knockout (CK) allele, a flox (neo) knockout allele, or a flox (Δneo) allele all being essentially the same phenotype, Tip110 deleted. That is, mice carrying one Tip110 wild-type allele and any one of the aforementioned Tip110 alleles are effectively $Tip110^{+/-}$ mice and as such will be referred to from here on as $Tip110^{+/-}$ mice. They can be distinguished though by their genotypes as noted in **Fig. 13B** where the wild-type allele presents as a 516 bp band and the knockdown allele presents as an 850 bp band for flox (neo) mice and in **Fig. 13C** where the wild-type allele presents as a 516 bp band and the "knockdown" allele with a frameshift mutation presents as a 350 bp band for flox (exon 12-18) mice. Flox (Δneo) mice were not used in these experiments.

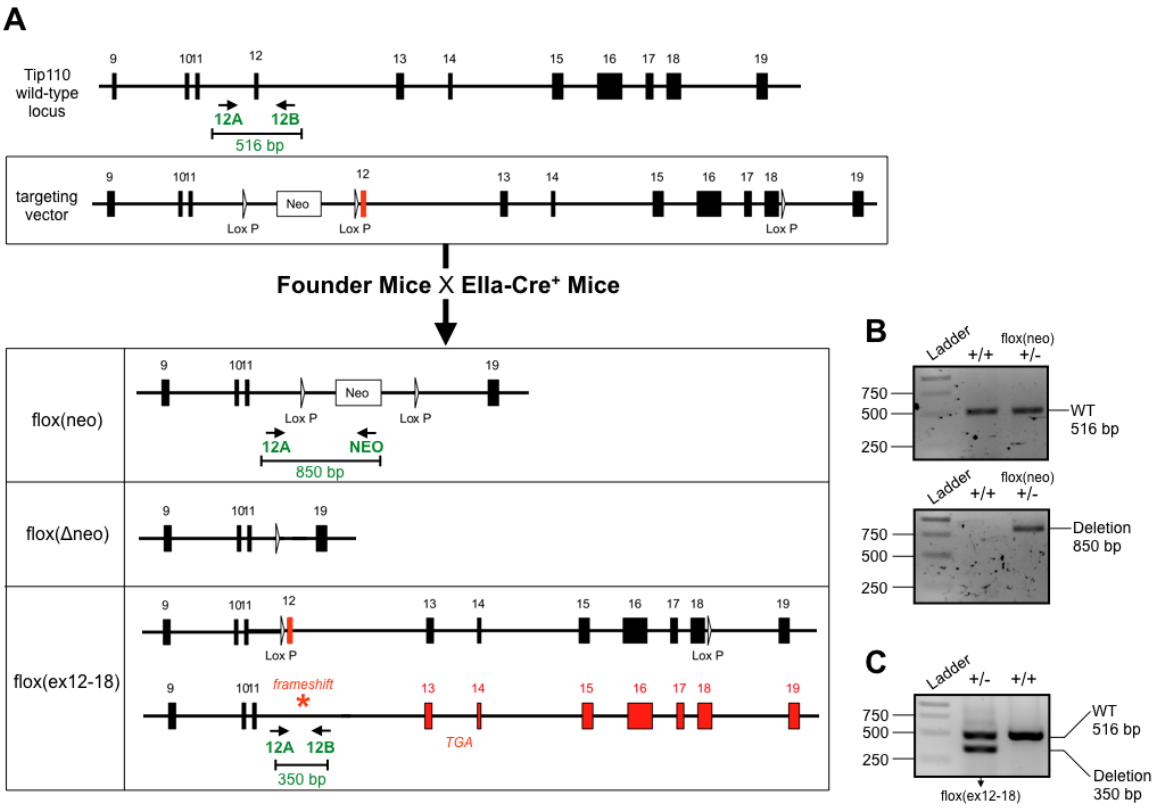
A
Tip110 wild-type locus
9
10
11
12
13
14
15
16
17
18
19
12A
12B
516 bp
targeting vector
Neo
Lox P
Lox P
Lox P
Founder Mice X Ella-Cre+ Mice
flox(neo)
12A
NEO
850 bp
flox(Δneo)
flox(ex12-18)
frameshift
TGA
12A
12B
350 bp
B
Ladder
+/+
flox(neo)
+/-
750
500
250
WT
516 bp
Deletion
850 bp
C
+/-
+/+
WT
516 bp
Deletion
350 bp
flox(ex12-18)

Figure 13. Tip110 targeting vector and segregation of the transgenes. (**A**) A tri-flox targeting vector with loxP sites flanking a neomycin resistance cassette (neo) and exons 12-18 of Tip110 was introduced into the genomic Tip110 locus for selection of ES cells. After selection and generation of tri-floxed transgenic mice, mating with EIIa-Cre^{+} mice was performed to produce Tip110 knockdown mice with a flox (neo) allele where exons 12-18 were deleted or a flox (Δneo) allele where neo and exons 12-18 are deleted. A flox (exon 12-18) allele was also generated where neo is deleted and exons 12-18 remain floxed for conditional targeting. In the lower-most panel of A, the flox (exon 12-18) allele details where the inadvertent deletion of exon 12 – which resulted in the frameshift-mediated introduction of a stop codon early in exon 13 – occurred. (**B**) Genotyping of mouse tail genomic DNA from flox (neo) mice was performed by PCR using three primers. PCR amplification with primers 12A and 12B produced a 516 bp DNA fragment for the WT Tip110 allele, while PCR amplification with primers 12A and NEO produced an 850 bp fragment for the excised allele. (**C**) Genotyping of mouse tail genomic DNA from flox (exon 12-18) mice was performed by PCR using one primer pair. PCR amplification with primers 12A and 12B produced a 516 bp DNA fragment for the WT Tip110 allele (upper band) while the same set of primers produced a 350 bp fragment for the exon 12-deleted allele (lower band).

Table 1. Genotyping analysis of newborn pups from Tip110+/- intercrosses

	+/+	+/-	-/-	Total # of pups
$Tip110^{Flox/+}$	51 (35.7%)	92 (64.3%)	0 (0%)	143
Tip110-KD	31 (36.9%)	53 (63.1%)	0 (0%)	84
Total	82 (36.3%)	145 (63.7%)	0 (0%)	227

Tip110 Affects Embryo Development and Post-Implantation Survival

To generate Tip110$^{-/-}$ mice, Tip110$^{+/-}$ mice were intercrossed. Genotyping analysis of pups from Tip110$^{+/-}$ intercrosses revealed that no Tip110$^{-/-}$ mice were ever able to survive past birth. Typical Mendelian inheritance ratios predict that Tip110$^{+/-}$ intercrosses would produce 25% wild-type offspring, 50% Tip110$^{+/-}$ offspring, and 25% Tip110$^{-/-}$ offspring. However, in genotyping over 200 pups from such a cross the ratios of offspring were ~36% wild-type and ~64% Tip110$^{+/-}$ with no pups at 6-12 days post-natal development ever being genotyped as Tip110$^{-/-}$ (**Table 1**). This suggests that homozygous loss of Tip110 causes embryonic lethality in mice.

To investigate when Tip110$^{-/-}$ mouse embryos failed to develop *in vivo,* mouse embryo implantation sites from Tip110$^{+/-}$ intercrosses were analyzed from embryos as early as 5.5 dpc. There were no overt differences between the gross morphology of embryo implantation sites between 5.5 and 7.5 dpc (data not shown). This is due in part to the small size of the embryo relative to the implantation site and suggests that embryos were developmentally comparable at these stages. At 8.5 dpc implantation sites between wild-type, Tip110$^{+/-}$, and Tip110$^{-/-}$ embryos were fairly comparable (**Fig. 14A**) but dissection of each embryo out of the uterus and careful analysis of the embryo growing in the decidua revealed that the majority tended to develop normally (**Fig. 14B**), that some embryos were underdeveloped (**Fig. 14C**), and that others were completely resorbed (**Fig. 14D**). At 9.5 dpc implantation sites between wild-type, Tip110$^{+/-}$, and Tip110$^{-/-}$ embryos revealed that some implantation sites were smaller and less vascularized than their counterparts but otherwise appear to be morphologically comparable (**Fig. 14E**). Further dissection of each 9.5 dpc embryo out of the uterus and careful analysis of each embryo growing in the decidua revealed two distinct phenotypes: one normal (**Fig. 14F**) and the other a

completely resorbed embryo (**Fig. 14G**). Analysis of embryo implantation sites at 10.5 dpc to 15.5 dpc revealed that Tip110$^{-/-}$ embryos were completely resorbed with distinctly smaller, underdeveloped, and less vascularized implantation sites compared to their wild-type and Tip110$^{+/-}$ counterparts (data not shown).

Analysis of whole embryos at 9.5 dpc revealed that compared to their wild-type (**Fig. 14H-K**) and Tip110$^{+/-}$ (data not shown) counterparts, Tip110$^{-/-}$ embryos possessed clear hallmarks of 9.5 dpc development such as embryo turning, heart formation, and somitogenesis but each was poor and incomplete (**Fig. 14L-O**). Although, Tip110$^{-/-}$ embryos were able to survive into 9.5 dpc development, they persisted in a severely underdeveloped and developmentally delayed state. These underdeveloped embryos have clear lack of S-shaped looping of the heart, less vascularization of the yolk sac, incomplete turning, poor somitogenesis and lack of proper development and closure of both the anterior and posterior neuropores; in addition, these embryos are significantly smaller in size that their littermates (**Fig. 14**, arrowheads).

Taken together these data suggest that embryos that lack Tip110 expression can survive through pre-implantation development and implantation but will perish shortly after post-implantation development initiates such that after 8.5 dpc or 9.5 dpc embryos lacking Tip110 are underdeveloped or more commonly completely resorbed and absent in any detectable fashion from the decidua and other extraembryonic tissues. Embryos that do survive into 9.5 dpc development are developmentally delayed and have a very distinct phenotype with some of the hallmarks of 9.5 dpc development being absent or poor. In addition, we confirmed that no Tip110$^{-/-}$ mice could survive to birth or post-natal development as they all perished *in utero*.

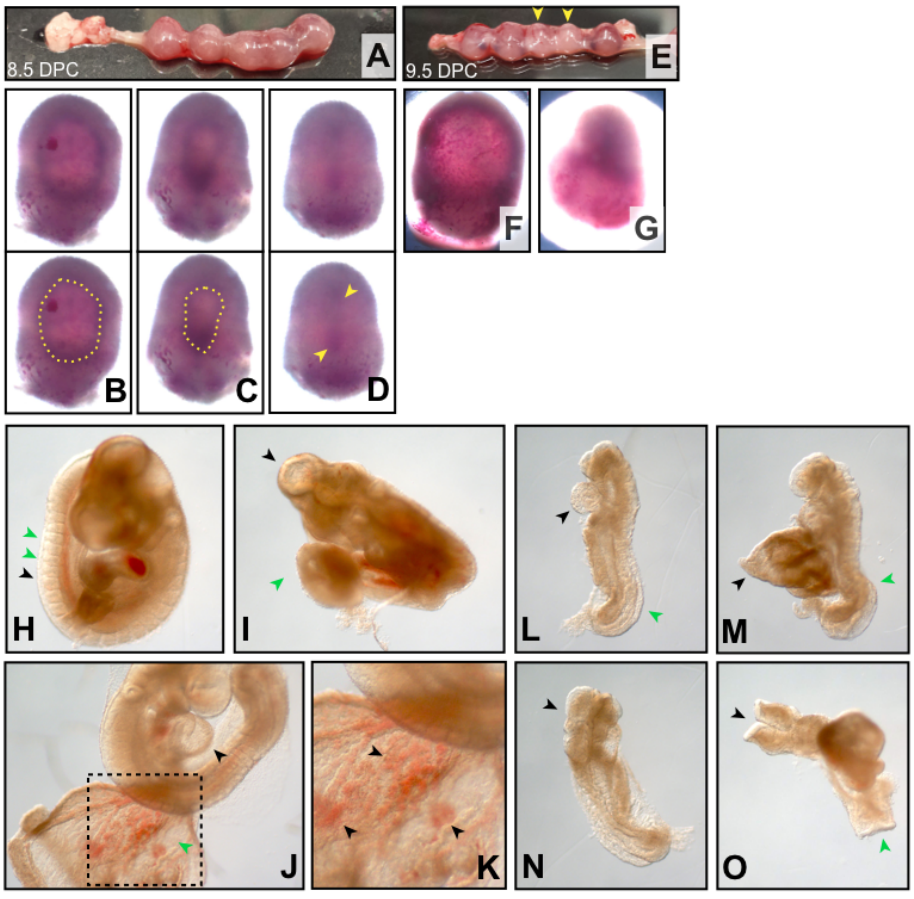
8.5 DPC
A
9.5 DPC
E
F
G
B
C
D
H
I
L
M
J
K
N
O

Figure 14. Impaired implantation and embryo development following Tip110$^{+/-}$ intercross. Uterine horns were isolated from plugged females at 8.5 dpc (**A**) and 9.5 dpc (**E**) after successful Tip110$^{+/-}$ intercrosses. Each implantation site was dissected to obtain an intact decidua and photographed using a bright field microscope. Decidua containing a normal embryo (**B** & **F**), an underdeveloped embryo (**C**), and a resorbed embryo (**D** & **G**) are shown. Embryos were also dissected from their implantation sites and other extraembryonic tissues at 9.5 dpc (**H-O**). Normal embryos (**H-K**) and underdeveloped embryos (**L-O**) were photographed using a stereoscopic dissecting microscope. Arrows in embryos show vascularization in some implantation sites (**E**), somitogenesis (**H**, green & **M**, green), embryo turning (**H**, black & **L**, green), anterior neuropore (**I**, **N** & **O**, black) and posterior neuropore (**I** & **O**, green), S-looping of heart (**J** & **L**, black), and yolk sac vascularization (**J**, green, **K** & **M**, black).

Tip110 is Expressed Ubiquitously in Early Post-Implantation Embryos

To better understand if and where Tip110 is expressed in post-implantation embryos, whole-mount immunohistochemistry was performed on 8.5 and 9.5 dpc embryos after successful $Tip110^{+/-}$ intercrosses. The data revealed that Tip110 was expressed in a generally ubiquitous fashion in post-implantation embryos, although there was prominent expression in certain areas throughout the body of the embryo. There was ubiquitous expression of Tip110 in 8.5 dpc embryos with prominent expression of Tip110 in the outer regions of the tail end of the embryo (**Fig. 15A & B**). 9.5 dpc embryos also showed a pattern of ubiquitous expression (**Fig. 15C & D**) but with clear expression of Tip110 in specific regions of the embryo such as in the anterior and posterior neuropore (**Fig. 15E & F**, respectively, arrowheads), in the developing heart and otic vesicle (**Fig. 15G**, arrowheads), and in the somites and the developing hindlimb **(Fig. 15H**, arrowheads**)**. In addition, Tip110 expression could also be detected clearly in the parietal and visceral yolk sac tissues derived from 9.5 dpc embryos **(Fig. 15I & J**, respectively).

Tip110 expression was also analyzed in underdeveloped and resorbed embryos at 8.5 and 9.5 dpc. These embryos showed several distinct phenotypes with no clear Tip110 expression (**Fig. 15K-M**). An underdeveloped 8.5 dpc embryo still in the yolk sac seemed to have minimal Tip110 expression with most being present in the tissue of the yolk sac **(Fig. 15K)**. An intact but resorbed 9.5 dpc decidua showed lack of prominent Tip110 expression throughout the extraembryonic tissues of the resorbed embryo **(Fig. 15L)**. A resorbed 9.5 dpc embryo with remnants of the allantois present showed no expression of Tip110 in the remaining resorbed embryo although there still some Tip110 expression in the allantois and in the maternal

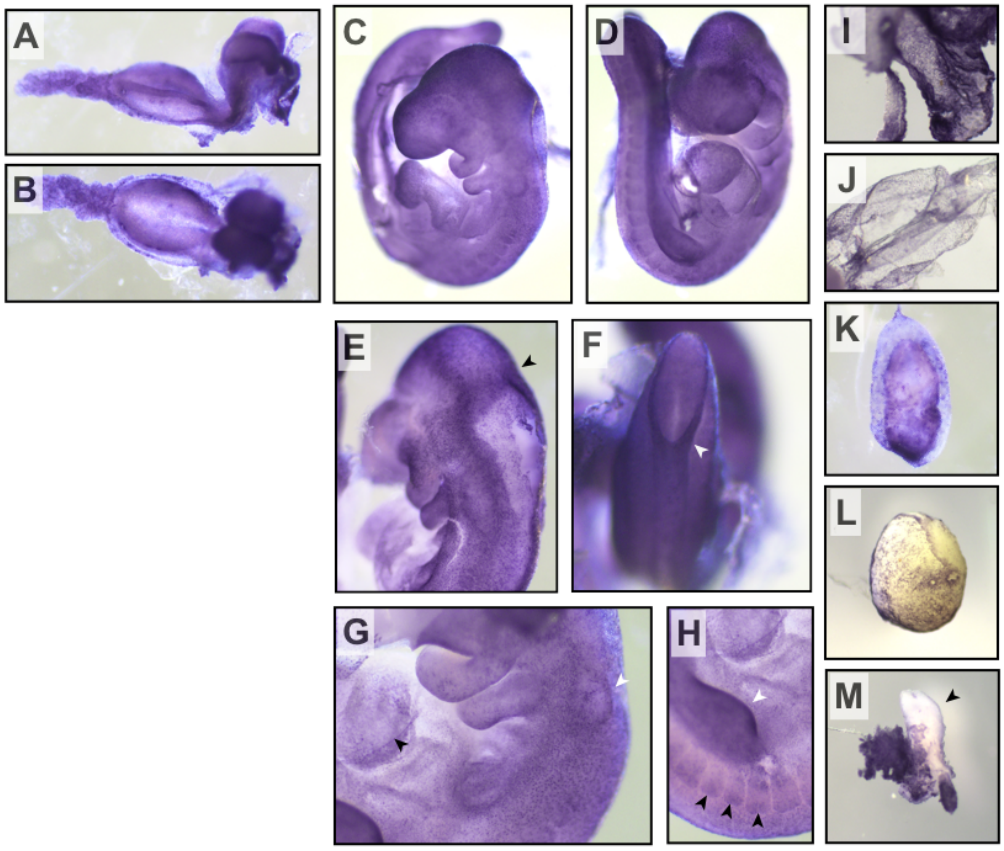
A
B
C
D
I
J
E
F
K
L
G
H
M

Figure 15. Tip110 Expression in Embryos and Extraembryonic Tissues. Uterine horns were isolated from plugged females at 8.5 dpc (**A** & **B**, **K**) and 9.5 dpc (**C**-**J**, **L** & **M**) after a successful Tip110+/- intercross. Each implantation site was dissected to obtain an intact embryo separated from its extraembryonic tissues where possible. Whole embryos were genotyped prior to staining by PCR using yolk sac-derived genomic DNA. To perform whole-mount immunohistochemistry 8.5 dpc and 9.5 dpc wild-type whole embryos (**A**-**H**), an underdeveloped embryo (**K**), resorbed embryos (**L** & **M**), and yolk sac tissues (**I**, parietal sac & **J**, visceral sac) were washed and stained with anti-Tip110 antibody or a control antibody (not shown) followed by anti-rabbit IgG HRP. Arrowheads show anterior (**E**) and posterior neuropores (**F**), heart (**G**, black arrow), otic vesicle (**G**, white arrow), hind limb (**H**, white arrow), somites (**H**, black arrow) and resorbed embryo remnant (**M**). Embryos were photographed using a stereoscopic dissecting microscope.

extraembryonic tissues connected to the embryo **(Fig. 15M)**. Taken together these data show that Tip110 is expressed ubiquitously throughout the embryo at 8.5 and 9.5 dpc, prominently in the neuropores, heart, otic vesicles, hind limbs, and somites of the developing 9.5 dpc embryo and can hardly if at all be detected in the resorbed tissues of $Tip110^{-/-}$ embryos.

Tip110 Heterozygosity Does Not Effect Cell Survival or Development

$Tip110^{+/-}$ mice used in these experiments survived for many generations with no overt or distinct phenotype as a result of their reduction in Tip110 protein expression (data not shown). As other data obtained here suggest, Tip110 heterozygosity did not affect the overall health of the mouse nor did it overtly affect fertility, cell survival, or embryonic development. In order to determine if there were more subtle effects of Tip110 reduction in $Tip110^{+/-}$ mice, experiments to investigate the effects of Tip110 reduction on gastrulation and organogenesis were performed.

After culturing blastocysts from $Tip110^{+/-}$ intercrosses *in vitro* to generate blastocyst-derived outgrowths, disaggregation of these masses was performed to first generate embryoid bodies (EB) and then cerebral organoids. EB provided an *in vitro* model to study gastrulation or the formation of the germ layers. Each of the three germ layers (endoderm, mesoderm, and ectoderm) gives rise to particular cell and tissue types in the developing embryo. As such, the EB model serves as a system to investigate the role of Tip110 in early differentiation and cell fate determination in the early embryo (*106, 107*). Cerebral organoids provided an *in vitro* model to study various aspects of organogenesis during mouse brain development in a manner that could not easily be done using living mice. These 3-dimensional structures form many of the cell types

and regions that we find naturally occurring in the developing brain so they serve as an *in vitro* model for organ development (*108*).

Wild-type and Tip110$^{+/-}$ EB were grown in KOSR mESC EB media (**Fig. 16A**) or FBS mESC EB media (**Fig. 16B**) *in vitro* for 14 days before western analysis. Another group of EB were neurally induced and grown for 11 days before another western analysis (**Fig. 16C**). These studies revealed that Tip110 knockdown does not dramatically affect the survival or growth potential of these EB. These data do however further support the idea that Tip110 expression is important for maintenance of cells in an undifferentiated state as Tip110 expression was higher in EB that had not been induced to spontaneously differentiate (**Fig. 16A & B**). EB that were allowed to persist in the early differentiated state tended to have more brachyury, a marker for mesoderm development (**Fig. 16A**), indicating they would most likely produce cells of a mesoderm lineage while the spontaneously differentiated EB had more Tuj1, a marker for ectoderm development (**Fig. 16B**), indicating they would be most likely produce cells of an ectoderm lineage, although the reason for this is unclear. Cerebral organoids derived from EB were grown *in vitro* for 40 days before being processed for western analysis or cryopreservation for later use. There was no difficulty associated with the ability to derive Tip110$^{+/-}$ mESC, EB, or organoids as compared to wild-type. Western analysis suggested that when compared to their wild-type counterparts neither Tip110$^{+/-}$ neurally induced EB (**Fig. 16C**) nor cerebral organoids (**Fig. 16D**) showed any differences in expression of markers for brain cells and general cell proliferation such as Vimentin, GFAP, or Egr1 and PCNA despite their reduction in Tip110 expression. In addition, Tip110$^{+/-}$ organoids grew just as well as their wild-type counterparts with no overt delays in growth or morphology (**Fig. 16E**).

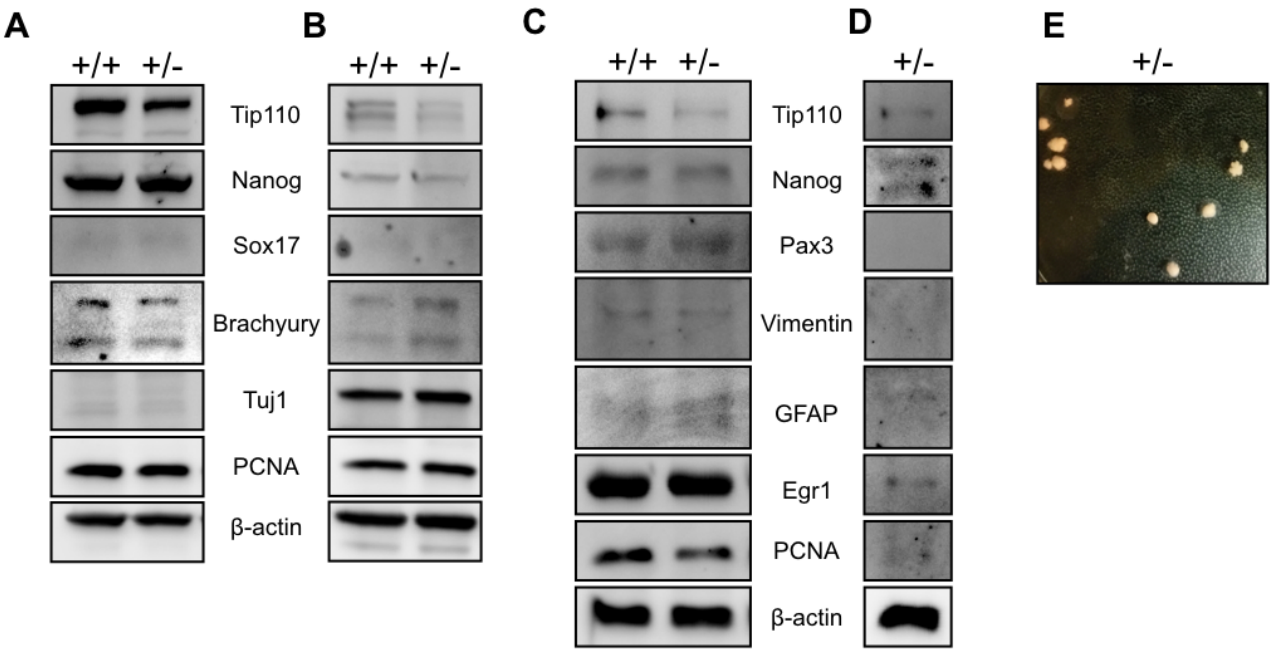
A
+/+ +/-
Tip110
Nanog
Sox17
Brachyury
Tuj1
PCNA
β-actin
B
+/+ +/-
C
+/+ +/-
Tip110
Nanog
Pax3
Vimentin
GFAP
Egr1
PCNA
β-actin
D
+/-
E
+/-

Figure 16. Derivation of Embryoid Bodies and Cerebral Organoids from Tip110-Deficient mESC. 3.5 dpc embryos were flushed from the uterine horns of superovulated or naturally mated females after successful $Tip110^{+/-}$ intercrosses. Wild-type, $Tip110^{+/-}$ and $Tip110^{-/-}$ blastocysts were cultured in KOSR-ESCM for at least nine days to form blastocyst-derived outgrowths. Outgrowths were then enzymatically disaggregated and cultured in FBS-ESCM to form mESC colonies. mESC were grown for at least two-weeks before enzymatic disaggregation and replating to form EB. EB were either grown in in KOSR mESC EB media (+KOSR, -FBS) or to support further differentiation in FBS mESC EB media (-KOSR, +FBS) for at least two-weeks. Western blot analysis was performed on lysates from EB grown in KOSR mESC EB media (**A**) and on EB grown in FBS mESC EB media (**B**), where ß-actin was included as an equal loading control. FBS-induced EB were either moved to neural induction media and grown for 11 days before another Western blot analysis or for up to five days before being (**C**) embedded in Matrigel and cultured in CODM (+B27, -Vitamin A) on an orbital shaker for three days followed by culturing in CODM (+B27, +Vitamin A) for 40 days. The 40-day old cerebral organoids were collected for Western blot analysis (**D**) and photographed (**E**).

Taken together these results suggest that Tip110 knockdown does not likely affect gastrulation or organogenesis. More specifically Tip110 reduction does not affect formation of germ layers or brain development in mice. That is, $Tip110^{+/-}$ mice likely proceed through the basics steps of their early and late development in a manner that is comparable to their wild-type littermates. As such, any of the subtle differences in proliferation or cell growth that Tip110 knockdown might have on the cells of the developing embryo can mostly be considered negligible as they do not affect overt or covert aspects of mouse development.

Summary

Tip110-CK mice were not generated but rather two populations of Tip110-KD or $Tip110^{+/-}$ mice were able to be generated. These $Tip110^{+/-}$ mice were then crossed to generate $Tip110^{-/-}$ offspring. The data obtained from such crosses reveal that Tip110 haplosufficiency does not impact embryo health and survival nor does it impact cell growth and proliferation in any meaningful capacity as all $Tip110^{+/-}$ mice exhibited no overt phenotype as a result of their haplosufficiency from the hemizygous knockout and survived and procreated just as well as their wild-type counterparts. Complete loss of Tip110, however, causes an early post-implantation death around 8.5 and 9.5 dpc. Most often at this time point embryos can be found in a completely resorbed state or in other more infrequent cases embryos can be found in an underdeveloped state *in vivo*. Tip110 is also expressed rather ubiquitously in 8.5 and 9.5 dpc embryos suggesting that it may be important for some cellular and developmental processes occurring at these stages. These data show clearly for the first time the necessity for Tip110 in a mammalian model and

highlight the critical role Tip110 plays in mammalian post-implantation development and embryogenesis.

CHAPTER IV

TIP110 IN THE PRE-IMPLANTATION DEVELOPMENT OF THE MOUSE

Rationale

Because Tip110 causes embryonic lethality fairly early on during post-implantation development it is likely that it may perturb some of the processes occurring during pre-implantation development as well. During pre-implantation development several rounds of cell division must occur to get the one-cell zygote to grow into a multicellular blastocyst. This blastocyst consists of both an inner cell mass (ICM) and a trophoectoderm (TE) cell outer layer. These cell populations respectively give rise to the embryo proper and extraembryonic tissues of the embryo. The inner cell mass itself is composed of a population of totipotent stem cells that can essentially differentiate into any cell type while the trophoectoderm cell layer is the first cell type to differentiate and although possessing some stemness, lacks the totipotent capacities of the the ICM. Because we know that Tip110 is critical, to some degree, for the survival and differentiation of stem cell populations it would be fair to presume that Tip110 expression might affect the cell divisions occurring the generate the blastocyst and that it might also be critical for the growth, differentiation, and survival of the mESC population developing in the ICM and the TE stem cells of the trophoectoderm.

To test these postulations, we observed the *in vitro* development of the early mouse embryo to determine if there were any aberrant changes in the morphology and cleavage rate of wild-type, $Tip110^{+/-}$, and $Tip110^{-/-}$ embryos. In addition, immunostaining to visualize the expression and

cellular localization of Tip110 in the early mouse embryo was performed. Also, an *in vitro* model for implantation was created and derivation of mESC from in wild-type, $Tip110^{+/-}$, and $Tip110^{-/-}$ embryos was performed. Lastly, to determine the molecular mechanisms at play in the $Tip10^{-/-}$ embryo compared to wild-type counterparts, whole-transcriptome microarray analysis of cellular RNA was performed. All of these experiments shed light onto the role of and necessity for Tip110 in stem cell and early mammalian embryo development.

Results

Tip110 is Expressed in the 2-cell Embryo and Blastocyst

The finding that $Tip110^{-/-}$ embryos died early in post-implantation development prompted an investigation into the role and/or necessity for Tip110 during pre-implantation development. We first determined whether Tip110 was expressed in the early embryo, if it was preferentially expressed in the inner cell mass or trophoectoderm, and whether Tip110 was localized in the cytoplasmic or nuclear compartment of each cell. To this end, blastocysts were flushed from the uterine horns of pregnant wild-type mice and processed for immunofluorescence staining. Confocal microscopy of immunostained blastocysts revealed that Tip110 was expressed in the cytoplasm of the inner cell mass cells of blastocysts and appeared to be higher in the trophoectoderm cells of the blastocyst with its localization being mostly nuclear (**Fig. 17**, bottom panel)**.** Included as a control was Oct4 (**Fig. 17**, top panel), which is critically involved in the self-renewal of undifferentiated embryonic stem cells and used as a marker for undifferentiated cells.

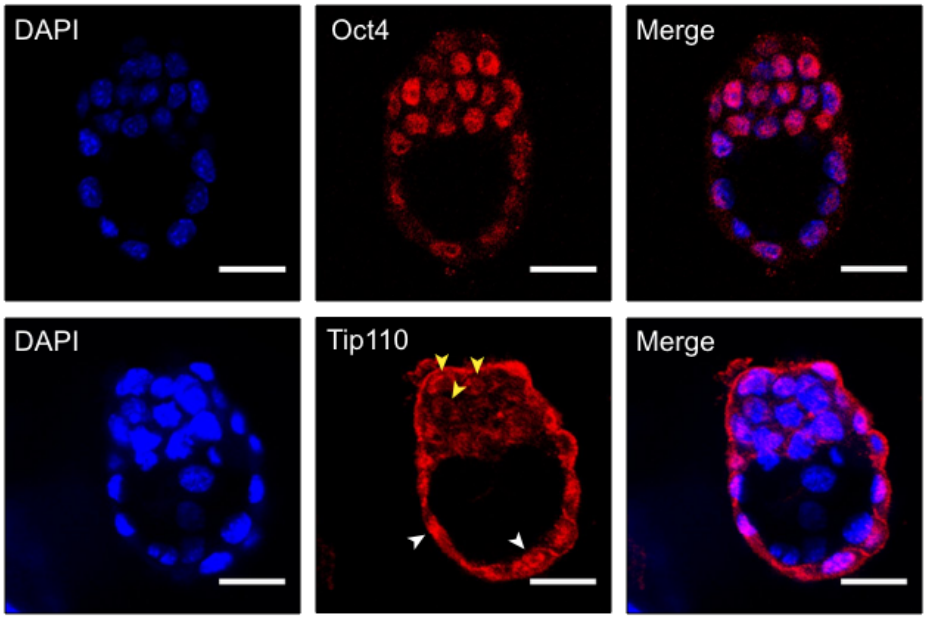
DAPI
Oct4
Merge
DAPI
Tip110
Merge

Figure 17. Oct4 and Tip110 expression in blastocysts. 3.5 dpc embryos were flushed from the uterine horns of superovulated or naturally mated females after successful wild-type intercrosses. The blastocysts were washed and stained with anti-Oct4 antibody (Top), or anti-Tip110 antibody (Bottom), followed by anti-mouse or rabbit Alexa Fluor 555. The blastocysts were then counterstained with DAPI for nuclei and photographed using a Zeiss LSM 510 confocal microscope. Tip110 expression in ICM and TE cells was shown by yellow and white arrowheads, respectively. Scale bar = 100 μm.

Expression of Tip110 throughout the cells of the blastocyst suggests that Tip110 might be necessary not only for post-implantation development but also pre-implantation development of the mouse. Using siRNA-mediated Tip110 knockdown in other studies we know that Tip110 is important for cell growth and is critical at a very early stage for maintenance of stemness (*7, 23*). Because of this it is not surprising that Tip110 can be detected in the blastocyst with an expression pattern that is fairly comparable to Oct4. Other data (not shown) reveals that Tip110 is also expressed in the 2-cell embryo similar to the blastocyst.

Tip110$^{-/-}$ Embryos Can Develop from Zygotes to Blastocysts

We next determined whether loss of Tip110 would have any adverse effects on the proliferative capacity and/or pluripotency of the early embryo. 2-cell embryos were isolated from the infundibulum of the oviducts of pregnant Tip110$^{+/-}$ mice at 1.5 dpc and cultured *in vitro* to monitor their ability to cleave to the blastocyst stage. After 5 days of culture, wild-type, Tip110$^{+/-}$, and Tip110$^{-/-}$ blastocysts were all able to cleave and make successive divisions from the 2-cell stage (**Fig. 18A**, Day 1) to blastocysts (**Fig. 18A**, Day 4 and 5) with no overt retardation in growth or any obvious morphological defects. On the 5th day of culture each intact blastocyst was transferred from KSOM culture to KOSR-ESCM to promote formation of stem cell-based blastocyst-derived outgrowths *in vitro*. After 3 more days of culture in KOSR-ESCM, each blastocyst, regardless of its genotype, hatched from its zona pellucida and was able to attach to the culture vessel to form a blastocyst outgrowth (**Fig. 18B**). A prominent distinction between wild-type and Tip110$^{+/-}$ blastocyst outgrowths and the Tip110$^{-/-}$ blastocyst outgrowth was that the wild-type and Tip110$^{+/-}$ outgrowths formed into distinct and organized globular masses while the

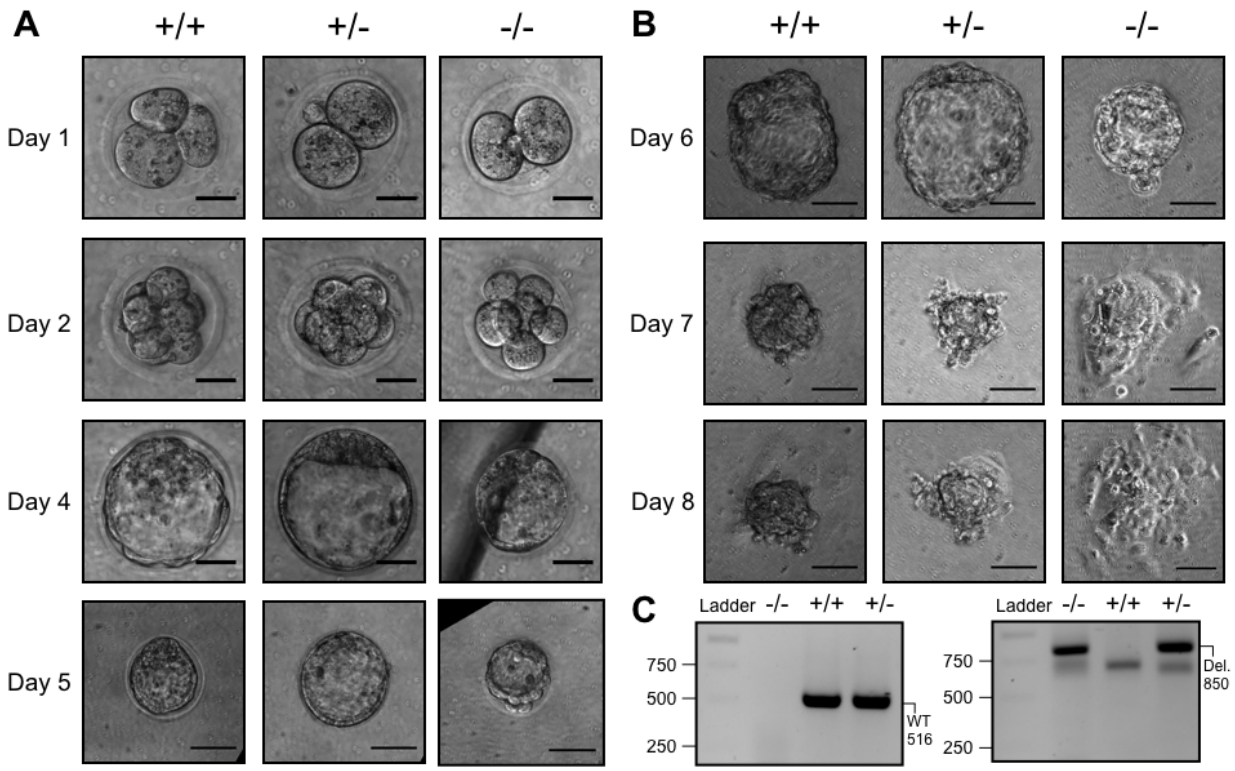
A
+/+
+/-
-/-
Day 1
Day 2
Day 4
Day 5
B
+/+
+/-
-/-
Day 6
Day 7
Day 8
C
Ladder
-/-
+/+
+/-
750
500
250
WT
516
Ladder
-/-
+/+
+/-
750
500
250
Del.
850

Figure 18. Culture of 2-cell embryos to blastocysts and blastocyst-derived outgrowths. 1.5 dpc embryos were isolated from the oviduct infundibulum of superovulated or naturally mated females after successful Tip110$^{+/-}$ intercrosses and cultured in KSOM+AA to grow to blastocysts over a five-day period (**A**). At the end of the 5-day culturing, the blastocysts were transferred to KOSR-ESCM and cultured for three days to generate blastocyst-derived outgrowths (**B**). The images were taken with a bright field microscope and are representative of three independent experiments. Scale bar = 100 μm. Genotyping of genomic DNA was performed by PCR (**C**) using three primers: 12A, 12B, and NEO as described in **Fig. 13**.

Tip110$^{-/-}$ outgrowths had less order and were mostly diffused. Tip110$^{-/-}$ blastocysts seem to be composed less of an ordered stem cell mass and more of the invasive differentiating cells derived from the trophoectoderm despite being cultured in media designed to promote growth of the inner cell mass stem cell population. These data show that wild-type and Tip110$^{+/-}$ blastocysts were able to form a prominent stem cell mass and had very few differentiated trophoblast giant cells surrounding them while the Tip110$^{-/-}$ blastocysts had a clear absence of a prominent stem cell mass and consisted mostly of what are likely differentiating trophoblast giant cells. The genotype of each outgrowth was confirmed by PCR amplification of DNA isolated from each day 8 outgrowth (**Fig. 18C**). Taken together, these data suggest that although Tip110 expression is neither necessary for successful cleavage of a 2-cell embryo to a blastocyst nor for blastocyst implantation, it is needed for proper formation of stem cell based blastocyst-derived outgrowths *in vitro*.

Tip110 is Essential for Derivation of mESC from Blastocysts

To further investigate the effects of Tip110 loss on survival of the early embryo and on formation of blastocyst-derived outgrowths, blastocysts were flushed from the uterine horns of pregnant Tip110$^{+/-}$ mice at 3.5 dpc. These blastocysts were cultured long-term individually *in vitro* in KOSR-ESCM. Culturing blastocysts *in vitro* revealed that long-term survival of blastocyst-derived outgrowths was prohibited by Tip110 loss **(Fig. 19A**, esp. Day 7-11**)**. Compared to the wild-type and Tip110$^{+/-}$ embryos, Tip110$^{-/-}$ embryos could survive *in vitro* culture and form blastocyst-derived outgrowths short-term but eventually seemed to switch from a proliferative state to a senescent or dying state. Tip110$^{-/-}$ blastocysts developed initially (**Fig.**

19A, Day 1 to Day 5 or 6**)** at a similar pace and with a comparable morphology to wild-type or Tip110$^{+/-}$ blastocysts. There was a non-significant fold change in size of outgrowths between Day 4 and Day 6 (**Fig. 19B**). However, there was a significant fold change in size between wild-type and Tip110$^{+/-}$ outgrowths and Tip110$^{-/-}$ outgrowths between Day 6 and Day 8 such that Tip110$^{-/-}$ outgrowths were on average 1.123 fold smaller than wild-type outgrowths and 0.790 fold smaller that Tip110$^{+/-}$ outgrowths. By Day 11 there were often little to no Tip110$^{-/-}$ cells remaining in culture. To ascertain the effects of Tip110 loss on stem cell self-renewal, blastocyst outgrowths were enzymatically disaggregated at 11 days and cultured in FBS-ESCM for up to 28 days to derive a mouse embryonic stem cell (mESC) population. There were no mESC derived from Tip110$^{-/-}$ blastocyst outgrowth, but a comparable number of mESC colonies from wild-type and Tip110$^{+/-}$ blastocyst outgrowths were obtained with indistinguishable morphology (**Fig. 19C**). Similar results were obtained when mouse embryonic fibroblast cells were used in the mESC cultures (data not shown). The cells derived from blastocyst-derived outgrowths and grown as mESC colonies were verified as stem cell populations using Nanog, Sox2, and Oct4 as markers for stemness in Western blot analysis (**Fig. 19D**). Both wild-type and Tip110$^{+/-}$ mESC expressed each of these pluripotency factors in a similar fashion. Genotyping was confirmed by collecting DNA from Day 8 outgrowths or from DNA isolated from mESC populations (**Fig. 19E**). Taken together, these data show that Tip110 is expressed in the blastocyst but only becomes essential for growth and survival after the blastocyst has implanted and begins to form a proliferating stem cell population. These data also further suggest that Tip110 haploinsufficiency does not negatively impact embryo survival and proliferation nor does it affect mESC derivation from blastocyst-derived outgrowths in Tip110$^{+/-}$ mice as the inability of mESC populations to survive is only observed in Tip110$^{-/-}$ mice.

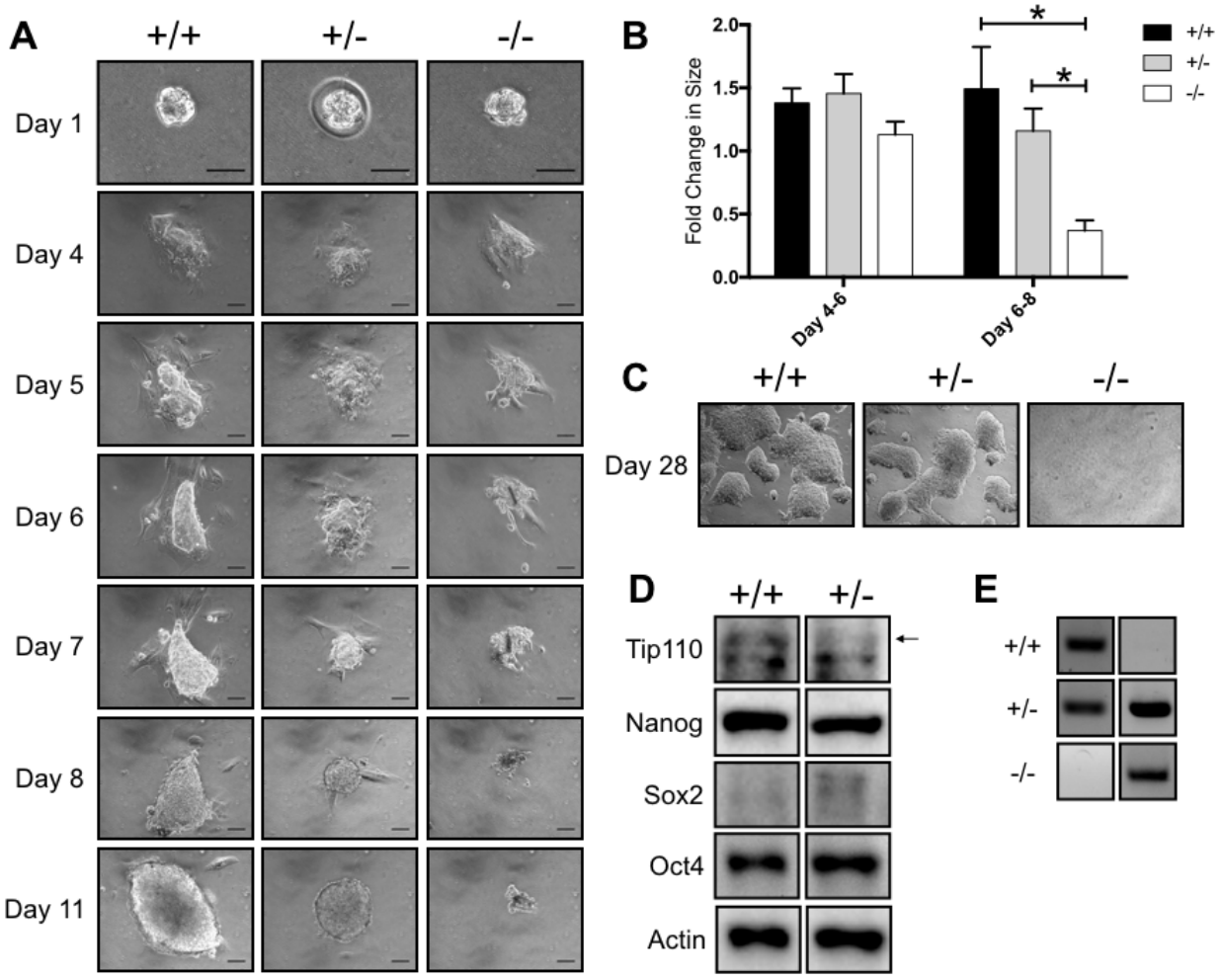
A
+/+
+/-
-/-
Day 1
Day 4
Day 5
Day 6
Day 7
Day 8
Day 11
B
Fold Change in Size
2.0
1.5
1.0
0.5
0.0
*
*
+/+
+/-
-/-
Day 4-6
Day 6-8
C
+/+
+/-
-/-
Day 28
D
+/+
+/-
Tip110
Nanog
Sox2
Oct4
Actin
E
+/+
+/-
-/-

Figure 19. Impaired derivation of mESC from Tip110$^{-/-}$ blastocyst outgrowths. 3.5 dpc embryos were flushed from the uterine horns of superovulated or naturally mated females after successful Tip110$^{+/-}$ intercrosses. Wild-type, Tip110$^{+/-}$ and Tip110$^{-/-}$ blastocysts were cultured in vitro in KOSR-ESCM for 11 days to form blastocyst-derived outgrowths (**A**). The fold-change in size of the outgrowth from day four to six and from day six to eight was calculated using ImageJ software (NIH) where the area of multiple outgrowths (n=3 per genotype) was calculated (**B**). The data were the mean ± S.E.M of triplicates and were representative of three independent experiments. Outgrowths were enzymatically disaggregated after 11 days of culture and cultured in vitro in FBS-ESCM to derive a mESC population (**C**). The stemness of the cells was confirmed by Western blot analysis of cell lysates obtained from mESC where ß-actin was included as an equal loading control (**D**). Tip110 was identified by an arrow. Genotyping of genomic DNA was performed by PCR using three primers (**E**). Scale bar = 100 μm. *: $p \leq 0.05$.

Tip110 Affects Genes Critical for Pluripotency, Growth, and Survival of ESC

To better understand the underlying molecular mechanisms of Tip110 function in stem cell based blastocyst outgrowths and in embryonic development, a whole-transcriptome array of wild-type and Tip110$^{-/-}$ cells was performed. Because 8.5 and 9.5 dpc embryos were often completely resorbed at the time of dissection it was difficult to collect reliable samples that could be easily distinguished from their extraembryonic and maternal tissues. As such, RNA for the Affymetrix array was isolated from 4-6 day old blastocyst-derived outgrowths and used for a whole transcriptome mouse array. The Affymetrix GeneChip WT Pico Kit and GeneChip Mouse Transcriptome Pico Assay 1.0 was used; it allows for a thorough analysis of picogram levels of RNA input and >23,000 protein-coding genes and >114,000 protein-coding mouse transcripts.

The array analysis output was first subjected to quality control analysis using the Affymetrix Expression Console (EC) software. To summarize the data and obtain a basic output for analysis the Affymetrix Transcriptome Analysis Console (TAC) software was used. Pathway analysis provided by the TAC software in addition to use of the DAVID (*109, 110*) and PANTHER (*101, 111*) classification systems and WIKI Pathways Beta (*102*) were employed to perform more elaborate data analysis. Sorting genes by biological function using the PANTHER system revealed that over 50% of genes affected by Tip110 had functions associated with metabolic and cellular processes while around 6% and 12% had to do with developmental processes and biological regulation respectively (**Fig. 20A**). Further breakdown of the genes associated with developmental processes revealed that 31% were associated with system development, 33% with germ layer development, and 19% with death (**Fig. 20B**). Over 50% of the genes associated with

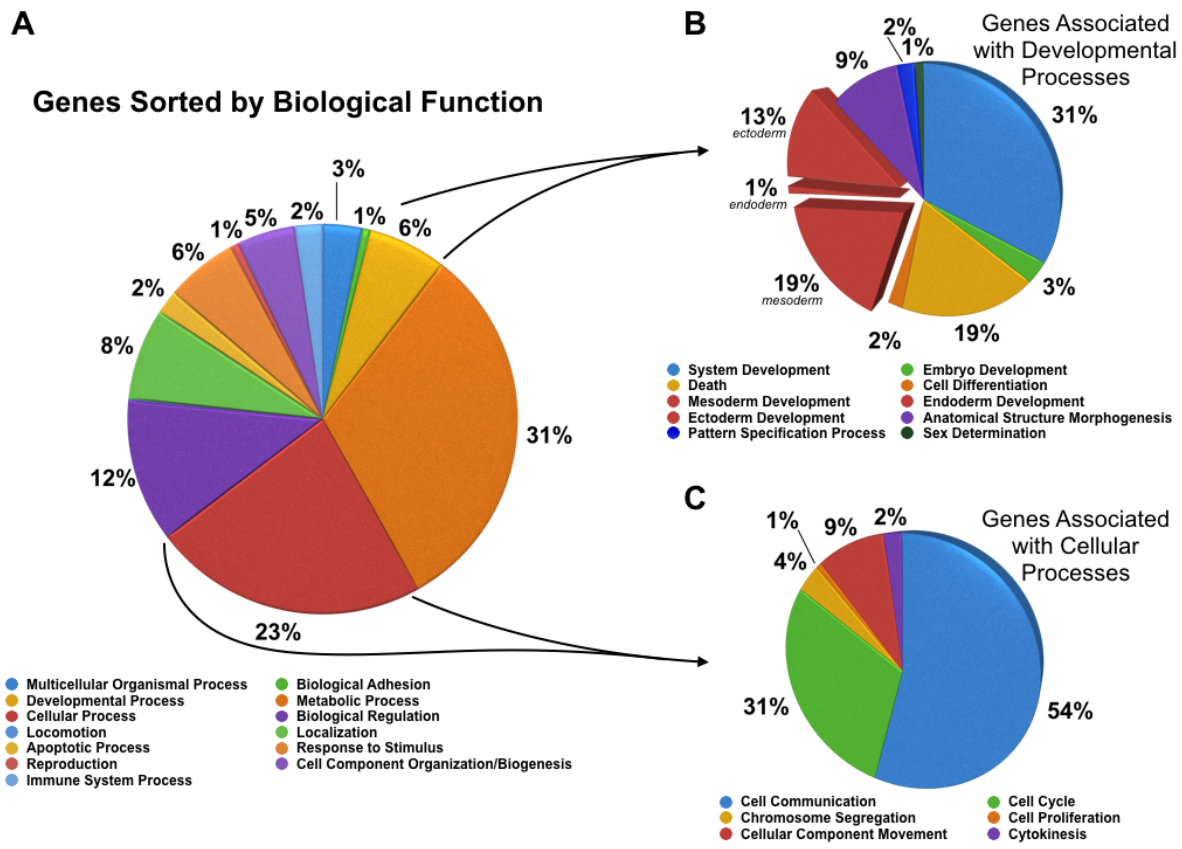
A
Genes Sorted by Biological Function
3%
1%
6%
31%
23%
12%
8%
2%
6%
1%
5%
2%
Multicellular Organismal Process
Developmental Process
Cellular Process
Locomotion
Apoptotic Process
Reproduction
Immune System Process
Biological Adhesion
Metabolic Process
Biological Regulation
Localization
Response to Stimulus
Cell Component Organization/Biogenesis
B
Genes Associated with Developmental Processes
2%
1%
9%
13%
ectoderm
1%
endoderm
19%
mesoderm
2%
19%
3%
31%
System Development
Death
Mesoderm Development
Ectoderm Development
Pattern Specification Process
Embryo Development
Cell Differentiation
Endoderm Development
Anatomical Structure Morphogenesis
Sex Determination
C
Genes Associated with Cellular Processes
1%
9%
2%
4%
31%
54%
Cell Communication
Chromosome Segregation
Cellular Component Movement
Cell Cycle
Cell Proliferation
Cytokinesis

Figure 20. Biological functions affected by Tip110. Functional analysis of genes from microarray analysis output using PANTHER classification system (GO-Slim) where genes were first categorized by biological process (**A**) and then further categorized as genes associated with developmental (**B**) or cellular processes (**C**). Each slice represents a percentage of both up- and down-regulated genes. All included genes met $\leq$ -1.5 or $\geq$ +1.5-fold change and $p \leq 0.05$ thresholds.

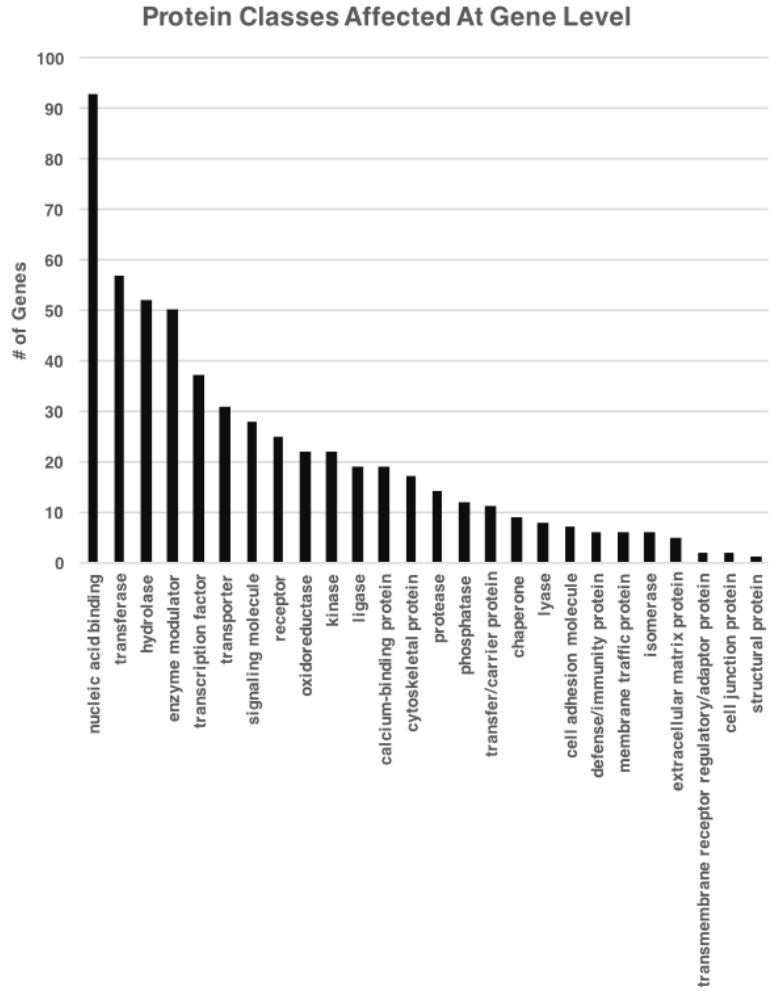
Protein Classes Affected At Gene Level
# of Genes
100
90
80
70
60
50
40
30
20
10
0
nucleic acid binding
transferase
hydrolase
enzyme modulator
transcription factor
transporter
signaling molecule
receptor
oxidoreductase
kinase
ligase
calcium-binding protein
cytoskeletal protein
protease
phosphatase
transfer/carrier protein
chaperone
lyase
cell adhesion molecule
defense/immunity protein
membrane traffic protein
isomerase
extracellular matrix protein
transmembrane receptor regulatory/adaptor protein
cell junction protein
structural protein

Figure 21. Protein classes affected by Tip110 knockout. Functional analysis of genes from microarray analysis output using PANTHER classification system where genes were categorized by protein class. Each bar represents a total of both up- and down-regulated genes. All included genes met $\leq$ -1.5 or $\geq$ +1.5-fold change and $p \leq 0.05$ thresholds.

cellular processes dealt with cellular communication while 31% dealt with cell cycle (**Fig. 20C**). The respective protein classes affected by Tip110 knockout were prominently associated with nucleic acid binding (>90 genes) although there were other protein classes such as transcription factors (>35 genes) and signaling molecules (>25 genes) that were also affected (**Fig. 21**).

Many of the genes found to be down-regulated in Tip110$^{-/-}$ outgrowths compared to wild-type were associated with pluripotency and self-renewal. Particularly, Nanog, Sox2, and Oct4 were shown to be significantly down-regulated in Tip110$^{-/-}$ outgrowths with respective fold changes of -152.02, -20.18, and -10.65 (**Table 2**). Importantly, Nanog expression had the greatest fold change of all genes associated with self-renewal and pluripotency. In addition, nearly all genes that bind to the Nanog promoter were shown to be down-regulated in this array with the exception of n-Myc which had an increase (+1.05) below the thresholds set in the array. Interestingly a potent activator of the Nanog promoter and other pluripotency genes (*112*), Zic3, was shown to be down-regulated by over 40-fold. All of this implicates Nanog as a critical contributor to the lack of stem cell self-renewal and survival in Tip110$^{-/-}$ cells.

A more critical analysis of pathways upstream of the Nanog promoter revealed that Tip110 loss perturbed regulation of the ESC pluripotency network and many signal transduction pathways in a way that may culminate in the overall down-regulation of the Nanog promoter (**Fig. 22**). Specifically, down-regulation of signal transduction ligands and receptors such as FGF4 (-17.8), Lifr (-2.2), Nodal (-1.84), TGF-β (-1.69), and others and signal transduction components such as mTOR (-2.33), rRas (-2.83), Akt1 (-1.84), and Raf1 (-1.53) and others may collectively contribute to a diminished capacity to generate a thriving self-renewing pluripotent stem cell

population as many of these components of signal transduction pathways are associated with ESC differentiation and pluripotency. Genes downstream of the Nanog promoter that promote pluripotency and self-renewal were also all down-regulated while some genes that are normally inhibited by Nanog (i.e. Gata6 and Gata4) were up-regulated (**Fig. 23**). In addition, other genes that promote self-renewal like Stat3 were shown to be down-regulated while genes that inhibit self-renewal like Erk1/2 were shown to be up-regulated. Although one specific pathway could not be implicated in the inability of Tip110$^{-/-}$ blastocyst-derived outgrowths to maintain their stemness and survive, the array analysis suggests that overall the pluripotency network (**Fig. 22**), mRNA processing (**Fig. 24**), proteasomal degradation (**Fig. 25**), and cell cycle and DNA replication associated pathways (**Fig. 26**) were the most perturbed by Tip110 loss.

To gain some insights into why post-implantation embryos do not survive *in vivo*, the array data were also analyzed to see if any genes critical for development of the ectoderm, endoderm, and mesoderm were perturbed. Although many of the genes associated with gastrulation may not be expressed in blastocyst outgrowths, some basic information about the general gene regulation occurring during gastrulation could be extrapolated. Overall, many genes associated with signal transduction, transcription regulation, cell growth, differentiation, and cycling during formation of the ectoderm, endoderm, and mesoderm were found to be down-regulated (**Table 3, Fig. 27**). While the genes that were found to be up-regulated were generally associated with negative regulation of signal transduction and other pathways, interestingly, several genes associated with expression in the placenta and differentiated trophoblast giant cells were shown to be up-regulated. Together these data suggest that Tip110 is necessary for ESC self-renewal and pluripotency in blastocyst derived stem cell populations through its role as a regulator of stem

Table 2. Genes that Bind and Regulate the Nanog Promoter

Gene Symbol	Fold Change	Promoter Interaction
Stat3	-1.05	
T (Brachyury)	-1.13	
Klf2	**-2.88**	
Klf4*	**-1.76**	*Distal Enhancer*
Klf5	**-3.24**	
Nanog	**-152.02**	
Sall4	-1.27	
Tcf3	-1.4	
GCNF	-1.28	*Negative Regulation*
p53	**-3.14**	
FoxD3	-1.2	
Oct4	**-10.65**	
Sox2	**-20.18**	*Proximal Promoter*
Esrrb	**-1.97**	
Zic3	**-41.23**	
n-Myc	1.05	

Genes with greater than a 1.5-fold change emphasized in bold. *Klf4 binds both the distal enhancer and proximal promoter of Nanog.

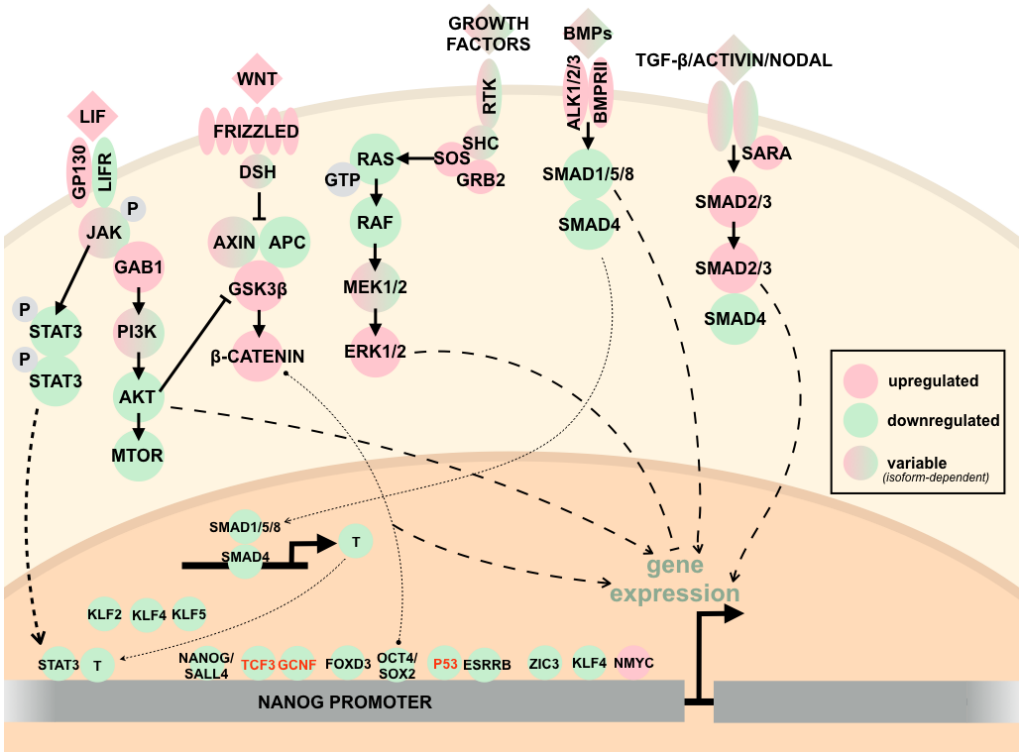
GROWTH FACTORS
BMPs
TGF-β/ACTIVIN/NODAL
WNT
LIF
FRIZZLED
RTK
ALK1/2/3
BMPRII
SARA
GP130
LIFR
DSH
SHC
RAS
SOS
GTP
GRB2
SMAD1/5/8
SMAD2/3
JAK
P
AXIN
APC
RAF
SMAD4
SMAD2/3
GAB1
GSK3β
MEK1/2
SMAD4
P
STAT3
PI3K
β-CATENIN
ERK1/2
P
STAT3
AKT
MTOR
upregulated
downregulated
variable
(isoform-dependent)
SMAD1/5/8
SMAD4
T
gene expression
KLF2
KLF4
KLF5
STAT3
T
NANOG/ SALL4
TCF3
GCNF
FOXD3
OCT4/ SOX2
P53
ESRRB
ZIC3
KLF4
NMYC
NANOG PROMOTER

Figure 22. Dysregulation of the ESC pluripotency signaling network in Tip110$^{-/-}$ cells. Affymetrix microarray analysis of four to six day old wild-type and Tip110$^{-/-}$ blastocyst-derived outgrowth cell RNA revealed the fold changes of genes in this network. Genes are shown in red when up-regulated, green when down-regulated, and by a red to green gradient when different isoforms of a gene are both up- and down-regulated. All genes are shown regardless of meeting the $\leq$ -1.5 or $\geq$ +1.5-fold change or $p \leq 0.05$ thresholds.

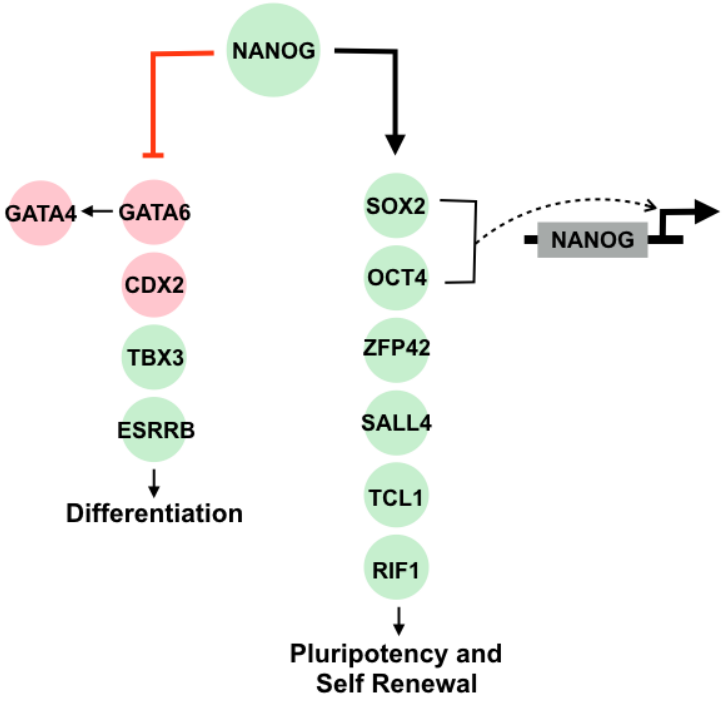
NANOG
GATA4
GATA6
CDX2
TBX3
ESRRB
Differentiation
SOX2
OCT4
NANOG
ZFP42
SALL4
TCL1
RIF1
Pluripotency and
Self Renewal

Figure 23. Dysregulation of genes downstream of Nanog in Tip110$^{-/-}$ cells. Nanog promoter activation and Nanog gene expression contribute to expression of genes associated with pluripotency and self-renewal and repression of genes associated with differentiation. Genes are shown in red when up-regulated and green when down-regulated. All genes are shown regardless of meeting the $\leq$ -1.5 or $\geq$ +1.5-fold change or $p \leq 0.05$ thresholds.

Table 3. Analysis of Gastrulation-Associated Genes

Endoderm Associated Genes

Gene	Change	Function
Gdf3	-8.66	cell growth and differentiation
Afp	1.57	organ development (liver and pancreas) and regeneration
Eomes	1.92	proliferation and differentiation (TE cells), endoderm specification
Gata6	1.98	differentiation and organgenesis (gut, lung, heart)
Dusp5	2.21	negative regulation of MAPK superfamily (MAPK/ERK, JNK, p38)
Fabp2	2.89	long chain FA transport and energy homeostasis

Ectoderm Associated Genes

Gene	Change	Function
Zic3	-41.23	regulation of ESC pluripotency, development, and differentiation
Pcolec2	-7.00	ECM degradation and collagen biosynthesis
Phc1	-5.61	transcription repression (esp. Hox genes in development)
Tubb3	-4.54	mitosis, axon guidance and maintenance, microtubules
Bcam	-2.91	signal transduction and cell adhesion
Wdr62	-2.82	neurogenesis, neuronal proliferation and migration
Nradd	-2.26	apoptosis, development and proliferation, MAPK/TNF signaling
Pabpc4	-2.22	RNA processing, regulation of mRNA stability and translation
Bnc2	-1.83	mRNA processing, transcription regulation, development
Pcnxl3	-1.75	integral component of membrane
Gas2l1	1.70	negative regulation of cell growth, differentiation, and transcription
Chrna4	6.51	ion (ACh) transport, ESC pluripotency
Tnfrsf10b	8.63	apoptosis induction and NF-kB activation

Mesoderm Associated Genes

Gene	Change	Function
Fgd1	-9.23	apoptosis, cell cycle, signal transduction (MAPK, Rho-GTPase)
Gdf3	-8.66	cell growth and differentiation
Spry2	-8.22	negative regulator of FGF pathways, proliferation, and apoptosis,
Pcolce2	-7.00	ECM degradation and collagen biosynthesis
Phc1	-5.61	transcription repression (esp. Hox genes in development)
Gm9847	-4.11	cell growth, negative regulator (JAK/STAT, IR, PK activity), protein modification/ubiquitination.
Ncln	-3.34	embryogenesis, axis formation and symmetry
Mbnl1	-2.61	alternative splicing, embryo development and differentiation
Nodal	-1.84	mesoderm formation and axial patterning
Lphn1	-1.84	regulation of exocytosis and GPCR signaling
Socs2	-1.83	negative regulator of cytokine mediated signaling (JAK/STAT) hormone/IGF signaling, apoptosis, cell growth
Myl12b	-1.75	mitosis (cytokinesis), cell shape, cell locomotion
Ddah2	-1.73	metabolism, NO biosynthesis and NO-mediated signaling
Tgfb1	-1.69	proliferation and differentiation, regulation of growth factors
Prl8a8	1.54	placenta (spongiotrophoblasts and trophoblast giant cells) ,GHRS
Cish	1.63	negative regulator of cytokine mediated signaling (JAK-STAT5)
Gas2l1	1.70	negative regulation of cell growth, differentiation, transcription
Eomes	1.92	proliferation/ differentiation (TE cells), mesoderm determination
Bmp6	2.42	cartilage and bone formation, cell differentiation and proliferation
Prl7c1	3.83	placenta (spongiotrophoblasts and trophoblast giant cells) ,GHRS
Fgd3	10.35	actin cytoskeleton (cell shape, filopodia), Rho/GTPase signaling
Prl8a9	46.22	placenta (spongiotrophoblasts and trophoblast giant cells) ,GHRS
Prl5a1	49.78	marker for invasive trophoblasts, GHRS

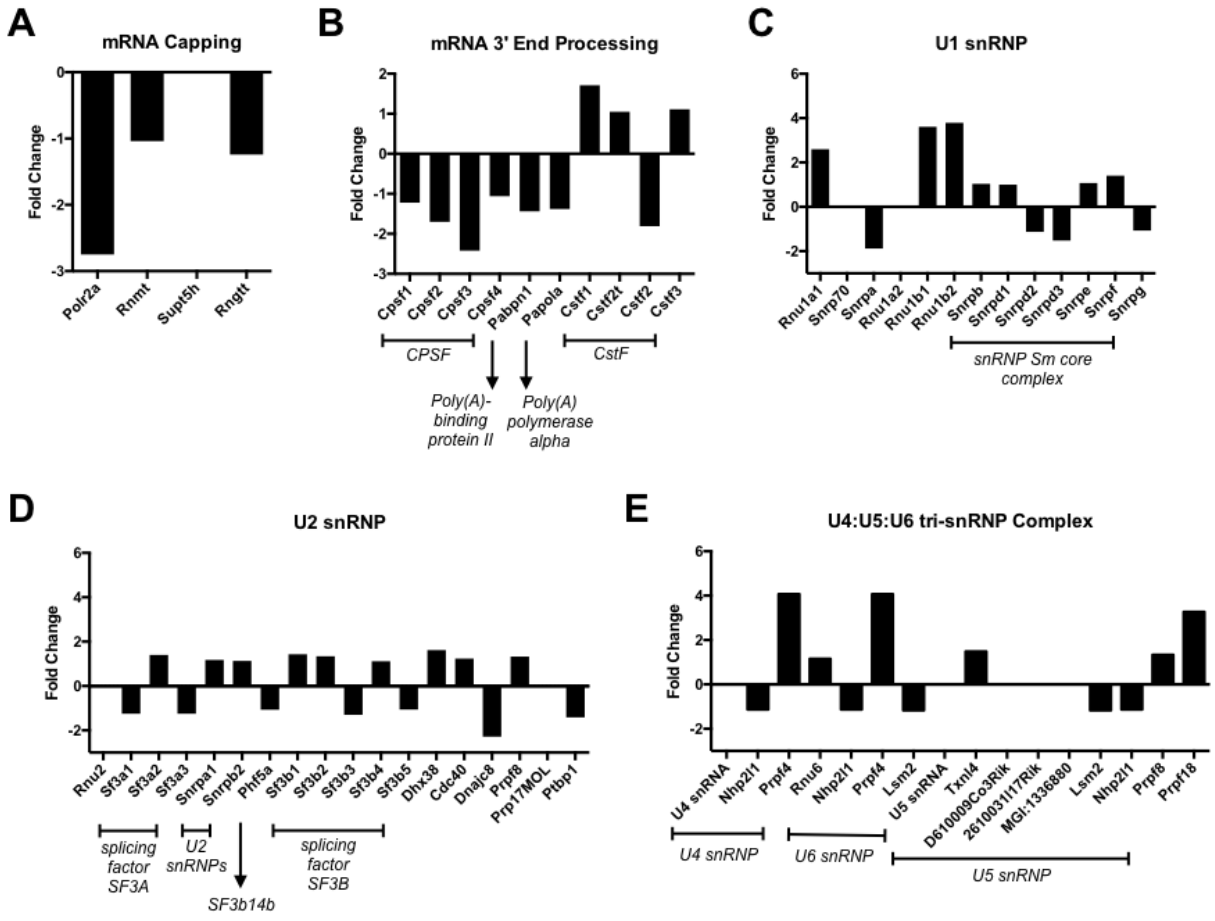
A
mRNA Capping
Fold Change
0
-1
-2
-3
Polr2a
Rnmt
Supt5h
Rngtt
B
mRNA 3' End Processing
Fold Change
2
1
0
-1
-2
-3
Cpsf1
Cpsf2
Cpsf3
Cpsf4
Pabpn1
Papola
Cstf1
Cstf2t
Cstf2
Cstf3
CPSF
CstF
Poly(A)-binding protein II
Poly(A) polymerase alpha
C
U1 snRNP
Fold Change
6
4
2
0
-2
Rnu1a1
Snrp70
Snrpa
Rnu1a2
Rnu1b1
Rnu1b2
Snrpb
Snrpd1
Snrpd2
Snrpd3
Snrpe
Snrpf
Snrpg
snRNP Sm core complex
D
U2 snRNP
Fold Change
6
4
2
0
-2
Rnu2
Sf3a1
Sf3a2
Sf3a3
Snrpa1
Snrpb2
Phf5a
Sf3b1
Sf3b2
Sf3b3
Sf3b4
Sf3b5
Dhx38
Cdc40
Dnajc8
Prpf8
Prp17MOL
Ptbp1
splicing factor SF3A
U2 snRNPs
splicing factor SF3B
SF3b14b
E
U4:U5:U6 tri-snRNP Complex
Fold Change
6
4
2
0
-2
U4 snRNA
Nhp2l1
Prpf4
Rnu6
Nhp2l1
Prpf4
Lsm2
U5 snRNA
Txnl4
D610009Co3Rik
2610031I17Rik
MGI:1336880
Lsm2
Nhp2l1
Prpf8
Prpf18
U4 snRNP
U6 snRNP
U5 snRNP

Figure 24. Dysregulation of mRNA processing and spliceosome associated genes in Tip110$^{-/-}$ cells. The Affymetrix Transcriptome Analysis Console software provided a list of genes associated with mRNA processing and their respective fold changes. This information was used to construct bar graphs depicting the fold change of each gene. Genes associated with mRNA capping (**A**), mRNA 3'-end processing (**B**), the U1 snRNP (**C**), the U2 snRNP (**D**), and the U4:U5:U6 snRNP complex (**E**) are included. All included genes are shown regardless of meeting $\leq$ -1.5 or $\geq$ +1.5-fold change and $p \leq 0.05$ thresholds.

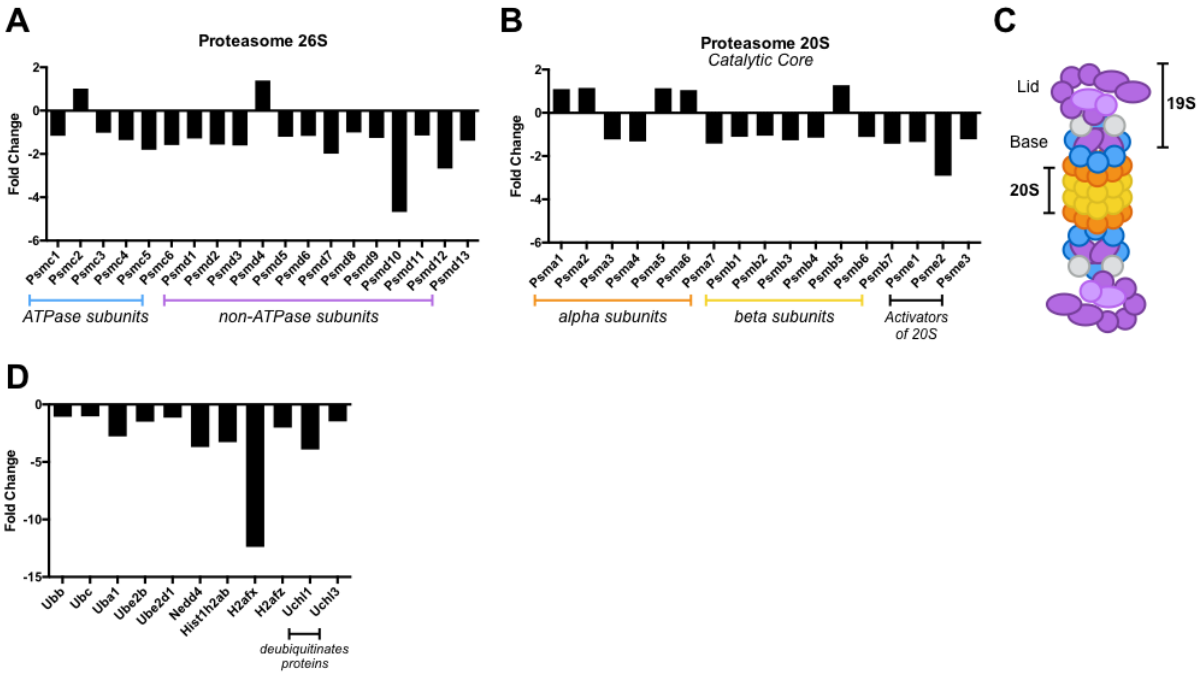
A
Proteasome 26S
Fold Change
2
0
-2
-4
-6
Psmc1
Psmc2
Psmc3
Psmc4
Psmc5
Psmc6
Psmd1
Psmd2
Psmd3
Psmd4
Psmd5
Psmd6
Psmd7
Psmd8
Psmd9
Psmd10
Psmd11
Psmd12
Psmd13
ATPase subunits
non-ATPase subunits
B
Proteasome 20S
Catalytic Core
Fold Change
2
0
-2
-4
-6
Psma1
Psma2
Psma3
Psma4
Psma5
Psma6
Psma7
Psmb1
Psmb2
Psmb3
Psmb4
Psmb5
Psmb6
Psmb7
Psme1
Psme2
Psme3
alpha subunits
beta subunits
Activators of 20S
C
Lid
Base
20S
19S
D
Fold Change
0
-5
-10
-15
Ubb
Ubc
Uba1
Ube2b
Ube2d1
Nedd4
Hist1h2ab
H2afx
H2afz
Uchl1
Uchl3
deubiquitinates proteins

Figure 25. Down-regulation of proteasome-mediated degradation in Tip110$^{-/-}$ cells. The Affymetrix Transcriptome Analysis Console software provided a list of genes associated with the 26S proteasome and their respective fold changes. This information was used to construct bar graphs depicting the fold change of each gene. Genes coding for proteins that make up the 26S proteasome (**A**), the catalytic core or 20S proteasome (**B**), an illustration of the 26S proteasome (**C**), and other genes associated with the proteasome degradation pathway are included (**D**). All included genes are shown regardless of meeting $\leq$ -1.5 or $\geq$ +1.5-fold change and $p \leq 0.05$ thresholds.

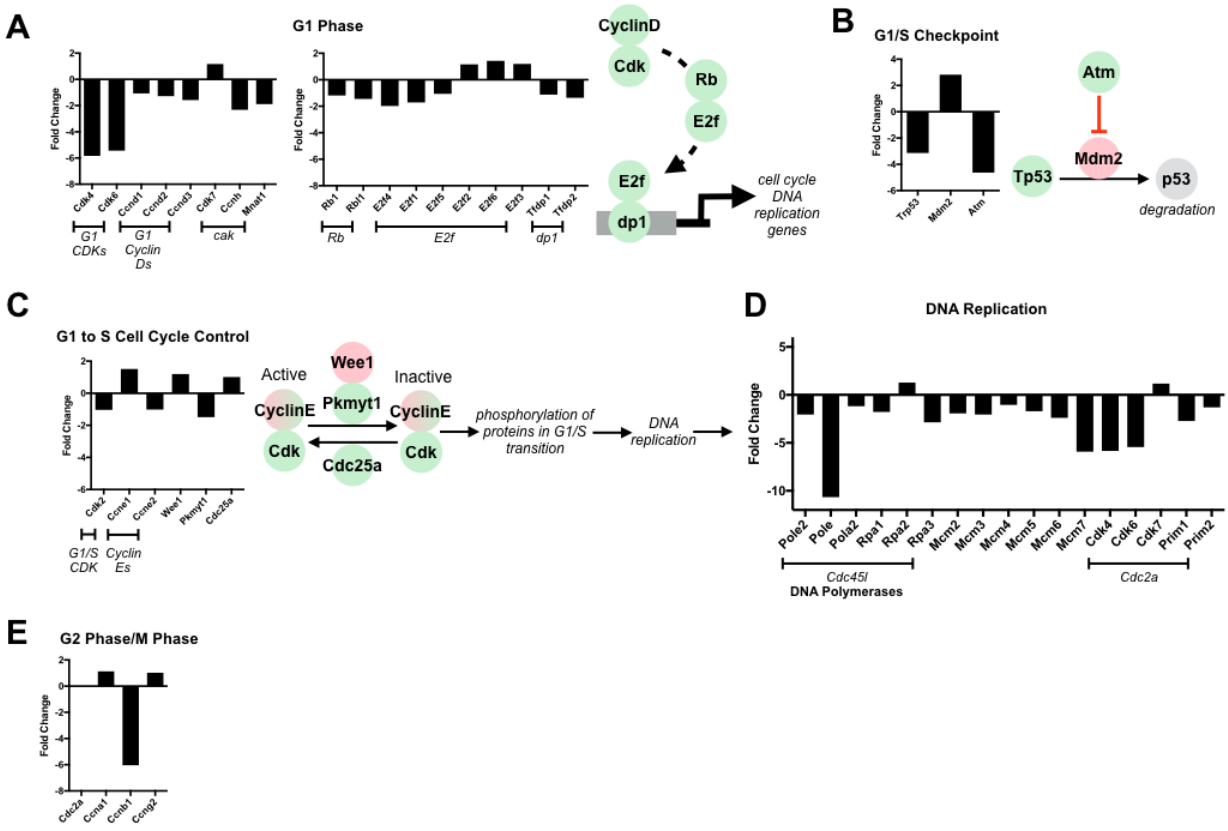
A
G1 Phase
Fold Change
Cdk4
Cdk6
Ccnd1
Ccnd2
Ccnd3
Cdk7
Ccnh
Mnat1
G1 CDKs
G1 Cyclin Ds
cak
Rb1
Rbl1
E2f4
E2f1
E2f5
E2f2
E2f6
E2f3
Tfdp1
Tfdp2
Rb
E2f
dp1
CyclinD
Cdk
Rb
E2f
E2f
dp1
cell cycle DNA replication genes
B
G1/S Checkpoint
Trp53
Mdm2
Atm
Atm
Mdm2
Tp53
p53
degradation
C
G1 to S Cell Cycle Control
Cdk2
Ccne1
Ccne2
Wee1
Pkmyt1
Cdc25a
G1/S CDK
Cyclin Es
Active
CyclinE
Cdk
Wee1
Pkmyt1
Cdc25a
Inactive
CyclinE
Cdk
phosphorylation of proteins in G1/S transition
DNA replication
D
DNA Replication
Pole2
Pole
Pola2
Rpa1
Rpa2
Rpa3
Mcm2
Mcm3
Mcm4
Mcm5
Mcm6
Mcm7
Cdk4
Cdk6
Cdk7
Prim1
Prim2
Cdc45l
DNA Polymerases
Cdc2a
E
G2 Phase/M Phase
Cdc2a
Ccna1
Ccnb1
Ccng2

Figure 26. Down-regulation of cell cycling and DNA replication genes in Tip110$^{-/-}$ cells. The Affymetrix Transcriptome Analysis Console software provided a list of genes associated with cell cycle and DNA replication and their respective fold changes. This information was used to construct bar graphs depicting the fold change of each gene. Genes associated with the G1 phase of the cell cycle (**A**), the G1/S checkpoint (**B**), G1/S cell cycle control (**C**), DNA replication (**D**), and G2 and M phases of the cell cycle (**E**) are included. All included genes are shown regardless of meeting $\leq$ -1.5 or $\geq$ +1.5-fold change and $p \leq 0.05$ thresholds.

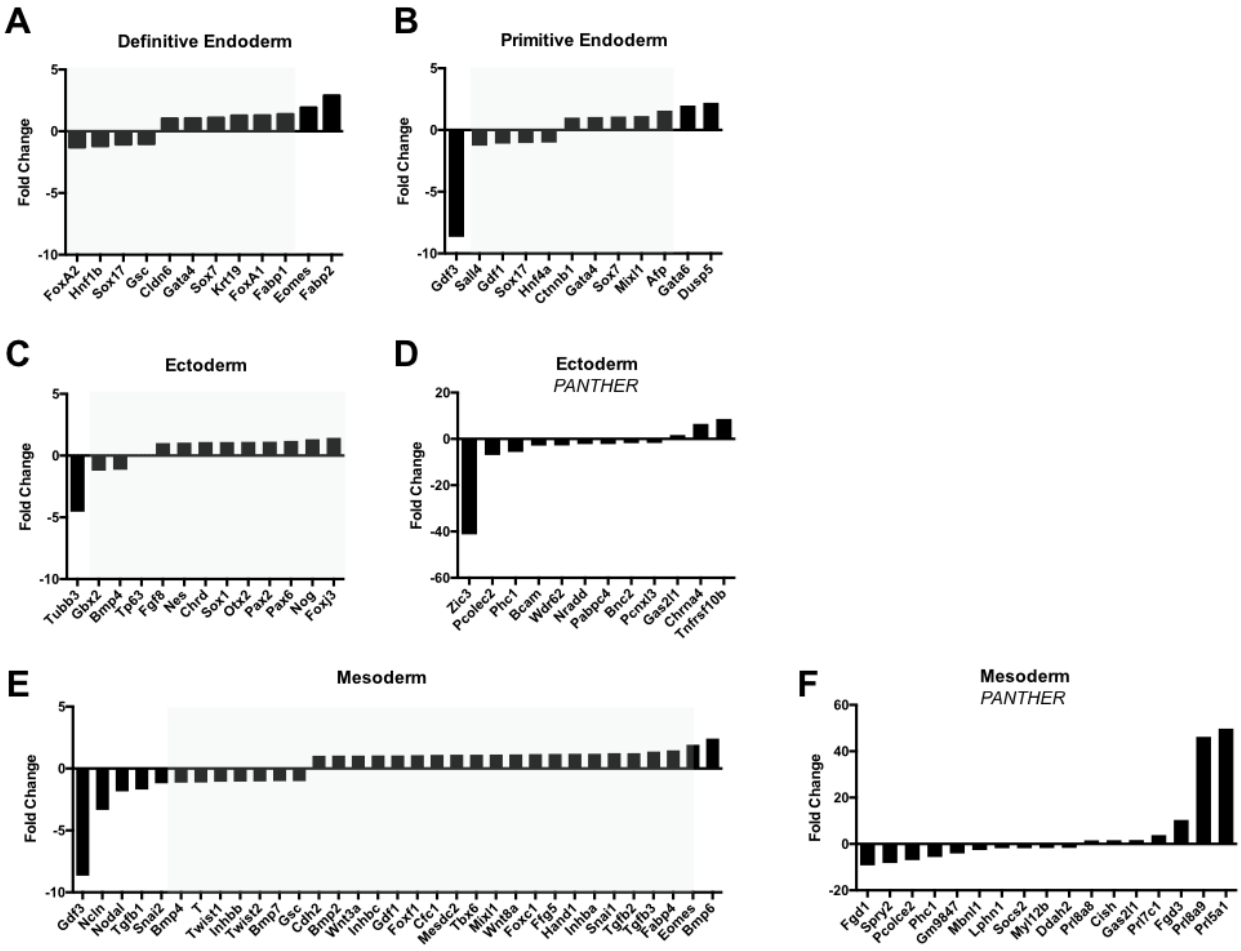
A
Definitive Endoderm
Fold Change
FoxA2 Hnf1b Sox17 Gsc Cldn6 Gata4 Sox7 Krt19 FoxA1 Fabp1 Eomes Fabp2
B
Primitive Endoderm
Fold Change
Gdf3 Sall4 Gdf1 Sox17 Hnf4a Ctnnb1 Gata4 Sox7 Mixl1 Afp Gata6 Dusp5
C
Ectoderm
Fold Change
Tubb3 Gbx2 Bmp4 Tp63 Fgf8 Nes Chrd Sox1 Otx2 Pax2 Pax6 Nog Foxj3
D
Ectoderm
PANTHER
Fold Change
Zic3 Pcolec2 Phc1 Bcam Wdr62 Nradd Pabpc4 Bnc2 Pcnxl3 Gas2l1 Chrna4 Tnfrsf10b
E
Mesoderm
Fold Change
Gdf3 Ncln Nodal Tgfb1 Snai2 Bmp4 T Twist1 Inhbb Twist2 Bmp7 Gsc Cdh2 Bmp2 Wnt3a Inhbc Gdf1 Foxf1 Cfc1 Mesdc2 Tbx6 Mixl1 Wnt8a Foxc1 Ffg5 Hand1 Inhba Snai1 Tgfb2 Tgfb3 Fabp4 Eomes Bmp6
F
Mesoderm
PANTHER
Fold Change
Fgd1 Spry2 Pcolce2 Phc1 Gm9847 Mbnl1 Lphn1 Socs2 Myl12b Ddah2 Prl8a8 Cish Gas2l1 Prl7c1 Fgd3 Prl8a9 Prl5a1

Figure 27. Dysregulation of germ layer associated genes in Tip110$^{-/-}$ cells. Functional analysis of genes from microarray analysis output using PANTHER classification system provided a list of genes associated with each germ layer and their respective fold changes. Additionally, genes generally accepted as markers for each germ layer were included. This information was used to construct bar graphs depicting the fold change of each gene. Genes associated with the definitive endoderm (**A**), primitive endoderm (**B**), ectoderm (**C** & **D**), and mesoderm (**E** & **F)** are included. Genes identified by PANTHER classification system include Dusp5 in B, and all genes in (**D**), and (**F**). A grey box indicates genes with fold changes outside the ≤ -1.5 or ≥ +1.5 threshold. All other genes meet the ≤ -1.5 or ≥ +1.5-fold change threshold.

cell factors. In addition, other cellular processes such as mRNA processing, splicing, proteasome degradation, cell cycle, and DNA replication were also shown to be dysregulated upon Tip110 loss.

Summary

These data revealed that Tip110$^{-/-}$ offspring developed from zygotes to blastocysts *in vivo* and from 2-cell embryos to blastocysts *in vitro* with no overt defects in morphology or cleavage rate. Tip110 immunostaining in 2-cell embryos and blastocysts revealed that Tip110 is expressed at both stages and is found in both the cytoplasmic and nuclear compartments. In the blastocyst Tip110 is expressed in the ICM and TE. Most interestingly, mESC can be derived from wild-type and Tip110$^{+/-}$ cells and grown indefinitely *in vitro* while Tip110$^{-/-}$ mESC could not be derived in LIF+2i culture in the presence and absence of MEF. Loss of Tip110 in mESC derived from blastocyst outgrowths, was clearly shown to perturb genes critical for stem cell pluripotency, growth, and survival such as Nanog, Oct4, and Sox2 suggesting that Tip110 is a critical regulator of stem cell factors. In this cell population there was also clear dysregulation of the ESC pluripotency network and down-regulation of Nanog promoter activation, cell cycling, DNA replication and other important processes.

CHAPTER V

DISCUSSION

In this study, we demonstrated that a complete loss of Tip110 expression during mouse embryonic development resulted in a non-viable phenotype with several important and distinct characteristics. Although the findings indicate that Tip110 did not likely affect fertilization, cleavage, or implantation, there was a clear necessity for the protein once the stem cell population of the embryo began to grow and proliferate so that complete loss of Tip110 resulted in dysregulation of the ESC pluripotency network and in marked reduction in stem cell factors such as Nanog, Oct4, Sox2 and others.

One important aspect of this study is that $Tip110^{-/-}$ mice were studied alongside wild-type and $Tip110^{+/-}$ mice. This study design revealed clearly that $Tip110^{+/-}$ mice did not represent a distinct intermediate phenotype but instead show a phenotype that was comparable if not indistinguishable from wild-type mice. Despite a reduction of Tip110 protein expression in $Tip110^{+/-}$ mice and a moderate decrease in some markers for proliferation or differentiation, $Tip110^{+/-}$ embryos successfully developed to blastocysts and blastocyst-derived stem cell populations. $Tip110^{+/-}$ embryos also proceeded through embryonic development similarly to their wild-type counterparts and grew and survived into adulthood with no overt phenotypic changes compared to wild-type mice. Moreover, an in-depth investigation into whether $Tip110^{+/-}$ mice exhibited more covert phenotypic changes revealed that Tip110 knockdown did not impair gastrulation or organogenesis *in vitro*. All of these results suggest that Tip110 haploinsufficiency produces viable cells and organisms but complete lack of Tip110 protein expression produces

changes in cell stemness and survivability such that cell death and embryonic lethality occur both *in vitro* and *in vivo*.

Tip110 was shown to be ubiquitously expressed in wild-type and Tip110$^{+/-}$ embryos at 8.5 and 9.5 dpc with higher expression in areas with more rapid proliferation and differentiation processes occurring at this developmental stage such as the neuropores, somites, hindlimb, and heart. Tip110$^{-/-}$ embryos were typically found in a resorbed or underdeveloped state with some variability between litters. Embryos that were underdeveloped or resorbed lacked clear and prominent Tip110 expression and were much smaller in size than their littermates. Underdeveloped embryos possessed a distinctly smaller and less vascularized implantation site (**Fig. 14**) despite the fact that the decidua, which is mostly maternal, was comparable in size regardless of the genotype. This data further highlights a role for Tip110 in the developing embryo and suggests why the protein is so indispensable and crucial for embryo survival and viability. Post-implantation experiments provided some clues as to when and where Tip110 was required during this stage of development but to understand its role in embryogenesis more clearly, a look at when Tip110 expression initiated in the early embryo revealed that Tip110 can be detected at early as the 2-cell stage (data not shown) and was clearly expressed throughout 3.5 dpc blastocysts (**Fig. 17**). Immunofluorescence staining also showed that Tip110 expression was prominent in the trophoectoderm (TE) layer of the embryo although it was also expressed in the inner cell mass at 3.5 dpc. Expression was mostly nuclear in the ICM and both nuclear and cytoplasmic in the TE cells. In the nucleus, Tip110 plays roles in a variety of processes but most notably regulation of pre-mRNA splicing and gene transcription (*49*).

Tip110$^{-/-}$ embryos could develop *in vivo* and *in vitro* from 2-cell embryos to blastocysts that can hatch from the zona pellucida and attach to the uterine lining or a culture vessel, but long-term survival beyond that point was impaired, namely stem cell populations cannot be derived from Tip110$^{-/-}$ blastocyst-derived outgrowths that formed after *in vitro* implantation. The cell population that did grow can only establish itself for several days before a senescent or dying state was induced. The inability of Tip110$^{-/-}$ cells to survive up to and not beyond the mESC state suggests that this protein is very critical at this stage for maintenance of cells in a pluripotent, self-renewing state. This finding is in agreement with our previous studies in hESC, HSC, and HPC showing that Tip110 expression in hESC and embryoid bodies is associated with their differentiation (*22*). We have also shown a potential reciprocal regulation between Tip110 and c-Myc expression (*7, 23*) and preferential regulation of alternative splicing of Oct4 by Tip110 to generate the major isoform Oct4a which is essential for self-renewal and maintenance of stem cells in an undifferentiated state (*7*). Whole transcriptome array analysis revealed a common theme that genes promoting self-renewal were down-regulated while the opposite was often true for those inhibiting self-renewal. Although one specific pathway could not be implicated as a causative factor in loss of stemness in Tip110$^{-/-}$ outgrowth cells, this trend was seen throughout such that the overall trend favored differentiation and did not support self-renewal and pluripotency (**Fig. 23, Fig. 28**). One standout gene that is critical for stemness was Nanog. Nanog is an important internal regulator of pluripotency and is necessary for maintenance of mESC self-renewal (*113*). There was not only potent down-regulation of Nanog but also down-regulation of nearly all genes that bind and activate the Nanog promoter and other pluripotency factors such as Oct4, Sox2, and Klf4. In addition, Zic3, a known activator of the Nanog promoter and transcription factor that is required for maintenance and regulation of pluripotency and self-

renewal in ESC (*112*) was down-regulated by over 40-fold. Zic3 plays a critical role in the classic pluripotency network by not only binding to the Nanog promoter but in its operating downstream of Nanog, Oct4, and Sox2 (*112*) (**Fig. 22 & 29**). These results together show that Tip110 is critical for pluripotency and self-renewal through maintenance and or regulation of genes associated with pluripotency and stemness and suggest Tip110 as an indispensable regulator of ESC pluripotency-associated processes.

The array data also showed that Tip110 knockout cells had a clear dysregulation of genes associated with cell cycling, DNA replication, mRNA processing, splicing, and proteasome degradation. The cell cycling network showed a marked trend of down-regulation especially in the G1 and S phases. G1 cyclin-dependent kinases, Cdk4 and Cdk6, were down-regulated by nearly 6-fold while other G1 phase proteins were also down-regulated (**Fig. 26A & D**). Interestingly, Pole, which codes for the catalytic subunit of DNA polymerase epsilon was down-regulated by over 10-fold (**Fig. 26D**). This gene is important in cell cycling, DNA repair, and DNA replication (*114, 115*) and its down-regulation might suggest key dysregulation leading to cell death. This down-regulation is likely linked to the down-regulation of genes associated with mRNA processing and splicing and the 26 proteasome (**Fig. 24 & 25**). As discussed above, Tip110 plays a critical role in mRNA processing (*49*). Thus, it is no surprise that most of the genes associated with these processes are down-regulated (**Fig. 24**). Genes associated with each snRNP are both up- and down-regulated (**Fig. 24C-E**), which have been found in Tip110 ortholog-deleted zebrafish (*13*). Tip110 knockout-induced down-regulation of the components of the 26S proteasome that make up the lid, base, and catalytic core might stabilize the proteins that should be degraded for survival and maintenance of ESC. All of these results raise the other

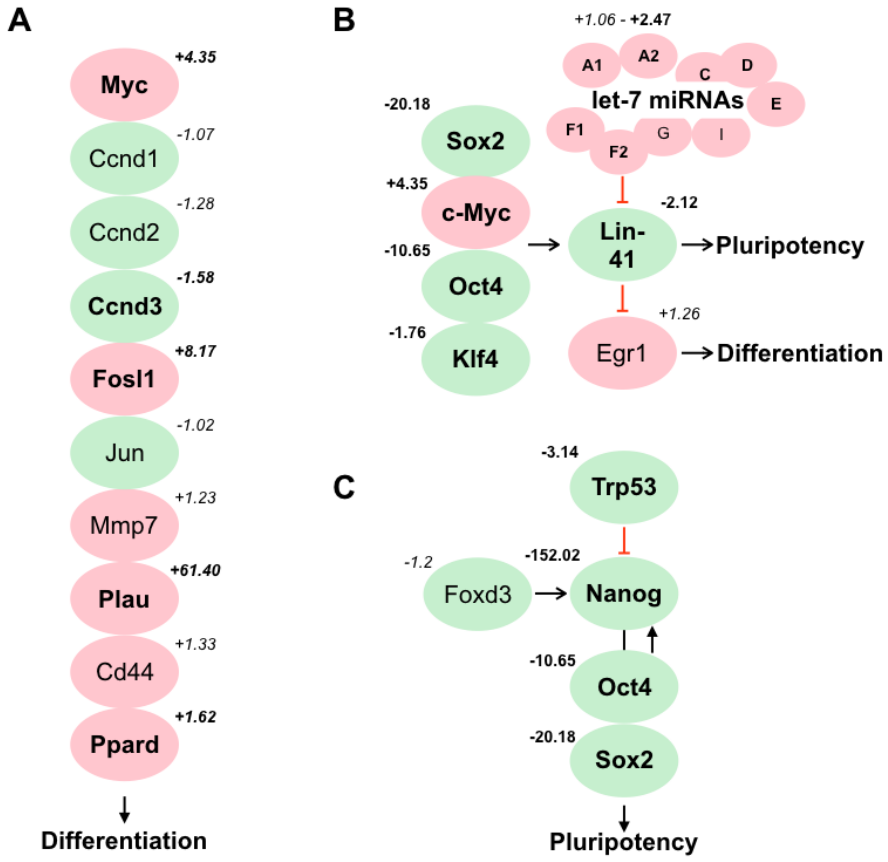
A
Myc
+4.35
Ccnd1
-1.07
Ccnd2
-1.28
Ccnd3
-1.58
Fosl1
+8.17
Jun
-1.02
Mmp7
+1.23
Plau
+61.40
Cd44
+1.33
Ppard
+1.62
Differentiation
B
+1.06 - +2.47
A1
A2
C
D
E
let-7 miRNAs
F1
F2
G
I
-20.18
Sox2
+4.35
c-Myc
-10.65
Oct4
-1.76
Klf4
-2.12
Lin-41
Pluripotency
+1.26
Egr1
Differentiation
C
-3.14
Trp53
-1.2
Foxd3
-152.02
Nanog
-10.65
Oct4
-20.18
Sox2
Pluripotency

Figure 28. Up-regulation of differentiation-associated genes and down-regulation of pluripotency-associated genes in Tip110$^{-/-}$ cells. A search of WIKI Pathways Beta provided a list of genes associated with the WNT signaling pathway and pluripotency, Let-7 ESC reprogramming, and ESC pluripotency and their respective fold changes. This information was used to construct bar graphs depicting the fold change of each gene. Genes associated with differentiation (**A**), Let-7 regulation of ESC reprogramming (**B**), and pluripotency (**C**) are included. All included genes are shown regardless of meeting ≤ -1.5 or $\geq +1.5$-fold change and $p \leq 0.05$. Genes with fold changes ≤ -1.5 or $\geq +1.5$ are indicated in bold.

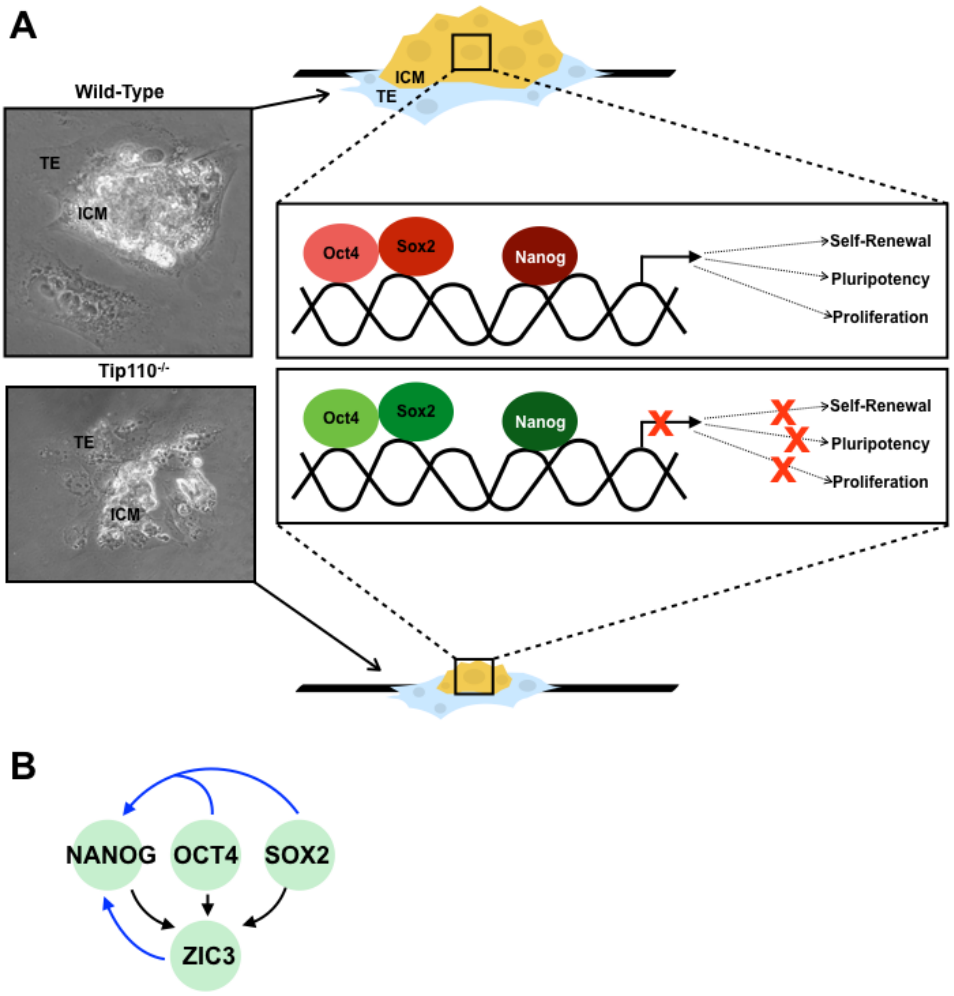
A
Wild-Type
TE
ICM
ICM
TE
Oct4
Sox2
Nanog
Self-Renewal
Pluripotency
Proliferation
Tip110-/-
TE
ICM
Oct4
Sox2
Nanog
Self-Renewal
Pluripotency
Proliferation
B
NANOG
OCT4
SOX2
ZIC3

Figure 29. Decreased expression of pluripotency genes in Tip110 knockout blastocyst-derived outgrowths. Pluripotency genes and their prospective effects as obtained from array outputs in wild-type outgrowths (**A**, Top) and Tip110-/- outgrowths (**A**, Bottom) are shown. The network between Zic3 and pluripotency factors Nanog, Oct4, and Sox2 are shown (**B**).

possibility that Tip110 loss causes dysregulation at the DNA, RNA, and protein level culminating in a phenotype that is neither conducive to pluripotency and self-renewal nor for homeostasis and survival.

Analysis of the genes identified with the PANTHER Classification System (*101*) and general markers associated with gastrulation and the development of each germ layer revealed many perturbations in signal transduction pathways, development-associated genes, and other processes such as cell cycling, cell growth, cell proliferation, and cell differentiation (**Table 3, Fig. 27**). Mesoderm-associated genes were most perturbed upon loss of Tip110, suggesting that Tip110 is critical for formation of mesoderm-associated cell lineages such as fat, muscle, bone, and immune cells including their mesenchymal and hematopoietic stem cell precursors. There was also down-regulation of many ectoderm-associated genes which might implicate Tip110 in neurogenesis. In addition, $Tip110^{-/-}$ cells had high levels of proteins expressed in the placenta (i.e. in spongiotrophoblasts and trophoblast giant cells) such as Prl5a1, Prl8a9, Prl7ac, and Prl8a8. This may also suggest that Tip110 is critical for maintenance of TE cells in an undifferentiated state such that when it is lost the cells are free to differentiate into the invasive, rapidly proliferating trophoblast giant cells.

Taken together these data suggest that knockout of Tip110 results in some very specific perturbations in signal transduction and maintenance of pluripotency and self-renewal networks such that a general phenotype supporting differentiation and poor long-term survival of stem cells is favored over a phenotype supporting maintenance of pluripotency, self-renewal, and survival. Much of this dysregulation can be attributed to loss of Nanog expression, down-

regulation of the Nanog promoter, and diminished expression of other regulators of stemness such as Oct4, Sox2, Klf4, and Zic3. Further investigation is certainly warranted to understand the effects of Tip110 knockout particularly in a more specific manner (i.e. at specific stages of development or in specific systems) to determine if it plays any critical roles in the development of certain organs or cells *in vivo*. Those studies are expected to provide more insights into its biological roles and functions.

CHAPTER VI

PERSPECTIVES AND FUTURE DIRECTIONS

Tip110 in Pluripotency

Previously reported data and the data presented here concerning Tip110 and its effects on stem cell factors and stem cell survival suggest that Tip110 might be important for pluripotency. Whether Tip110 is essential or required for pluripotency though, remains unclear. Tip110 expression is associated with the cycling of HSC through regulation of c-Myc and Gata2 (*6, 23*); also, its expression is associated with the differentiation state of the cell as well as the expression of pluripotency factors Nanog, Oct4, and Sox2 (*22*). In addition, Tip110 expression can be increased with the overexpression of c-Myc and this increase can lead to preferential splicing of Oct4 in the Oct4a isoform which is associated with pluripotency (*7*). These data coupled to the data reported here that showed that Tip110 was detected throughout development and was required for embryonic development and for derivation of mESC *in vivo* collectively make the case for Tip110 as a critical regulator of development and stem cell survival. To concisely describe Tip110 as a pluripotency factor though will require more work.

Because Tip110 is essential for processes like pre-mRNA splicing and has roles in regulation of gene expression/transcription, its role in stemness may be directly tied to these processes making it less of a stem cell or pluripotency factor and more of a housekeeping gene. This is an important point raised by Martello et. al. when attempting to define the criteria for establishing a gene product as a pluripotency factor (*116*). True pluripotency factors, when lost or dysregulated,

can result in stem cell or embryo death but more importantly they have impacts on cell fate determination. As such, a deeper investigation of the effects of Tip110 loss on lineage specification processes might be necessary. Additional experiments that test the reprogramming capacity of Tip110 as well as experiments that concisely determine whether the mESC population described here are dying because of perturbations in housekeeping/homeostatic functions or because of a true inability to self-renew are also necessary. Collectively, the work presented here provide further evidence to support roles for Tip110 in stem cell pluripotency and self-renewal and show that Tip110 is critical in development and embryogenesis. However, there is still need to further investigate what other more specific roles Tip110 has in each of these processes as well as to concisely determine if we should describe it as a pluripotency factor or a simply a housekeeping gene.

Another point to consider is that the array analysis of Tip110$^{-/-}$ cells revealed that c-Myc was up-regulated by over 4-fold despite nearly all other stem factors showing clear down-regulation. In the literature c-Myc is consistently described as a stem cell factor that is required for self-renewal and pluripotency, and in fact is one of the stem cell factors discovered by Yamanaka as being essential for reprogramming of cells back to a pluripotent state (*117*). In addition, c-Myc is a regulator of Tip110 expression and it can be regulated by Tip110 (*7, 23*). Because of this it is unclear why c-Myc expression would be increased when Tip110 is lost. One could conjecture that c-Myc levels increase in an attempt to compensate for Tip110 loss but this is contradicted by our understanding that reductions in Tip110 expression are correlated with reductions in c-Myc (the inverse is also true). If the Tip110$^{-/-}$ cells used here are, despite their poor health and survivability, cells with stemness and an initial degree of pluripotency and self-renewal the cells

will require c-Myc expression. Without Tip110 though, there might be dysregulation of gene expression and signal transduction that leads to an increased expression of c-Myc, at least initially. We might also conjecture that the c-Myc levels in these cells actually could be on a decline. A time-course experiment might reveal that further culture of the $Tip110^{-/-}$ cells would result in a lower level of c-Myc expression.

If c-Myc might have been initially up-regulated, we can correlate that with array data that shows that activators of Myc such as Wnt, Shh, and Egf are modestly up-regulated in the absence of Tip110. As well, Aeg-1 which is required for Myc expression and is regulated by Myc also showed a modest up-regulation. We also know that Myc is a transcriptional gene target of Stat3. Because these cells are grown in the presence of Lif (which leads to the recruitment of Stat after Lif-R dimerization) activation of the Lif/Stat3 pathway would take place and could possibly lead to the up-regulation of c-Myc even in the absence of Tip110.

Collectively these data, although paradoxical, show an up-regulation of Myc and regulators of Myc expression. However, it is unclear why c-Myc levels are higher in the absence of Tip110. Future experiments to verify the results provided by the array are certainly necessary as well as experiments to determine the effects of complete loss of Tip110 on c-Myc regulation.

Tip110 in Embryology and Stem Cell Biology

Tip110 is important for development across several different species and results in lethality during embryogenesis or shortly after post-natal development initiates, further suggesting it as an

essential protein or housekeeping gene. The ubiquitous expression of the protein *in vitro* also supports this notion. If one were to continue to investigate the role of Tip110 in development or development-associated processes it would be most interesting to make use of conditional knockout models where Tip110 loss could be induced in a more controlled fashion at later stages of post-implantation development (i.e. beyond the 8.5 and 9.5 dpc cutoffs we were restricted to here) to determine if it has any additional organ-specific or tissue-specific mechanisms of action. In addition, histology and pathology-oriented work would certainly be insightful.

It would also be interesting to investigate the role of Tip110 loss and overexpression in a mouse model to compare what the effects are on tumor development and survival *in vitro* since it is clear that the protein plays some important roles in cancer. This is evidenced by its high expression in cancerous cell and tissues, by its regulation and interaction with oncogenes, and by its regulation of p53 and HIF proteins. In addition, it is a critical contributor to mRNA splicing, transcription processes, and regulation of proteasomal degradation processes. A deeper investigation into the dysregulation of these cellular processes when Tip110 is altered in a cancerous cell line or tissue biopsy would likely yield some interesting results.

The role of Tip110 in stem cell maintenance and self-renewal is so far one of its more interesting functions. The array data presented here showed some very compelling data that the protein is critical in the maintenance of expression of Nanog, Oct4, and Sox2. A deeper look into the array data and into the remaining RNA isolated from the blastocyst-derived stem cell population with complete loss of Tip110 might also reveal more compelling information about the role of Tip110 in stem cell biology. The cells produced in these experiments are the only true Tip110 knockout

cells produced from a transgenic mouse cross and have provided a whole new area of potential exploration as far as the role of Tip110 in stemness in concerned. It is clear now that the protein is important in both hESC and mESC cell survival and proliferation and future work will hopefully answer in a more concise manner why and how this is so.

Additional Roles of Tip110

Additional studies other than those presented in this dissertation have provided clues about the role of Tip110 in the interaction with cell cycle regulator Sap155, in the regulation of small RNA, and in the nuclear translocation of cellular proteins. In addition, the differences in size, expression, and degradation of human Tip110 and mouse Tip110 have also been investigated. Each of these areas can certainly warrant further investigation – to provide some direction for potential experiments the results obtained so far concerning these topics will be briefly discussed.

Tip110 and Sap155 – Direct or Indirect Interaction?

Previous unpublished experiments (Timani et al) revealed several proteins that might interact with Tip110. Of particular interest was the Sap155 protein. Sap155 is a protein associated with splicing and cell cycle related processes (*118*). Confirming an interaction between Tip110 and Sap155 might provide insights into some additional spliceosome-associated components Tip110 interacts with during regulation of pre-mRNA splicing processes and other roles for Tip110 in the cell cycle. Initial analysis of Sap155 revealed that the protein is fairly abundant at the

endogenous level in HeLa, Jurkat, NIH3T3, and 293T cells (data not shown). Despite this several attempts to immunoprecipitate Tip110 and Sap115 were unsuccessful (**Fig. 30**). Immunoprecipitation of either Tip110 or Sap155 from 293T cell lysates transfected with Tip110 followed by Western blot analysis to detect Tip110 and Sap155 failed to demonstrate a clear interaction (either direct or indirect) between the two proteins (**Fig. 30A**). This does not mean there is no direct or indirect interaction between Tip110 and Sap155 but does suggest that other methods might be employed to better detect the interaction such as a pulldown, yeast two-hybrid, or tandem affinity purification assay. It is likely that the Sap155 antibody (sc102102, Santa Cruz Biotech.) used here was not good for immunoprecipitation as there was no detection of Sap155 after IP for Sap155 despite the clear detection of the protein in the western blot input (**Fig. 30B**). Because of the role both Tip110 and Sap155 play in the splicing process and their effects on the cell cycle it would certainly be worthwhile to investigate this particular subject further in the future.

Tip110 Regulation of small RNA

In other attempts to better understand the functions of Tip110, a search of the conserved domains and motifs on the protein was conducted. Using the NCBI Conserved Domain Database (*44*) a new conserved domain on the Tip110 protein, NOP25, with homology similar to a protein in the Nop25 superfamily called Nucleolar protein 12 was discovered (**Fig. 1A** & **B**). Nucleolar protein 12 is part of the yeast nuclear pore complex-associated pre-60S ribosomal subunit. Proteins in this particular family function as exonucleases that are required for the 5'-end maturation of 25S and 5.8S rRNA. This information coupled to previously established information that showed that

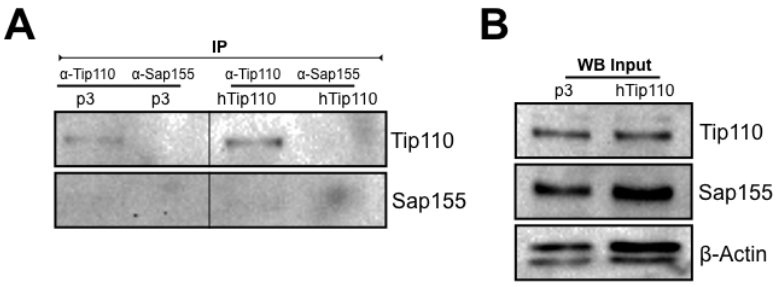
A
IP
α-Tip110
α-Sap155
α-Tip110
α-Sap155
p3
p3
hTip110
hTip110
Tip110
Sap155
B
WB Input
p3
hTip110
Tip110
Sap155
β-Actin

Figure 30. Immunoprecipitation cannot detect interaction between Tip110 and Sap155. 293T cells were transfected with either pcDNA3 (p3, as a transfection control) or recombinant human Tip110. (**A**) Cell lysates were immunoprecipitated using either anti-Tip110 antibody or anti-Sap155 antibody followed by Western blotting for Tip110 and Sap155. Western blot inputs are included for reference (**B**). β-Actin was included as a loading control for Western blotting. The data are representative of three independent experiments.

Tip110 interacts with certain snRNP during spliceosome recycling and other domains that support its role in the 3'-end processing of pre-mRNA suggested that Tip110 might, to some degree, be able to affect the regulation of small RNA. To investigate this, studies were first conducted to determine what effect, if any, changes in Tip110 protein expression might have on 28S, 18S, 5.8S, and 5S rRNA and on U1, U2, U4, U5, and U6 snRNA levels in 293T cells. To do this Tip110 was either overexpressed or knocked down using transfection techniques. The efficiency of each transfection was confirmed with western blot analysis and the levels of the aforementioned RNA were then measured using RT-PCR and qRT-PCR (data not shown).

These studies revealed that changes in Tip110 protein expression by overexpression or siRNA-mediated knockdown do not have a significant impact on the levels of ribosomal or small nuclear RNA *in vitro* (**Fig. 31**). There were occasions where subtle changes in expression were noted in both the RT-PCR and qRT-PCR experiments but the changes were often difficult to reproduce and sometimes contradictory. These results do not however mean that changes in Tip110 levels would not affect the processing of these RNA *in vitro*. As such, this area could certainly be explored further in the future.

It might also be worthwhile to investigate the role of Tip110 in the regulation of long noncoding RNA (lncRNA). lncRNA have roles in a variety of processes including gene expression, protein translation, cell differentiation, cell fate determination, organogenesis, and tissue homeostasis (*119*). Because Tip110 has RNA binding abilities and can serve as a regulator of many cellular processes including RNA splicing, processing, and modification it would not be surprising if it

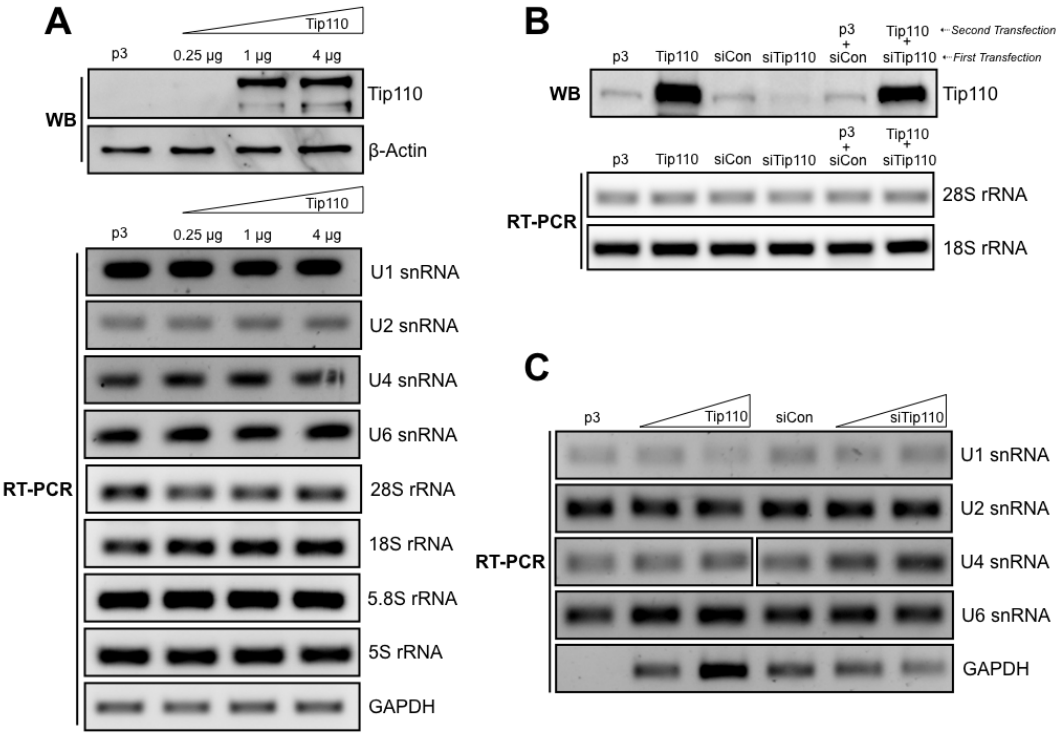
A
Tip110
p3
0.25 μg
1 μg
4 μg
WB
Tip110
β-Actin
Tip110
p3
0.25 μg
1 μg
4 μg
RT-PCR
U1 snRNA
U2 snRNA
U4 snRNA
U6 snRNA
28S rRNA
18S rRNA
5.8S rRNA
5S rRNA
GAPDH
B
p3
Tip110
siCon
siTip110
p3 + siCon
Tip110 + siTip110
←Second Transfection
←First Transfection
WB
Tip110
RT-PCR
28S rRNA
18S rRNA
C
p3
Tip110
siCon
siTip110
RT-PCR
U1 snRNA
U2 snRNA
U4 snRNA
U6 snRNA
GAPDH

Figure 31. Regulation of rRNA and snRNA by Tip110 *in vitro*. (**A**) 293T cells were transfected with pcDNA3 (p3) or increasing amounts of recombinant Tip110. pc3 was used as a transfection and reference control. Western analysis was performed to confirm the success of the transfection and β-actin was used as a loading control. Total RNA was isolated from these cells and converted to cDNA. RT-PCR reactions were then performed to detect snRNA (U1, U2, U4, and U6) and rRNA (28S, 18S, 5.8S, and 5S). GAPDH was used a loading control for the RT-PCR reactions. (**B**) 293T cells were transfected with recombinant Tip110 or siRNA to induce Tip110 knockdown. pc3 and siCon were used as a transfection controls. Western analysis was performed to confirm the success of the transfection. Total RNA was isolated from these cells and converted to cDNA. RT-PCR reactions were performed to detect 28S and 18S rRNA. (**C**) 293T cells were transfected with increasing amounts of Tip110 or siRNA to induce Tip110 knockdown. pc3 and siCon were used as a transfection controls. Total RNA was isolated from these cells and converted to cDNA. RT-PCR reactions were performed to detect snRNA (U1, U2, U4, and U6). GAPDH was used a loading control for the RT-PCR reactions.

could bind to and/or contribute to the processing, modification, and regulation of lncRNA. The array data presented here revealed that ~56% of the total genes (36,703 of 65, 956) affected by Tip110 were noncoding. Genes in this noncoding category include: lncRNA, miRNA, mitochondrial tRNA scaRNA, snRNA, snoRNA, and many other unidentified RNA. Moreover, the array data also revealed that loss of Tip110 led to important perturbations in RNA processing and spliceosome-associated genes.

It would certainly be advisable to investigate any trends in the functions of the noncoding RNA that are affected by Tip110 loss as well as what neighboring genes surround them. In addition, a look at the effects of Tip110 loss and overexpression on capping and end modifications is also warranted. Lastly, detecting Tip110 interactions with different RNA is necessary. Thus far it has been shown that Tip110 can bind U6 snRNA and the 7SK RNA but certainly the RNA binding protein likely interacts with many other RNA species transiently or otherwise. This information would provide a clear picture for the role Tip110 plays in RNA processing and regulation outside of serving as a recycling factor for the spliceosome and regulator of pre-mRNA splicing.

Nuclear Translocation of YB-1 by Tip110

Previous studies revealed that overexpression of Tip110 resulted in the translocation of certain proteins (i.e. Usp4, Usp11, Usp15, and YB-1) that were normally localized in the cytoplasm to the nucleus (**Fig. 32**, YB-1 translocation). The mechanism and reason for this translocation however was unclear. To better understand this, wild-type Tip110 and Tip110 mutants lacking either the N-terminus (Tip110ΔNT) or the nuclear localization signals of Tip110 (Tip110ΔNLS)

were used in immunofluorescence experiments. The N-terminus of Tip110 contains several HAT domains which are required for its protein-protein interactions; so the thought was that if the translocation capacity of Tip110 required direct interaction it would not occur in the absence of this domain. The nuclear localization signals are required for the protein to enter the nucleus so if they are removed the translocation might also be perturbed assuming these domains are required for this process. The data from these immunofluorescence experiments revealed that indeed The N-terminus (data not shown) and NLS (**Fig. 34**) of Tip110 are required for translocation of YB-1 to the nucleus. In addition, these studies suggested that the translocation was likely mediated through importin-α (**Fig. 34**). Tip110 and YB-1 can only interact with importin-α simultaneously when Tip110 has its N-terminus or NLS sequences (**Fig. 34B**) which may explain why YB-1 cannot translocate to the nucleus in immunofluorescence experiments using cells transfected with Tip110ΔNT or Tip110ΔNLS. Other recently published data concerning this matter revealed that this same phenomena occurs between Tip110 and USP4 and that both the N-terminal HAT domains and NLS sequences of Tip110 are necessary for the translocation to occur (*46*). Certainly there are other proteins that Tip110 may translocate to the nucleus aside from the ones described here. As such, it would be interesting to identify these proteins and to determine the significance of their translocation and what biological processes the translocation is necessary for.

Post-Translational Modification and Instability of Tip110

Previously it was mentioned that human Tip110 (hTip110) and mouse Tip110 (mTip110), although similar, have some very distinct properties. hTip110 is larger than mTip110 after PAGE

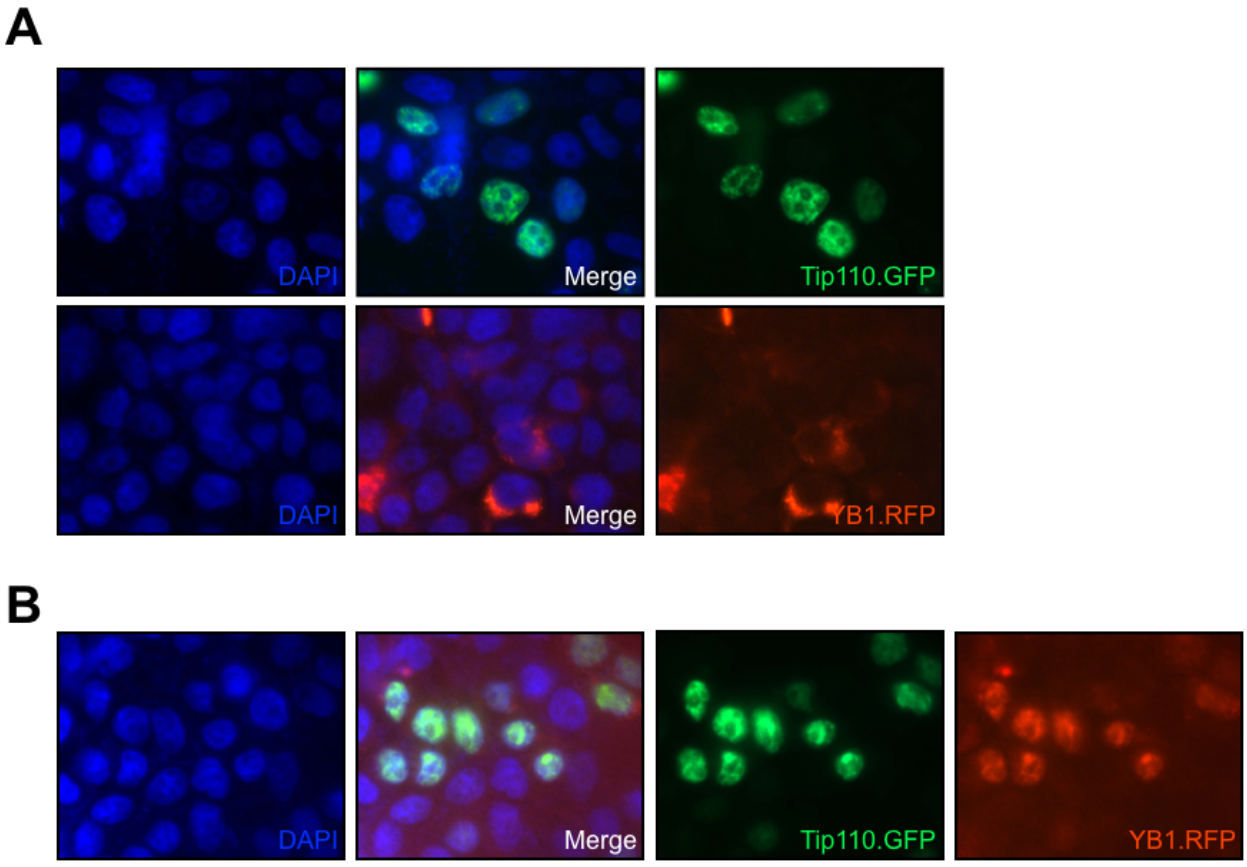
A
DAPI
Merge
Tip110.GFP
DAPI
Merge
YB1.RFP
B
DAPI
Merge
Tip110.GFP
YB1.RFP

Figure 32. Tip110 Induces the Nuclear Translocation of YB-1 *In Vitro*. (**A**) 293T cells were transfected with recombinant Tip110.GFP (Top) or recombinant YB1.RFP (Bottom). 48 hrs. after transfection cells were fixed, counterstained with DAPI for nuclei, and mounted for immunofluorescence detection. (**B**) 293T cells were co-transfected with recombinant Tip110.GFP and recombinant YB1.RFP (Bottom). 48 hrs. after transfection cells were fixed, counterstained with DAPI for nuclei, and mounted for immunofluorescence detection.

A

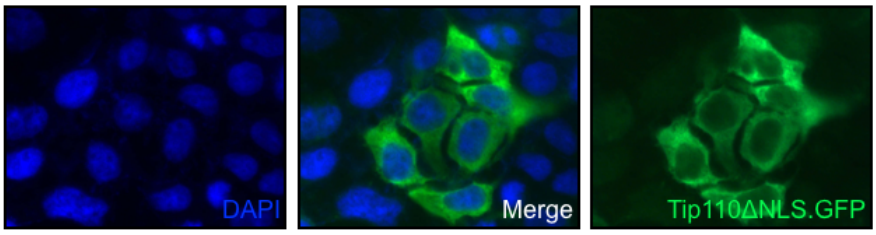
DAPI
Merge
Tip110ΔNLS.GFP

B

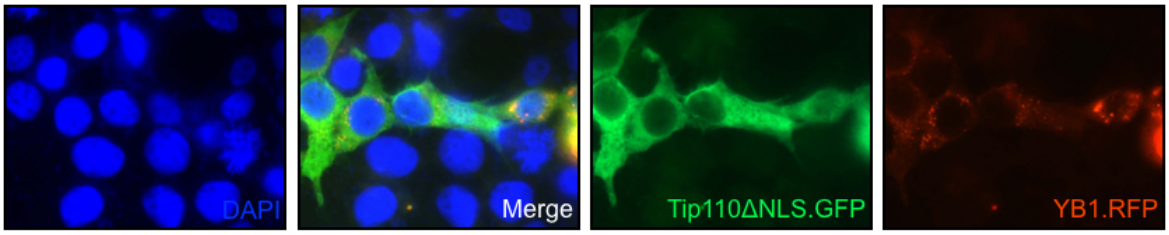
DAPI
Merge
Tip110ΔNLS.GFP
YB1.RFP

Figure 33. Nuclear translocation of YB-1 is inhibited by co-expression with Tip110ΔNLS mutant. (**A**) 293T cells were transfected with recombinant Tip110ΔNLS.GFP. 48 hrs. after transfection cells were fixed, counterstained with DAPI for nuclei, and mounted for immunofluorescence detection. (**B**) 293T cells were co-transfected with recombinant Tip110ΔNLS.GFP and recombinant YB1.RFP. 48 hrs. after transfection cells were fixed, counterstained with DAPI for nuclei, and mounted for immunofluorescence detection.

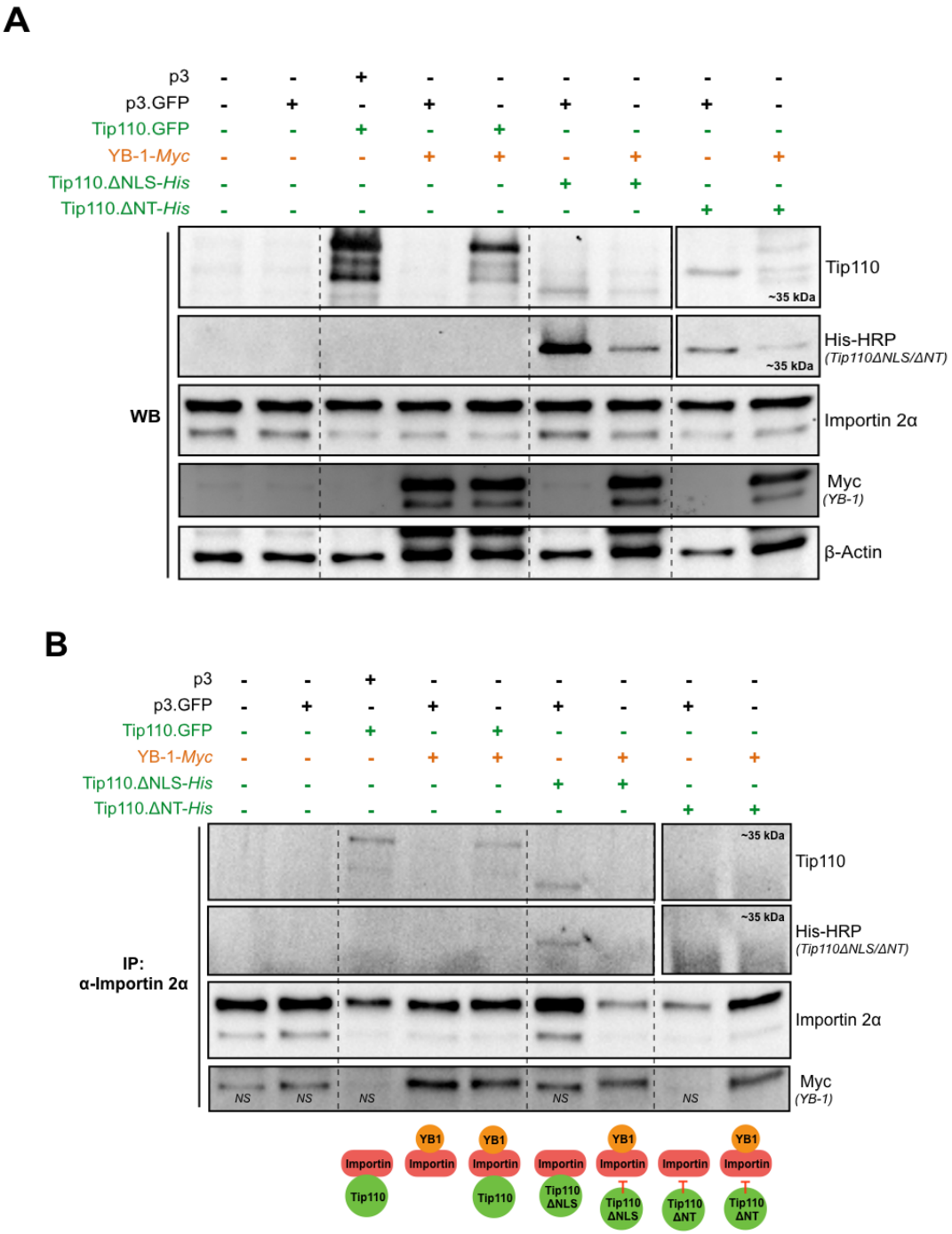
A
p3
p3.GFP
Tip110.GFP
YB-1-Myc
Tip110.ΔNLS-His
Tip110.ΔNT-His
WB
Tip110
~35 kDa
His-HRP
(Tip110ΔNLS/ΔNT)
~35 kDa
Importin 2α
Myc
(YB-1)
β-Actin
B
p3
p3.GFP
Tip110.GFP
YB-1-Myc
Tip110.ΔNLS-His
Tip110.ΔNT-His
IP:
α-Importin 2α
~35 kDa
Tip110
~35 kDa
His-HRP
(Tip110ΔNLS/ΔNT)
Importin 2α
NS
NS
NS
NS
NS
Myc
(YB-1)
Importin
Tip110
YB1
Importin
Importin
Tip110
Importin
Tip110 ΔNLS
YB1
Importin
Tip110 ΔNLS
Importin
Tip110 ΔNT
YB1
Importin
Tip110 ΔNT

Figure 34. Tip110 and YB-1 co-immunoprecipitate with Importin-2α *in vitro* when the NLS and N-terminus of Tip110 are undisturbed. 293T cells were transfected with pcDNA3 (p3), p3.GFP, Tip110.GFP, Tip110ΔNLS.His, Tip110ΔNT.His, and/or YB-1.Myc in various combinations as described. (**A**) 48 hrs. after transfection cell lysates were subjected to Western analysis for Tip110 (the anti-Tip110 antibody detected all Tip110 constructs while the anti-His-HRP antibody best detected Tip110ΔNLS.His and Tip110ΔNT.His), Importin-2α, or YB-1 (anti-myc antibody). β-Actin was included as a loading control for Western blotting. (**B**) Cell lysates were also immunoprecipitated using Importin-2α followed by western blotting for Tip110, Importin-2α, or YB-1. A schematic is shown (bottom) to provide a summary representation of the interactions of Tip110 and YB-1 with Importin-2α. NS = non-specific bands.

despite their predicted molecular weight being essentially the same (**Fig. 2**). Also, hTip110 is very unstable when expressed in mouse cells and tissues despite the mouse protein being expressed fairly well in human cells. Experiments designed to determine which PTM, if any, was responsible for the differences between hTip110 and mTip110 involved creation of several mutant Tip110 constructs and use of enzymatic and other biological inhibitors. Treating immunoprecipitated cell lysates from cells transfected with a Tip110 expression plasmid with calf intestinal phosphatase (CIP), tunicamycin, or endoglycosidase H (endo H) indicated that neither serine, threonine, or tyrosine phosphorylation nor N-glycosylation (also confirmed by site-directed mutagenesis) was likely responsible for the differences in size or stability observed between h- and mTip110 **(Fig. 36A & B)**. Subsequently, a series of mutated hTip110 and mTip110 hybrid constructs were created to better identify what loci on the protein may be associated with the size and stability differences between hTip110 and mTip110 **(Fig. 35)**.

N- and C-terminal deletion mutants were created in identical fashions for both hTip110 and mTip110 to determine which terminus, if any, contributed most to the discrepancies between the proteins **(Fig. 35C & D)**. Surprisingly, the data showed that in 293T cells the size difference between hTip110 and mTip110 was conserved on both termini so that the human ΔNT (aa 671-963) and ΔCT (aa 1-670) mutants were both larger than their mouse counterparts **(Fig. 36C)**. There are also stability differences between the constructs. That is, human ΔNT was more stable than mouse ΔNT while the inverse was true for the ΔCT mutants. These data suggest that the size difference between mTip110 and hTip110 is not specific to one particular portion of the protein. It may be likely that there is a PTM dispersed throughout the protein that accounts for

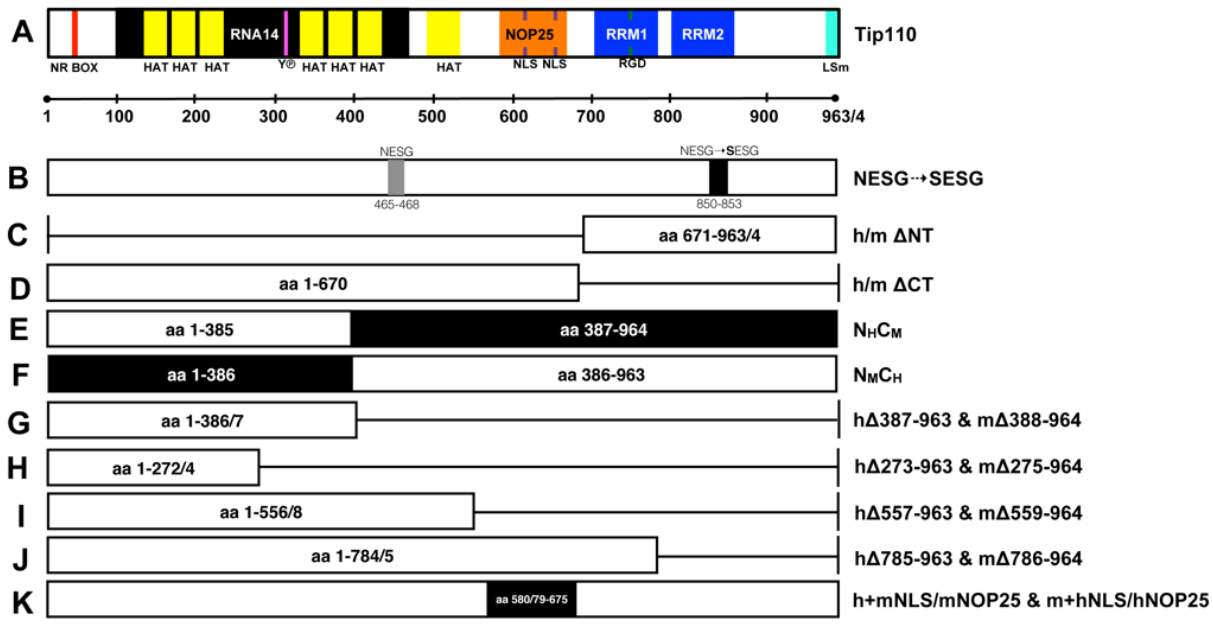
A
RNA14
NOP25
RRM1
RRM2
Tip110
NR BOX
HAT HAT HAT
Y
HAT HAT HAT
HAT
NLS NLS
RGD
LSm
1
100
200
300
400
500
600
700
800
900
963/4
B
NESG
465-468
NESG→SESG
850-853
NESG⇢SESG
C
aa 671-963/4
h/m ΔNT
D
aa 1-670
h/m ΔCT
E
aa 1-385
aa 387-964
NHCM
F
aa 1-386
aa 386-963
NMCH
G
aa 1-386/7
hΔ387-963 & mΔ388-964
H
aa 1-272/4
hΔ273-963 & mΔ275-964
I
aa 1-556/8
hΔ557-963 & mΔ559-964
J
aa 1-784/5
hΔ785-963 & mΔ786-964
K
aa 580/79-675
h+mNLS/mNOP25 & m+hNLS/hNOP25

Figure 35. Schematic of Tip110 and mutant Tip110 constructs. (**A**) Wild-type Tip110 with its conserved domains detailed along with their respective positions. (**B-K**) shows h- and mTip110 mutants created by PCR and restriction enzyme cloning techniques. (**B**) hTip110 with its N-glycosylation sites shown, where the amino acid site represented by the black box was mutated from NESG to SESG using site directed mutagenesis. (**C**) N-terminal deletion mutant for hTip110 and mTip110 where amino acids 1–670 are deleted. (**D**) C-terminal deletion mutant for hTip110 and mTip110 where amino acids 671–963/4 are deleted. (**E**) Domain swapped mutant with a hTip110 N-terminus and a mTip110 C-terminus (NHCM). (**F**) Domain swapped mutant with a hTip110 C-terminus and a mTip110 N-terminus (NMCH). (**G**) Mutant with deletion in amino acids 387–963 (hTip110) and 388–964 (mTip110). (**H**) Mutant with deletion in amino acids 273–963 (hTip110) and 275–964 (mTip110). (**I**) Mutant with deletion in amino acids 557–963 (hTip110) and 559–964 (mTip110). (**J**) Mutant with deletion in amino acids 785–963 (hTip110) and 786–964 (mTip110). (**K**) Represents two mutants: hTip110 with NLS/NOP25-like site (580–675) of mTip110 and mTip110 with NLS/NOP25-like site (579–675) of hTip110. *Abbreviations: aa - amino acid, h - human, and m - mouse.*

this. The stability pattern was also surprising as there is no obvious explanation for why the proteins would have an inverse pattern of stability, although differences in plasmid preparation cannot be ruled out as a causative factor. Similar trends were also observed in NIH3T3 cells (data not shown).

Swapping of N- and C- terminal domains between hTip110 and mTip110 revealed that any construct containing hTip110 was unstable in NIH3T3 cells **(Fig. 35E & F, & 36E)** while constructs containing either mTip110 or hTip110 were stable in 293T cells (data not shown). In the NIH3T3 cells it is important to note that the domain swapped constructs (N-terminus of mTip110 + C-terminus of hTip110 — N_mC_h and N-terminus of hTip110 + C-terminus of mTip110 — N_hC_m) were slightly more stable than the wild-type hTip110, with the N_hC_m construct being the most stable – this suggests that the N-terminus of hTip110 (aa 1-386) contributes, at least in part, to the stability of hTip110 **(Fig. 36D)**. Addition of the proteasome inhibitor MG132, increased the expression of all of the constructs in NIH3T3 cells but did not restore the hTip110 containing constructs to the levels of recombinant mTip110. Mutants expressing only amino acids 1-386 and 1-387 of hTip110 and mTip110 respectively **(Fig. 35G)** were created to confirm the role of the N-terminus of Tip110 on its size and stability and revealed that the 386 amino acid hTip110 construct is indeed larger than its 387 amino acid mouse counterpart but not necessarily more stable (data not shown).

To further investigate the differences between hTip110 and mTip110 constructs, serially truncated mutants were created by progressively shortening the 963 amino acid hTip110 protein to 785, 557, and 273 amino acids; and the mTip110 protein to 786, 559, and 275 amino acids

(Fig. 35H-J). The results revealed that the shorter the Tip110 construct was the more unstable it became - with the 785/786 amino acid construct being expressed in a similar fashion as wild-type hTip110 and mTip110 **(Fig. 36E)**. This indicates that amino acids 785-963 (containing RRM2 and LSm motif) are not crucial for proper Tip110 expression. While constructs of 557/559 and 273/275 amino acids were degraded in 293T and NIH3T3 cells where expression could only be detected properly upon the addition of proteasome inhibitors MG132 or epoxomicin **(Fig. 36E)**. Most interestingly, in all of these constructs hTip110 proved to be larger in size than mTip110 by ~10 kDa (data not shown) further implying that there is some modification dispersed rather evenly (adding about 10 kDa per third of Tip110) throughout the protein contributing to the overall ~30 kDa size difference between mTip110 and hTip110.

BLAST analysis of hTip110 versus mTip110 revealed that the region with the highest degree of dissimilarity between hTip110 and mTip110 was between amino acids 273/275 and 785/786 **(Fig. 1)**. This region contains the 2 NLS sites of Tip110, RRM1, and a conserved domain with similarity to nucleolar protein 12 (Nop25) — a highly conserved RNA binding, nucleolar protein that is involved in nucleolar architecture and maintenance and in 5'-end maturation of 5.8S and 25S rRNA (*44*). To better understand how this site with similarity to Nop25 might contribute to the size and (in)stability of Tip110, the NOP25/NLS domain was swapped between h- and mTip110 **(Fig. 35K)**. Although the stability of hTip110$^{mNLS/mNop25}$ decreased slightly in 293T and NIH3T3 cells, there were no other significant observations or conclusions to be made (the size differences between WT and mutant Tip110 is due to loss of the his-tag in mutants) **(Fig. 36F)**. The only remaining domain within the region of high dissimilarity that was not tested was the RRM1 domain. The sequence of the RRM1 domain between m- and hTip110 is not

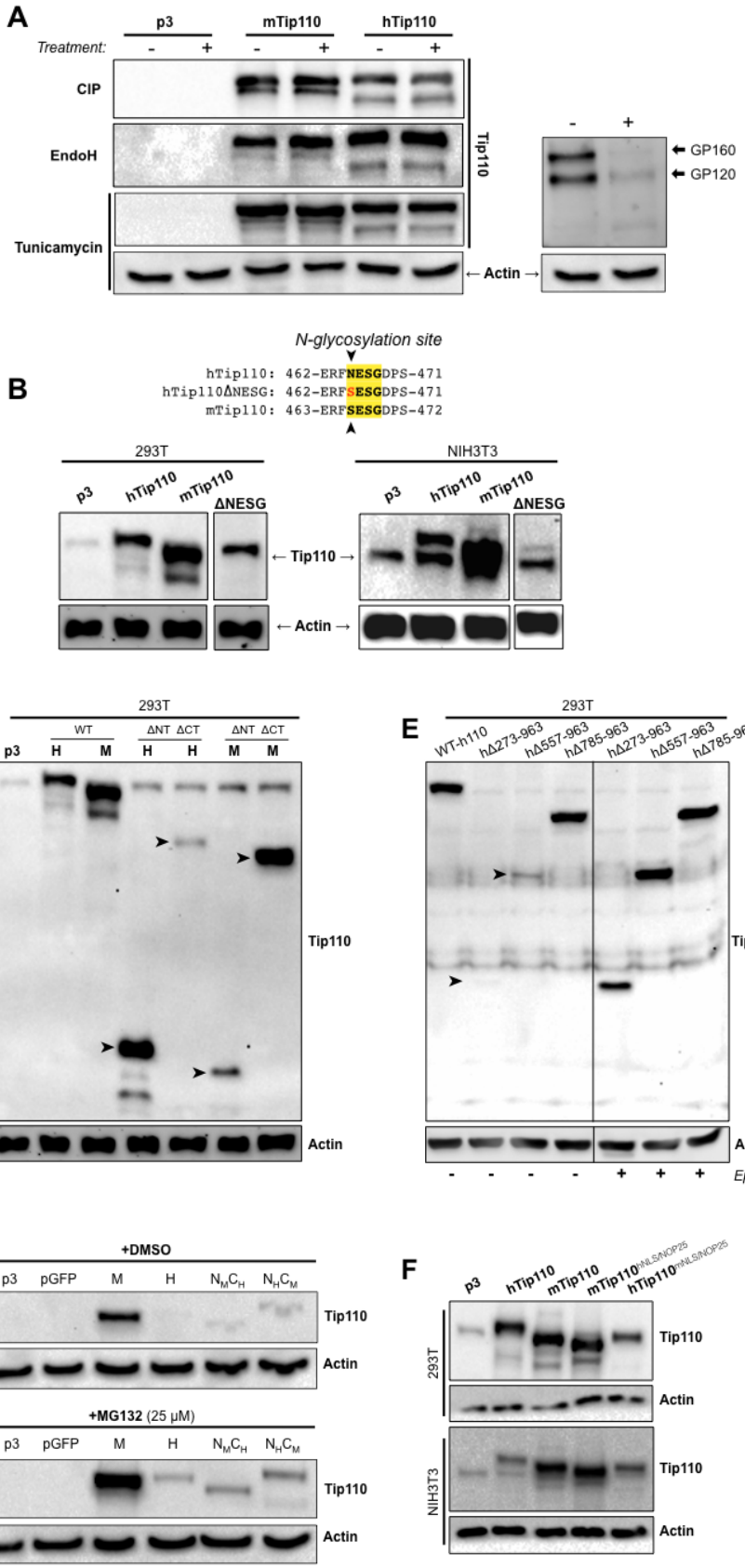
A
p3
mTip110
hTip110
Treatment:
CIP
EndoH
Tunicamycin
Tip110
Actin
GP160
GP120
B
N-glycosylation site
hTip110: 462-ERFNESGDPS-471
hTip110ΔNESG: 462-ERFSESGDPS-471
mTip110: 463-ERFSESGDPS-472
293T
NIH3T3
p3
hTip110
mTip110
ΔNESG
Tip110
Actin
C
293T
WT
ΔNT ΔCT
p3
H
M
Tip110
Actin
D
+DMSO
p3
pGFP
M
H
NMCH
NHCM
Tip110
Actin
NIH3T3
+MG132 (25 μM)
E
293T
WT-h110
hΔ273-963
hΔ557-963
hΔ785-963
Tip110
Actin
Epoxomicin
F
p3
hTip110
mTip110
mTip110hNLS/NOP25
hTip110hNLS/NOP25
293T
NIH3T3
Tip110
Actin

Figure. 36. Identification of post-translational modifications of Tip110 via Western Blot analysis. (**A**) 293T cells were transfected with pcDNA3 (p3), human Tip110, or mouse Tip110 constructs and treated with calf intestinal phosphatase (CIP), endoglycosidase H (endo H), or tunicamycin according to the manufacturer's recommendations. A control is shown to right where 293T cells were first transfected with recombinant GP120 and then treated with tunicamycin. (**B**) 293T cells transfected with p3, human Tip110, mouse Tip110, or the hTip110-ΔNESG mutant. A sequence alignment (top) details how the hTip110-ΔNESG mutant was converted to be similar to the equivalent site for mouse Tip110. (**C**) 293T cells were transfected with pcDNA3 (lane 1) and the following Tip110 plasmid DNA constructs: WT recombinant human Tip110 and mouse Tip110 (lanes 2 and 3, respectively), hTip110 ΔNT and ΔCT mutants (lanes 4 and 5, respectively), mTip110 ΔNT and ΔCT mutants (lanes 6 and 7, respectively). (**D**) NIH3T3 cells were transfected with pcDNA3 (lane 1) or recombinant GFP (lane 2) and the following Tip110 plasmid DNA constructs: mouse Tip110 (lane 3), human Tip110 (lane 4), the NMCH construct (lane 5), and the NHCM construct (lane 6). Top: Cells in the absence of MG132 (DMSO control). Bottom: Cells in the presence of MG132 (25 μM) for 20 h. (**E**) 293T cells were transfected with the following Tip110 plasmid DNA constructs: WT recombinant human Tip110 (lane 1), hTip110 amino acids with 273–963, 557 963, and 785–963 deleted in the absence of epoxomicin (DMSO control; lanes 1, 2, 3, and 4, respectively), hTip110 amino acids with 273–963, 557–963, and 785–963 deleted in the presence of epoxomicin (lanes 5, 6, and 7, respectively). (**F**) 293T (top) and NIH3T3 (bottom) cells were transfected with the following plasmid DNA constructs: pcDNA3 (lane 1), human Tip110 (lane 2), mouse Tip110 (lane 3), mTip110 with the NLS/NOP25 site of hTip110 (lane 4), hTip110 with the NLS/NOP25 site of mTip110 (lane 5). For all experiments cell lysates were typically collected for western blot

analysis 48 hours after transfection. β-Actin was included as a loading control for Western blotting.

significantly different though, suggesting that it is not likely contributing to the difference between h- and mTip110 proteins.

Taking all of these data together, it seems that there may not be a PTM at a singular locus that is responsible for the h- and mTip110 size discrepancy but rather a PTM that is dispersed throughout the various domains of the protein that contributes to the size difference observed between the mouse and human homologs. The data also indicate that the degradation of hTip110 in NIH3T3 cells occurs through proteasome-mediated pathways as the stability of the protein could be restored, to an extent, through introduction of MG132 or epoxomicin to cell cultures. It is important to note that we do know (from unpublished data) that overexpression of exogenous Tip110 can increase endogenous levels of the protein in 293T and K562 cells. The data show that it is possible for exogenous or ectopic expression to alter the steady-state levels of Tip110 to some degree, but these changes, as previously mentioned, reflect an increase rather than a decrease. This increase is mediated through the ability of the protein to interact with a specific site within its own 3' UTR. This phenomenon seems to reflect that Tip110 itself can increase the stability or at least the expression of endogenous levels of Tip110. We see this not only *in vitro* in NIH3T3 cells, but also *in vivo* in our transgenic mice, and *ex vivo* in mouse embryonic fibroblasts overexpressing hTip110 – that hTip110 is unstable in mouse cells and tissues. Whether this has anything to do with the 3' UTR has yet to be investigated. These data add another level of complexity to what we already know especially considering that mTip110 is expressed very well in human cells. These particular phenomena seem to be unique to Tip110 as there are no other classes of proteins that display these specific expression characteristics or differences between homologs with such high similarity. The differences between hTip110 and

mTip110 also suggest that they may function differently from one another *in vivo* although this difference has yet to be clearly identified. It is also important to note that we are limited to some degree in the cell lines we have investigated as our studies concerning hTip110 stability in mouse are limited only to NIH3T3 cells and the cells and tissues derived from our transgenic mouse model.

Studies involving the *in vitro* expression of hTip110 and mTip110 are not the only example of this protein stability phenomena occurring between hTip110 and mTip110. *In vivo* analysis of hTip110 expressed in a transgenic mouse model revealed a similar discrepancy. A transgenic mouse model overexpressing hTip110 was created and surprisingly, only hTip110 mRNA and not protein could be detected in the mouse embryonic fibroblasts (tg-MEF) derived from these mice (*19*). Only upon treatment with proteasome inhibitors (i.e. MG132, epoxomicin, or bortezomib) could hTip110 be detected in the tg-MEF, suggesting that hTip10 detection was hindered by proteasome-mediated degradation in the transgenic mice, as previously observed in *in vitro* experiments. This was confirmed further when it was shown that MG132 could increase exogenous hTip110 expression in NIH3T3 cells but had no effect on exogenous Tip110 in 293T cells. Interestingly, hTip110 is more ubiquitinated than mTip110 in NIH3T3 cells while mTip110 was shown to be more inhibitory to the global proteasome activity in the cell than hTip110. This suggests that hTip110 is less stable than mTip110 because it is more ubiquitinated than mTip110 but it is not clear why the hTip110 protein would be processed (i.e. ubiquitinated and degraded) differently in mouse cells and tissues than in human since they have such a high degree of similarity. These data highlight the importance of ubiquitin-proteasome system (UPS)-

mediated degradation in mouse cells and tissues and indicate that the hTip110 protein is more sensitive to this process.

Moreover, hTip110 but not mTip110 can interact with and serve as a substrate for USP15 - a deubiquitinating enzyme (*19*). Not only do these proteins interact with one another but co-expression of hTip110 with USP15 changes the localization of USP15 from cytoplasmic (and nucleolar) to an almost exclusive nuclear co-localization with hTip110. This interaction might suggest that hTip110 could be protected from UPS-mediated degradation through its interaction and subsequent deubiquitination by USP15 but this is not necessarily the case. In fact, when USP15 is knocked down, thus decreasing the deubiquitination of Tip110, there is actually more expression of hTip110 in tg-MEF. One explanation for this seemingly contradictory phenomena is that hTip110 is ubiquitinated by both K11/K48 and K63 ubiquitination. Proteins modified with K11 or K48 ubiquitination are targeted for degradation by the 26S proteasome while proteins with K63 ubiquitination are not. If USP15 preferentially deubiquitinates the K63 linkages of Tip110 leaving only K11 or K48 linkages it would make Tip110 more susceptible to 26S mediated degradation while USP15 knockdown would allow for the K63 linkages to remain and thus prevent Tip110 from being degraded. Also, it is important to note that there are other USP (i.e. USP4 and USP11) that Tip110 can interact with (*10, 59*). These USP could dominate when USP15 is knocked-down and also allow for deubiquitination of Tip110 in a fashion that favors a more stable protein. Collectively these data show that hTip110 is (de)ubiquitinated and subsequently processed in the UPS in a different manner than mTip110. That is, hTip110 is more ubiquitinated than mouse and more sensitive to UPS-mediated degradation than mouse when expressed in mouse cells and tissues.

All those above-mentioned studies have provided further insights into some of the mechanisms by which Tip110 is regulated. There is currently no clear answer for why hTip110 is not processed in the same manner in mouse and human cells/tissues or the reason for why deubiquitination of a protein would result in its destabilization. Comparing the global ubiquitin-proteasome system between mouse and human might reveal clues as to why. Further investigation will surely lead to an answer for why this protein displays such a distinct and characteristic size and expression phenomena between species.

REFERENCES

1. T. Nagase, Prediction of the coding sequences of unidentified human genes. IV. The coding sequences of 40 new genes (KIAA0121-KIAA0160) deduced by analysis of cDNA clones from human cell line KG-1. *DNA Res.* **2**, 167-174 (1995).
2. M. Bell, S. Schreiner, A. Damianov, R. Reddy, A. Bindereif, p110, a novel human U6 snRNP protein and U4/U6 snRNP recycling factor. *EMBO J.* **21**, 2724-2735 (2002).
3. A. Damianov, S. Schreiner, A. Bindereif, Recycling of the U12-type spliceosome requires p110, a component of the U6atac snRNP. *Mol. Cell. Biol.* **24**, 1700-1708 (2004).
4. K. Harada, A. Yamada, D. M. Yang, K. Itoh, S. Shichijo, Binding of a SART3 tumor-rejection antigen to a pre-mRNA splicing factor RNPS1: A possible regulation of splicing by a complex formation. *Int. J. Cancer* **93**, 623-628 (2001).
5. K. Licht, J. Medenbach, R. Lührmann, C. Kambach, A. Bindereif, 3'-cyclic phosphorylation of U6 snRNA leads to recruitment of recycling factor p110 through LSm proteins. *RNA* **14**, 1532-1538 (2008).
6. Y. Liu, X. Huang, K. A. Timani, H. E. Broxmeyer, J. J. He, MicroRNA-124 targets Tip110 expression and regulates hematopoiesis. *Stem Cells Development* **24**, 2009-2017 (2015).
7. Y. Liu, K. Timani, X. Ou, H. E. Broxmeyer, J. J. He, C-MYC Controlled TIP110 protein expression regulates OCT4 mRNA splicing in human embryonic stem cells. *Stem Cells and Development* **22**, 6 (2013).

8. J. Medenbach, S. Schreiner, S. B. Liu, R. Luhrmann, A. Bindereif, Human U4/U6 snRNP recycling factor p110: Mutational analysis reveals the function of the tetratricopeptide repeat domain in recycling. *Mol. Cell. Biol.* **24**, 7392-7401 (2004).

9. I. Novotny, M. Blazikova, D. Stanek, P. Herman, J. Malinsky, In vivo kinetics of U4/U6.U5 tri-snRNP formation in Cajal bodies. *Mol. Biol. Cell* **22**, 513-523 (2011).

10. E. J. Song *et al.*, The Prp19 complex and the Usp4(Sart3) deubiquitinating enzyme control reversible ubiquitination at the spliceosome. *Genes Dev.* **24**, 1434-1447 (2010).

11. D. Stanek, K. M. Neugebauer, Detection of snRNP assembly intermediates in Cajal bodies by fluorescence resonance energy transfer. *J. Cell Biol.* **166**, 1015-1025 (2004).

12. D. Stanek, S. D. Rader, M. Klingauf, K. M. Neugebauer, Targeting of U4/U6 small nuclear RNP assembly factor SART3/p110 to Cajal bodies. *J. Cell Biol.* **160**, 505-516 (2003).

13. N. S. Trede *et al.*, Network of coregulated spliceosome components revealed by zebrafish mutant in recycling factor p110. *Proc. Natl. Acad. Sci. U. S. A.* **104**, 6608-6613 (2007).

14. I. Novotny *et al.*, SART3-Dependent Accumulation of Incomplete Spliceosomal snRNPs in Cajal Bodies. *Cell Reports* **10**, 429-440 (2015).

15. S. Rüegger, T. S. Miki, D. Hess, H. Großhans, The ribonucleotidyl transferase USIP-1 acts with SART3 to promote U6 snRNA recycling. *Nucleic Acids Res.* **43**, 3344-3357 (2015).

16. Y. Liu *et al.*, Tip110, the human immunodeficiency virus type 1 (HIV-1) Tat-interacting protein of 110 kDa as a negative regulator of androgen receptor (AR) transcriptional activation. *J. Biol. Chem.* **279**, 21766-21773 (2004).

17. Y. Liu, J. L. Li, B. O. Kim, B. S. Pace, J. J. He, HIV-1 tat protein-mediated transactivation of the HIV-1 long terminal repeat promoter is potentiated by a novel nuclear tat-interacting protein of 110 kDa, Tip110. *J. Biol. Chem.* **277**, 23854-23863 (2002).

18. K. A. Timani, Y. Liu, J. J. He, Tip110 interacts with YB-1 and regulates each other's function. *BMC Mol. Biol.* **14**, 7 (2013).

19. K. A. Timani, Y. Liu, A. Suvannasankha, J. J. He, Regulation of ubiquitin-proteasome system-mediated Tip110 protein degradation by USP15. *Int. J. Biochem. Cell Biol.* **54**, 10-19 (2014).

20. W. N. Zhao, Y. Liu, K. A. Timani, J. J. He, Tip110 protein binds to unphosphorylated RNA polymerase II and promotes its phosphorylation and HIV-1 long terminal repeat transcription. *J. Biol. Chem.* **289**, 190-202 (2014).

21. L. Long *et al.*, The U4/U6 recycling factor SART3 has histone chaperone activity and associates with USP15 to regulate H2B deubiquitination. *J. Biol. Chem.* **289**, 8916-8930 (2014).

22. Y. Liu, M. R. Lee, K. Timani, J. J. He, H. E. Broxmeyer, Tip110 maintains expression of pluripotent factors in and pluripotency of human embryonic stem cells. *Stem Cells and Development* **21**, 829-833 (2012).

23. Y. Liu *et al.*, TIP110/p110(nrb)/SART3/p110 regulation of hematopoiesis through CMYC. *Blood* **117**, 5643-5651 (2011).

24. M. Ito *et al.*, Identification of SART3-derived peptides capable of inducing HLA-A2-restricted and tumor-specific CTLs in cancer patients with different HLA-A2 subtypes. *Int. J. Cancer* **88**, 633-639 (2000).

25. K. Furugaki *et al.*, Intraperitoneal administration of a tumor-associated antigen SART3, CD40L, and GM-CSF gene-loaded polyplex micelle elicits a vaccine effect in mouse tumor models. *PLoS One* **9**, 14 (2014).

26. K. Harada *et al.*, Mouse homologue of the human SART3 gene encoding tumor-rejection antigen. *Jpn. J. Cancer Res.* **91**, 239-247 (2000).

27. K. Iseki *et al.*, Evaluation of a new oil adjuvant for use in peptide-based cancer vaccination. *Cancer Sci.* **101**, 2110-2114 (2010).

28. T. Minami *et al.*, Identification of SART3-derived peptides having the potential to induce cancer-reactive cytotoxic T lymphocytes from prostate cancer patients with HLA-A3 supertype alleles. *Cancer Immunology Immunotherapy* **56**, 689-698 (2007).

29. E. R. Mohamed *et al.*, Capability of SART3(109-118) peptide to induce cytotoxic T lymphocytes from prostate cancer patients with HLA class I-A11,-A31 and-A33 alleles. *Int. J. Oncol.* **34**, 529-536 (2009).

30. T. Ono *et al.*, Antitumor effects of systemic and local immunization with a CTL-directed peptide in combination with a local injection of OK-432. *Clin. Cancer Res.* **12**, 1325-1332 (2006).

31. Y. Yamaguchi *et al.*, Feasibility study of adoptive immunotherapy for metastatic lung tumors using peptide-pulsed dendritic cell-activated killer (PDAK) cells. *Anticancer Res.* **25**, 2407-2415 (2005).

32. D. Yang *et al.*, Identification of a gene coding for a protein possessing shared tumor epitopes capable of inducing HLA-A24-restricted cytotoxic T lymphocytes in cancer patients. *Cancer Res.* **59**, 4056-4063 (1999).

33. Z. H. Zhang *et al.*, A mutation in SART3 gene in a Chinese pedigree with disseminated superficial actinic porokeratosis. *Br. J. Dermatol.* **152**, 658-663 (2005).

34. Z. H. Zhang *et al.*, Reassessment of microarray expression data of porokeratosis by quantitative real-time polymerase chain reaction. *J. Cutan. Pathol.* **37**, 371-375 (2010).

35. Y. Zhou *et al.*, Identification of three novel frameshift mutations of the MVK gene in four Chinese families with disseminated superficial actinic porokeratosis. *Br. J. Dermatol.* **169**, 193-195 (2013).

36. K. Fukuda, Y. Takao, Y. Miyazaki, K. Itoh, A. Yamada, New type of natural antibodies reactive to cytotoxic T lymphocyte-directed cancer vaccine peptides. *Immunobiology* **209**, 245-253 (2004).

37. N. Kawamoto *et al.*, IgG reactive to CTL-directed epitopes of self-antigens is either lacking or unbalanced in atopic dermatitis patients. *Tissue Antigens* **61**, 352-361 (2003).

38. J. P. Petschek, M. J. Mermer, M. R. Scheckelhoff, a. a. Simone, J. C. Vaughn, RNA editing in Drosophila 4f-rnp gene nuclear transcripts by multiple A-to-G conversions. *J. Mol. Biol.* **259**, 885-890 (1996).

39. A. Hubert *et al.*, A functional genomics screen identifies an Importin-a homolog as a regulator of stem cell function and tissue patterning during planarian regeneration. *BMC Genomics* **16**, 18 (2015).

40. J. Gu, S. Shimba, N. Nomura, R. Reddy, Isolation and characterization of a new 110 kDa human nuclear RNA-binding protein (p110nrb). *Biochim. Biophys. Acta* **1399**, 1-9 (1998).

41. X. F. Ding *et al.*, Nuclear receptor-binding sites of coactivators glucocorticoid receptor interacting protein 1 (GRIP1) and steroid receptor coactivator 1 (SRC-1): Multiple motifs with different binding specificities. *Mol. Endocrinol.* **12**, 302-313 (1998).

42. D. M. Heery, E. Kalkhoven, S. Hoare, M. G. Parker, A signature motif in transcriptional co-activators mediates binding to nuclear receptor. *Nature* **387**, 733-736 (1997).

43. J. Torchia *et al.*, The transcriptional co-activator p/CIP binds CBP and mediates nuclear-receptor function. *Nature* **387**, 677-684 (1997).

44. A. Marchler-Bauer *et al.*, CDD: conserved domains and protein three-dimensional structure. *Nucleic Acids Res.* **41**, D348-D352 (2013).

45. J. R. Lamb, S. Tugendreich, P. Hieter, Tetraco peptide repeat interactions - To TPR or not to TPR. *Trends Biochem. Sci.* **20**, 257-259 (1995).

46. J. K. Park, T. Das, E. J. Song, E. E. Kim, Structural basis for recruiting and shuttling of the spliceosomal deubiquitinase USP4 by SART3. *Nucleic Acids Res.*, (2016).

47. P. Allard, P. Beaulieu, A. Aprikian, S. Chevalier, Bombesin modulates the association of Src with a nuclear 110-kd protein expressed in dividing prostate cells. *J. Androl.* **21**, 367-375 (2000).

48. Y. Liu, J. Liu, Z. Wang, J. J. He, Tip110 binding to U6 small nuclear RNA and its participation in pre-mRNA splicing. *Cell & Bioscience* **5**, 40 (2015).

49. A. Whitmill, K. A. Timani, Y. Liu, J. J. He, Tip110: Physical properties, primary structure, and biological functions. *Life Sci.* **149**, 79-95 (2016).

50. A. Mayeda *et al.*, Purification and characterization of human RNPS1: A general activator of pre-mRNA splicing. *EMBO J.* **18**, 4560-4570 (1999).

51. D. A. Pomeranz Krummel, A. M. MacMillan, It takes two to tangle: Prp24 and spliceosome assembly. *Nat. Struct. Mol. Biol.* **21**, 503-504 (2014).

52. S. D. Rader, C. Guthrie, A conserved Lsm-interaction motif in Prp24 required for efficient U4/U6 di-snRNP formation. *RNA* **8**, 1378-1392 (2002).

53. G. A. Matera, Z. Wang, A day in the life of the splicesome. *Nature Reviews Molecular Cell Biology* **15**, 108-121 (2014).

54. R. McNamara, J. McCann, S. A. Gudipaty, I. D'Orso, Transcription factors mediate the enzymatic disassembly of promoter-bound 7sk snrnp to locally recruit p-tefb for transcription elongation. *Cell Reports* **5**, 1256-1268 (2013).

55. C. Jeronimo *et al.*, Systematic analysis of the protein interaction network for the human transcription machinery reveals the identity of the 7SK capping Eenzyme. *Mol. Cell* **27**, 262-274 (2007).

56. B. Sobhian *et al.*, HIV-1 Tat assembles a multifunctional transcription elongation complex and stably associates with the 7SK snRNP. *Mol. Cell* **38**, 439-451 (2010).

57. M. Jiang *et al.*, Androgen-responsive gene database: Integrated knowledge on androgen-responsive genes. *Mol. Endocrinol.* **23**, 1927-1933 (2009).

58. V. Torres-Estay *et al.*, Androgen receptor in human endothelial cells. *J. Endocrinol.* **224**, R131-R137 (2015).

59. M. E. Sowa, E. J. Bennett, S. P. Gygi, J. W. Harper, Defining the human deubiquitinating enzyme interaction landscape. *Cell* **138**, 389-403 (2009).

60. J. Cao, Q. Yan, Histone ubiquitination and deubiquitination in transcription, DNA damage response, and cancer. *Front. Oncol.* **2**, 1-9 (2012).

61. K. A. Timani, Y. Liu, Y. Fan, K. S. Mohammad, J. J. He, Tip110 regulates the cross talk between p53 and hypoxia-inducible factor 1α under hypoxia and promotes survival of cancer cells. *Molecular and Cellular Biology* **35**, 2254-2264 (2015).

62. P. B. Rahl *et al.*, c-Myc regulates transcriptional pause release. *Cell* **141**, 432-445 (2010).

63. A. Matz *et al.*, Regulation of neuronal survival and morphology by the E3 ubiquitin ligase RNF157. *Cell Death Differ.*, 1-17 (2014).

64. L. Cui, K. Osada, A. Imaizumi, K. Kataoka, K. Nakano, Feasibility of a subcutaneously administered block/homo-mixed polyplex micelle as a carrier for DNA vaccination in a mouse tumor model. *J. Control. Release* **206**, 220-231 (2015).

65. K. Fukuda, Expression of the SART3 antigens in oral cancers. *The Kurume Medical Journal* **48**, 55-58 (2001).

66. T. B. Hartmann *et al.*, Identification of selectively expressed genes and antigens in CTCL. *Exp. Dermatol.* **17**, 324-334 (2008).

67. N. Kawagoe *et al.*, Expression of the SART3 tumor rejection antigen in renal cell carcinoma. *J. Urol.* **164**, 2090-2095 (2000).

68. M. Koga *et al.*, Analysis of cellular localization of SART3 tumor antigen by a newly established monoclonal antibody: Heterotopic expression of SART3 on the surface of B-lineage leukemic cells. *Oncol. Rep.* **11**, 785-789 (2004).

69. Y. Komohara *et al.*, Anti-cancer vaccine candidates in specific immunotherapy for bladder carcinoma. *Int. J. Oncol.* **29**, 1555-1560 (2006).

70. Y. Miyagi *et al.*, Induction of cellular immune responses to tumor cells and peptides in colorectal cancer patients by vaccination with SART3 peptides. *Clin. Cancer Res.* **7**, 3950-3962 (2001).

71. E. Mizukoshi *et al.*, Comparative analysis of various tumor-associated antigen-specific T-cell responses in patients with hepatocellular carcinoma. *Hepatology* **53**, 1206-1216 (2011).

72. K. Murayama *et al.*, Expression of the SART3 tumor-rejection antigen in brain tumors and induction of cytotoxic T lymphocytes by its peptides. *J. Immunother.* **23**, 511-518 (2000).

73. F. Niiya *et al.*, Expression of SART3 tumor-rejection antigen in gastric cancers. *Jpn. J. Cancer Res.* **91**, 337-342 (2000).

74. M. Noguchi *et al.*, Induction of cellular and humoral immune responses to tumor cells and peptides in HLA-A24 positive hormone-refractory prostate cancer patients by peptide vaccination. *Prostate* **57**, 80-92 (2003).

75. T. Sasatomi *et al.*, Expression of tumor rejection antigens in colorectal carcinomas. *Cancer* **94**, 1636-1641 (2002).

76. Y. Suefuji *et al.*, Expression of SART3 antigen and induction of CTLs by SART3-derived peptides in breast cancer patients. *Br. J. Cancer* **84**, 915-919 (2001).

77. N. Suzuki *et al.*, Detection of peptide-specific cytotoxic T-lymphocyte precursors used for specific immunotherapy of pancreatic cancer. *Int. J. Cancer* **98**, 45-50 (2002).

78. M. Tanaka *et al.*, Development of a new diagnostic tool for pancreatic cancer: simultaneous measurement of antibodies against peptides recognized by cytotoxic T lymphocytes. *The Kurume Medical Journal* **53**, 63-70 (2006).

79. S. Tanaka *et al.*, Expression of tumor-rejection antigens in gynecologic cancers. *Jpn. J. Cancer Res.* **91**, 1177-1184 (2000).

80. N. Tsuda *et al.*, Expression of a newly defined tumor-rejection antigen SART3 in musculoskeletal tumors and induction of HLA class I-restricted cytotoxic T lymphocytes by SART3-derived peptides. *J. Orthop. Res.* **19**, 346-351 (2001).

81. J. P. Petschek, M. R. Scheckelhoff, M. J. Mermer, J. C. Vaughn, RNA editing and alternative splicing generate mRNA transcript diversity from the Drosophila 4f-rnp locus. *Gene* **204**, 267-276 (1997).

82. K. Cockburn, J. Rossant, Making the blastocyst: lessons from the mouse. *J. Clin. Invest.* **120**, 995-1003 (2010).

83. N. Dard, M. Breuer, B. Maro, S. Louvet-Vallée, Morphogenesis of the mammalian blastocyst. *Mol. Cell. Endocrinol.* **282**, 70-77 (2008).

84. S. K. Dey *et al.*, Molecular cues to implantation. *Endocr. Rev.* **25**, 341-373 (2004).

85. L. Robb, P. P. Tam, Gastrula organiser and embryonic patterning in the mouse. *Semin. Cell Dev. Biol.* **15**, 543-554 (2004).

86. P. P. Tam, R. R. Behringer, Mouse gastrulation: the formation of a mammalian body plan. *Mech. Dev.* **68**, 3-25 (1997).

87. A. Schnerch, C. Cerdan, M. Bhatia, Distinguishing between mouse and human pluripotent stem cell regulation: the best laid plans of mice and men. *Stem Cells* **28**, 419-430 (2010).

88. I. Ginis *et al.*, Differences between human and mouse embryonic stem cells. *Dev. Biol.* **269**, 360-380 (2004).

89. H. E. Shamseldin *et al.*, Identification of embryonic lethal genes in humans by autozygosity mapping and exome sequencing in consanguineous families. *Genome Biol.* **16**, 116 (2015).

90. V. E. Papaioannou, R. R. Behringer, Early embryonic lethality in genetically engineered mice: diagnosis and phenotypic analysis. *Vet. Pathol.* **49**, 64-70 (2012).

91. A. J. Copp, Death before birth: clues from gene knockouts and mutations. *Trends Genet.* **11**, 87-93 (1995).

92. Y. G. Gangloff *et al.*, Disruption of the mouse mTOR gene leads to early postimplantation lethality and prohibits embryonic stem cell development. *Mol. Cell. Biol.* **24**, 9508-9516 (2004).

93. K. Takeda *et al.*, Targeted disruption of the mouse Stat3 gene leads to early embryonic lethality. *Proc. Natl. Acad. Sci. U. S. A.* **94**, 3801-3804 (1997).

94. C. Luo *et al.*, Superovulation strategies for 6 commonly used mouse strains. *J Am Assoc Lab Anim Sci* **50**, 471-478 (2011).

95. A. Nagy, M. Gertsenstein, K. Vintersten, R. Behringer, *Manipulating the Mouse Embryo: A Laboratory Manual, Third Edition*. (Cold Spring Harbor Laboratory Press, New York, 2003), pp. 764.

96. A. Czechanski *et al.*, Derivation and characterization of mouse embryonic stem cells from permissive and nonpermissive strains. *Nat. Protoc.* **9**, 559-574 (2014).

97. G. R. Martin, Isolation of a pluripotent cell line from early mouse embryos cultured in medium conditioned by teratocarcinoma stem cells. *Proc. Natl. Acad. Sci. U. S. A.* **78**, 7634-7638 (1981).

98. M. A. Lancaster, J. A. Knoblich, Generation of cerebral organoids from human pluripotent stem cells. *Nat. Protoc.* **9**, 2329-2340 (2014).

99. K. Sasai *et al.*, Targeted disruption of Aurora A causes abnormal mitotic spindle assembly, chromosome misalignment and embryonic lethality. *Oncogene* **27**, 4122-4127 (2008).

100. I. A. Graef *et al.*, Neurotrophins and netrins require calcineurin/NFAT signaling to stimulate outgrowth of embryonic axons. *Cell* **113**, 657-670 (2003).

101. H. Mi, A. Muruganujan, J. T. Casagrande, P. D. Thomas, Large-scale gene function analysis with the PANTHER classification system. *Nat. Protoc.* **8**, 1551-1566 (2013).

102. T. Kelder *et al.*, Mining biological pathways using WikiPathways web services. *PLoS One* **4**, e6447 (2009).

103. M. Lakso *et al.*, Efficient in vivo manipulation of mouse genomic sequences at the zygote stage. *Proc. Natl. Acad. Sci. U. S. A.* **93**, 5860-5865 (1996).

104. Y. Higashi *et al.*, Generation of the floxed allele of the SIP1 (Smad-interacting protein 1) gene for Cre-mediated conditional knockout in the mouse. *Genesis* **32**, 82-84 (2002).

105. M. Holzenberger *et al.*, Cre-mediated germline mosaicism: a method allowing rapid generation of several alleles of a target gene. *Nucleic Acids Res.* **28**, E92 (2000).

106. S. M. Dang, M. Kyba, R. Perlingeiro, G. Q. Daley, P. W. Zandstra, Efficiency of embryoid body formation and hematopoietic development from embryonic stem cells in different culture systems. *Biotechnol. Bioeng.* **78**, 442-453 (2002).

107. H. Kurosawa, Methods for inducing embryoid body formation: in vitro differentiation system of embryonic stem cells. *J Biosci Bioeng* **103**, 389-398 (2007).

108. M. A. Lancaster *et al.*, Cerebral organoids model human brain development and microcephaly. *Nature* **501**, 373-379 (2013).

109. d. W. Huang, B. T. Sherman, R. A. Lempicki, Systematic and integrative analysis of large gene lists using DAVID bioinformatics resources. *Nat. Protoc.* **4**, 44-57 (2009).

110. d. W. Huang, B. T. Sherman, R. A. Lempicki, Bioinformatics enrichment tools: paths toward the comprehensive functional analysis of large gene lists. *Nucleic Acids Res.* **37**, 1-13 (2009).

111. H. Mi, S. Poudel, A. Muruganujan, J. T. Casagrande, P. D. Thomas, PANTHER version 10: expanded protein families and functions, and analysis tools. *Nucleic Acids Res.* **44**, D336-342 (2016).

112. L. S. Lim, F. H. Hong, G. Kunarso, L. W. Stanton, The pluripotency regulator Zic3 is a direct activator of the Nanog promoter in ESCs. *Stem Cells* **28**, 1961-1969 (2010).

113. S. P. Medvedev, A. I. Shevchenko, S. M. Zakian, Molecular basis of Mammalian embryonic stem cell pluripotency and self-renewal. *Acta Naturae* **2**, 30-46 (2010).

114. P. D. Jenik, R. E. Jurkuta, M. K. Barton, Interactions between the cell cycle and embryonic patterning in Arabidopsis uncovered by a mutation in DNA polymerase epsilon. *Plant Cell* **17**, 3362-3377 (2005).

115. E. E. Henninger, Z. F. Pursell, DNA polymerase ε and its roles in genome stability. *IUBMB Life* **66**, 339-351 (2014).

116. G. Martello, A. Smith, The nature of embryonic stem cells. *Annu. Rev. Cell Dev. Biol.* **30**, 647-675 (2014).

117. K. Takahashi, S. Yamanaka, Induction of pluripotent stem cells from mouse embryonic and adult fibroblast cultures by defined factors. *Cell* **126**, 663-676 (2006).

118. M. M. Luke *et al.*, The SAP, a new family of proteins, associate and function positively with the SIT4 phosphatase. *Mol. Cell. Biol.* **16**, 2744-2755 (1996).

119. S. U. Schmitz, P. Grote, B. G. Herrmann, Mechanisms of long noncoding RNA function in development and disease. *Cell. Mol. Life Sci.* **73**, 2491-2509 (2016).

Amanda J. Whitmill

EDUCATION

University of North Texas Health Science Center at Fort Worth - Fort Worth, TX 2011-2016
Department of Cell Biology, Immunology and Microbiology - Ph.D.

Texas A&M University-Corpus Christi - Corpus Christi, TX 2007-2011
School of Science and Technology - B.S.

RESEARCH EXPERIENCE

University of North Texas Health Science Center at Fort Worth - Fort Worth, TX 2011-Present
PhD Candidate/Graduate Teaching Assistant

Conducted research to investigate the role of Tip110 in embryonic and stem cell development.

Publications

Whitmill, A., Liu, Y., Timani, K.A., He, J.J. (2016). Tip110 Deletion Led To Embryonic Lethality And Impaired Embryonic Stem Cell Pluripotency, Self-Renewal And Survival Through Down-Regulation Of Stem Cell Factors Nanog, Oct4, And Sox2. (Pending Publication).

Whitmill, A., Timani, K.A., Liu, Y., He, J.J. (2016). Tip110: Physical Properties, Primary Structure, and Biological Functions. *Life Sciences*. 149: 79-95.

Liu, Y., Timani, K.A., Whitmill, A., Zhang, X., Broxmeyer, H.E., He, J.J.. (2016). Self-regulation of Tip110 Expression Through Preferential Usage of the Proximal Polyadenylation Site Within its 3' Untranslated Region. (Pending Publication).

Timani, K.A., Liu, Y., Whitmill, He, J.J. (2016). Tip110 Regulates TNF-α-Induced NF-kB Activation by Targeting IkB and p65. (Pending Publication).

Presentations

Whitmill, A. He, J.J. 2016. Disruption of the Mouse Tip110 Gene Leads to Early Post-implantation Lethality and Prohibits Embryonic Stem Cell Development. Experimental Biology 2016. San Diego, CA. Poster Presentation.

Whitmill, A. 2014. Getting to and Surviving in Graduate School. 2014 TAMUCC BUILD Symposium. Corpus Christi, TX. Oral Presentation.

Whitmill, A., He, J.J. 2013. Characterization of the Regulatory Mechanisms of Tip110 in Early Embryonic Development and Beyond. UNTHSC 21st Annual Research Appreciation Day. Fort Worth, TX. Poster Presentation.

Texas A&M University-Corpus Christi - Corpus Christi, TX 2009-2011
Research Assistant

Conducted seminal research to investigate the role of non-thermal ionized plasma treatment as a potential cancer therapy.

Publications

Thiyagarajan, M., Waldbeser, L., Whitmill, A. (2012). THP-1 Leukemia Cancer Treatment Using a Portable Plasma Device. *Stud. Health. Technol. Inform*. 173:515-7.

Whitmill, A., Waldbeser, L., Magesh, T. (2010). Effects of Ionized Plasma on Acute Monocytic Leukemia Cells. *Fall 2010 TAMUCC McNair Scholars Journal*.

Presentations

Whitmill, A., Waldbeser, L., Magesh, T. 2011. Effects of Non-Thermal Ionized Plasma on THP-1 Acute Monocytic Leukemia Cells. National Conference on Undergraduate Research, Ithaca, NY. Oral Presentation.

Whitmill, A., Waldbeser, L., Magesh, T. 2011. Induction of Apoptosis in Leukemia Cells by Non-Thermal Ionized Plasma. 7th Annual LSAMP Symposium, Prairie View, TX. Poster Presentation.

Whitmill, A., Waldbeser, L., Magesh, T. 2010. Effects Ionized Plasma on Acute Monocytic Leukemia Cells. 8th Annual Pathways Student Research Symposium, West Texas A&M University, Canyon, TX. Poster Presentation.

Whitmill, A., Waldbeser, L., Magesh, T. 2010. Effects of Non-Thermal Ionized Plasma on THP-1 Acute Monocytic Leukemia Cells. SACNAS Conference, Anaheim, CA. Poster Presentation.

Whitmill, A., Waldbeser, L., Magesh, T. 2010. Effects Ionized Plasma on Acute Monocytic Leukemia Cells. 10th Annual TAMUCC Undergraduate Research Symposium, Corpus Christi, TX. Oral Presentation.

Whitmill, A., Waldbeser, L., Magesh, T. 2010. Effects Ionized Plasma on Acute Monocytic Leukemia Cells. McNair Research Symposium, University of California - Berkeley, Berkeley, CA. Oral Presentation.

Alford, K., Whitmill, A., Waldbeser, L. 2009. Effects of Cortisol on the Pathogenicity of *Neisseria meningitidis*. Sigma Xi Annual Research Conference, Houston, TX. Poster Presentation.

Whitmill, A., Alford, K., Waldbeser, L. 2009. Effects of Cortisol on the Pathogenicity of *Neisseria meningitidis*. 9th Annual TAMUCC Undergraduate Research Symposium, Corpus Christi, TX. Poster Presentation.

HONORS & AWARDS

Graduate

- Graduate Student Travel Award (‘16)
- American Physiological Society Minority Travel Fellow Award (‘16)
- Division of Student Affairs Scholarship Recipient (‘15-‘16)
- Division of Student Affairs Scholarship Recipient (‘14-‘15)
- Division of Student Affairs Scholarship Recipient, (‘12-‘13)
- Minority Opportunities in Research and Education Program Participant (‘11-‘14)

Undergraduate

- Ronald E. McNair Scholar (‘10-‘11)
- Louis Stokes Alliance for Minority Participation (‘09-‘11)
- 3rd Place in Undergraduate Poster Presentation at 7th Annual LSAMP Symposium (‘11)
- Community Outreach Scholarship Recipient (‘08)

ASSOCIATIONS

Graduate

- Sigma Xi Member (‘16-Present)
- American Association for the Advancement of Science (‘15-Present)
- Sustainability Program Member (‘13-‘14)
    - *Title*: Sustainability Liaison
- Graduate Student Association (‘11-Present)
- Black Graduate Student Association (‘11-Present)

Undergraduate

- Association of Women in Science, (‘09-‘11)
    - *Title*: Historian, Fall ‘10
- Alpha Epsilon Delta – Pre-Professional Honor Society (‘07-‘08)